Schweizerische Eidgenossenschaft
Confédération suisse
Confederazione Svizzera
Confederaziun svizra

Eidgenössisches Departement für Umwelt, Verkehr, Energie und Kommunikation UVEK
Département fédéral de l'environnement, des transports, de l'énergie et de la communication DETEC
Dipartimento federale dell'ambiente, dei trasporti, dell'energia e delle comunicazioni DATEC

Bundesamt für Strassen
Office fédéral des routes
Ufficio federale delle Strade

Influence of sustained actions and loading rate on the strength of reinforced concrete structures

Influence de la durée et de la vitesse de chargement sur la résistance des structures en béton

Einfluss der Belastungsdauer und -geschwindigkeit auf den Widerstand von Betontragwerken

Ecole Polytechnique Fédérale de Lausanne (EPFL)
Laboratoire de Construction en Béton (IBETON)

D. Tasevski
M. Fernández Ruiz
A. Muttoni

Projet de recherche AGB 2013/001 sur demande du groupe de l'AGB
(Groupe de Travail et de Recherche en Matière de Ponts)

March 2020 **699**

Schweizerische Eidgenossenschaft
Confédération suisse
Confederazione Svizzera
Confederaziun svizra

Eidgenössisches Departement für Umwelt, Verkehr, Energie und Kommunikation UVEK
Département fédéral de l'environnement, des transports, de l'énergie et de la communication DETEC
Dipartimento federale dell'ambiente, dei trasporti, dell'energia e delle comunicazioni DATEC

Bundesamt für Strassen
Office fédéral des routes
Ufficio federale delle Strade

Influence of sustained actions and loading rate on the strength of reinforced concrete structures

Influence de la durée et de la vitesse de chargement sur la résistance des structures en béton

Einfluss der Belastungsdauer und -geschwindigkeit auf den Widerstand von Betontragwerken

Ecole Polytechnique Fédérale de Lausanne (EPFL)
Laboratoire de Construction en Béton (IBETON)

D. Tasevski
M. Fernández Ruiz
A. Muttoni

Projet de recherche AGB 2013/001 sur demande du groupe de l'AGB
(Groupe de Travail et de Recherche en Matière de Ponts)

March 2020 **699**

Impressum

Instance de recherche et équipe de projet

Direction du projet
Prof. Dr. Aurelio Muttoni

Membres
Darko Tasevski
Dr. Miguel Fernández Ruiz

Commission de suivi

Président
Dr. Martin Käser

Membres
Dr. Fritz Hunkeler (jusqu'à 2018)
Prof. Dr. Walter Kaufmann
Prof. Dr. Albin Kenel
Prof. Dr. Ueli Angst
Dr. Manuel Alvarez (jusqu'à 2018)
Daniele Stroligo
Stéphane Cuennet

Auteur de la demande

Groupe de travail et de recherche en matière de ponts (AGB)

Source

Le présent document est téléchargeable gratuitement sur http://www.mobilityplatform.ch.

Contents

Summary

Sustained loading scenarios on reinforced concrete structures, with increased strains and deformations due to concrete creep effects, are traditionally associated with the serviceability limit state behaviour, but they can also have an effect at the ultimate limit state. The present report investigates the effect of load duration and loading rate on the ultimate strength of reinforced concrete members.

It is well known that a rapid application of the load has a rather beneficial influence on the concrete compressive strength. On the other hand, if the concrete compressive stress at ultimate limit state is larger than about 80% of its nominal strength, usually measured by tests with a duration of 1 to 2 minutes, sustained loads (permanent actions and variable loads with a duration longer than a couple hours) can also have a detrimental effect on the material strength. The resulting strength reduction is due to the development of nonlinear creep associated to material damage (propagation and growth of micro-cracks). This can occur because the concrete stress level due to sustained load is usually higher at the ultimate limit state than at the serviceability limit state, as the actions are increased and the concrete compressive strength is reduced to account for uncertainties related to actions, material strength, dimensions, calculation of internal forces and resistance models.

For the design of new structures, the concrete compressive strength reduction due to a high level of sustained loading can usually be neglected because it is compensated by the beneficial increase of the compressive strength due to continued cement hydration. In fact, it is well known that the concrete strength keeps increasing after the reference age of 28 days and that after some months/years, the compressive strength can be more that 20% higher than at 28 days. However, neglecting the sustained loading effect can be on the unsafe side when:

(i) the maximum design load is applied on a relatively young concrete (when failure can occur before the strength increase due to continued cement hydration can develop)
(ii) the effective concrete compressive strength has been assessed after 28 days (in particular when assessing existing structures, where no additional strength increase due to continued cement hydration can be expected)

In codes of practice (in Switzerland SIA 262:2013 and EN 1992-1-1/CH-NA:2014), this effect is considered by a reduction of the design compressive concrete strength by a factor varying between 0.85 and 1.0 (or even an increase by 1.2 for very rapid loads). The value of 1.0 is typically used in the design of new structures, for which the governing design situation occurs when the effect of continued cement hydration is sufficient to compensate the strength decrease due to sustained loading or if the compressive stress at design level due to sustained loading does not exceed 85 to 90% of the compressive strength. The lower value of 0.85 refers to the more severe condition when the concrete strength is assessed after some years/decades and the contribution of rapid loads is negligible. Because this reduction is applied to the design concrete compressive strength, it effectively affects all cases where the resistance directly depends on the concrete compressive strength (compression members, compression zone due to bending, upper limit of the shear resistance in members with shear reinforcement, compression on locally loaded areas, etc.).

According to SIA 262:2013 and EN 1992-1-1/CH-NA:2014 (but not EN 1992-1-1:2004), this reduction also applies to the shear resistance of members without shear reinforcement (the shear resistance is reduced by the same coefficient as the compressive concrete strength). Because the concrete strength increase due to continued cement hydration has a smaller influence on the shear resistance (which is approximately proportional to $f_{ck}^{1/3}$), the reduction following this approach is particularly severe when assessing existing structures in shear without shear reinforcement, as the concrete strength increase after some decades is often not sufficient to compensate the strength reduction due to sustained load.

Main objectives

The present research project has the following objectives:

(i) to investigate the difference between sustained constant load and slow loading rates (the latter being typical for the classical construction process, where the maximal stress due to permanent loads will be reached some months after concrete casting)
(ii) to propose a verification procedure for complex loading histories
(iii) to clarify whether loading durations of a couple of hours or days can affect the concrete strength
(iv) to propose an improvement of code provisions with respect to the design compressive strength
(v) to verify whether a shear strength reduction due to sustained loading is necessary for members without shear reinforcement.

Effect of constant sustained load

Based on an improved mechanical model, which has been validated by additional test series on unreinforced concrete cylinders loaded in compression, it has been shown that the strength reduction, which can reach approximately 20%, is more severe under a constant sustained load than in the case of loads increased with a slow rate. In addition, because the strength reduction is associated to creep with material damage, the age of loading plays a major role. The strength reduction is very rapid in case of loading of concrete at young age (for a concrete age at loading of 7 days, the 20% strength reduction is reached in a couple of hours after the application of the sustained load), but it is very slow for old concretes (several months of sustained loading are needed to reach the reduction of 20% for an old concrete). All these considerations show the importance of the strength increase due to continued cement hydration and the age of assessing the concrete strength.

In addition, both the mechanical model and the conducted tests show that the detrimental effect of sustained loading and of slow loading rates on the compressive strength is associated with a larger deformation capacity at failure. This effect can be very beneficial and can potentially compensate the detrimental effect described above, allowing for a better redistribution of internal forces, reducing stress concentrations in concrete (for example in the compression zone) and allowing for an increase of the reinforcement activation in compression before concrete failure.

Complex loading history patterns

For a detailed verification of structures with a complex loading history, the cumulative damage estimation approach of Palmgren-Miner (used for instance for a detailed fatigue verification according to SIA 262:2013) has been adapted to account for time-dependent effects, leading to consistent results. Some simplifications of typical practical cases have been analysed:

(i) variation of constant stress rates or variation of constant strain rates
(ii) constant slow stress rate after a rapid initial stress increase (typically accounting for the stress increase during construction when additional permanent loads are added over a couple of months after a rapid construction)
(iii) rapid stress increase after a period of sustained loading (simulating rapid variable actions acting in addition to permanent loads)
(iv) influence of the duration of variable actions.

For practical design considerations, it must be remembered that the effect of a slow loading rate is partially accounted for in code provisions in an implicit manner, because design equations have been calibrated on laboratory tests with typical durations between approximately 20 minutes and a couple of hours. This means that a strength decrease of about 6% has already been accounted for and the strength decrease of 15% for the

sustained load effect on structural members according to current codes of practice is fully justified (instead of 20% observed in laboratory tests under uniaxial compression). This also allows reducing the period when the detrimental sustained loading effect is not fully compensated by the favourable strength increase due to continued cement hydration (a couple of weeks after 28 days for a low early age strength class concrete, a couple of months in case of an ordinary concrete, but up to several years in case of concrete with a high early age strength class).

According to the simulation of the simplified load histories, it can be assumed that for loading durations up to one hour, variable loads may be considered as sufficiently rapid to neglect their influence on the compressive strength. The present work also shows that the design provision in SIA 262:2013 for the strength reduction factor should be slightly adapted.

Shear-critical members

To verify whether a shear strength reduction due to sustained loading is necessary also for members without shear reinforcement, two test series with varying loading rates were conducted on slender and squat members. Both series, as well as a comparison with other test series found in the scientific literature, show that there is no marked decrease of the shear strength for longer durations of application of the load or for lower loading rates compared to typical shear tests. This can be explained by the favourable effect of the stress redistribution due to the nonlinear creep associated with sustained loading or slow loading rates. Furthermore, loading rates higher than typical shear tests show a consistent increase of the strength, possibly governed by the favourable geometry of cracking patterns. Based on the present work, for the assessment of shear critical existing structures, it can be assumed that the strength reduction factor η_t for calculating the design value of the shear stress limit according to SIA 262:2013 can be omitted.

So far, very little research has been conducted on the effect of sustained loading on the punching shear resistance, which was not part of this research project. As a consequence, additional considerations are needed before the strength reduction factor for calculating the design value of the shear stress limit in SIA 262:2013 can be removed.

Résumé

Les scenarios de chargement des structures en béton dans lesquels les déformations et les flèches augmentent à cause des effets du fluage sont traditionnellement associés à l'état limite de service, mais ils peuvent aussi avoir un effet à l'état limite ultime. Le présent rapport étudie l'effet du fluage dû à la durée et à la vitesse de chargement sur la résistance ultime des éléments en béton armé.

Il est bien connu qu'une application rapide de la charge a un effet plutôt favorable sur la résistance à la compression du béton. Cependant, si la compression dans le béton à l'état limite ultime dépasse 80% de la résistance, mesurée habituellement lors d'essais d'une durée d'une à deux minutes, les charges soutenues (actions permanentes et variables d'une durée dépassant quelques heures) peuvent avoir un effet défavorable sur la résistance du matériau. La réduction de résistance qui en découle est due au développement de fluage non linéaire accompagné d'un endommagement du matériau (propagation et développement de microfissures). Cette situation peut se produire car le niveau considéré de contrainte dû aux charges soutenues est habituellement plus grand à l'état limite ultime qu'à l'état limite de service du fait que les actions doivent être majorées et la résistance à la compression du béton réduite pour tenir compte des incertitudes sur les actions, la résistance des matériaux, les dimensions ainsi que les modèles de calcul des efforts et des résistances.

Lors du dimensionnement de structures nouvelles, la réduction de la résistance à la compression due à un haut niveau de charge soutenue peut habituellement être négligée car elle est compensée par l'effet bénéfique de l'augmentation de la résistance à la compression due à la poursuite du processus d'hydratation du ciment. En effet, il est bien connu que la résistance du béton continue d'augmenter après l'âge de référence de 28 jours et qu'après quelques mois ou années, la résistance à la compression peut être 20% plus grande qu'à 28 jours. Cependant, le fait de négliger l'effet des charges soutenues peut être du côté de l'insécurité quand :

(i) la charge de dimensionnement maximale est appliquée à un béton relativement jeune, de sorte que la rupture peut se produire avant que le développement de la résistance additionnelle due à la poursuite de l'hydratation du ciment puisse se développer, ou
(ii) la résistance à la compression effective du béton a été déterminée après l'âge de 28 jours, en particulier lors de l'évaluation de structures existantes, de sorte que l'augmentation ultérieure due à la poursuite de l'hydratation du ciment sera faible

Les normes de dimensionnement (en Suisse SIA 262:2013 et EN 1992-1-1/CH-NA:2014) considèrent cet effet par une réduction de la valeur de dimensionnement de la résistance à la compression du béton par un facteur entre 0.85 et 1.0 (voire une augmentation à 1.2 dans le cas de charges appliquées très rapidement). La valeur de 1.0 est typiquement utilisée pour le dimensionnement de nouvelles structures dans lesquelles la situation de dimensionnement déterminante se produit lorsque l'effet de la poursuite de l'hydratation du ciment est suffisant pour compenser la diminution de résistance due aux charges soutenues ou si le niveau de compression de dimensionnement sous charges soutenues ne dépasse pas 85 à 90 % de la résistance à la compression. La valeur inférieure de 0.85 s'applique au cas le plus sévère dans lequel la résistance à la compression est déterminée après plusieurs années ou décennies et lorsque l'effet de chargements rapides est négligeable. Puisque cette réduction s'applique à la résistance à la compression de dimensionnement, elle touche tous les cas dans lesquels la résistance dépend directement de la résistance à la compression du béton (éléments comprimés, zone de compression des éléments fléchis, limite supérieure de la résistance à l'effort tranchant des éléments avec armature transversale, zone d'application de charges concentrées, etc.)

Selon SIA 262:2013 et EN 1992-1-1/CH-NA:2014 (mais pas selon EN 1992-1-1:2004), cette réduction s'applique également à la résistance à l'effort tranchant des éléments sans armature transversale (la résistance à l'effort tranchant est réduite par le même coefficient que la résistance à la compression). Puisque l'augmentation de la résistance à la

compression du béton a une influence plus faible sur la résistance à l'effort tranchant (qui est approximativement proportionnelle à $f_{ck}^{1/3}$), la réduction selon cette approche est particulièrement sévère pour la vérification de structures existantes soumises à l'effort tranchant sans armature transversale, car l'augmentation de la résistance du béton au cours du temps n'est souvent pas suffisante pour compenser la diminution de résistance due aux charges soutenues.

Objectifs de l'étude

Ce projet de recherche a les buts suivants :

(i) étudier la différence entre une charge soutenue constante et une augmentation graduelle (le deuxième cas étant représentatif du processus classique de construction, dans lequel la contrainte maximale due aux charges permanentes est atteinte plusieurs mois après le bétonnage)
(ii) proposer une procédure de vérification pour les histoires de chargement complexes
(iii) clarifier si des durées de chargement de quelques heures peuvent influencer la résistance du béton
(iv) proposer une amélioration des normes de dimensionnement pour la résistance à la compression
(v) vérifier si une réduction de la résistance à l'effort tranchant due aux charges soutenues est nécessaire pour les éléments sans armature transversale

Structure du rapport

Le rapport est structuré en trois parties principales qui traitent des différents objectifs et qui sont précédés de la section 1, qui présente une introduction au rapport et un état de l'art bibliographique.

La première partie principale est traitée dans les sections 2-5 et traite de la résistance à la compression uniaxiale du béton. La section 2 présente une approche analytique permettant d'étudier de façon cohérente la réponse à long terme du béton sous une charge soutenue constante. La section 3 présente les résultats d'une campagne expérimentale sur la réponse du béton à résistance normale sous diverses contraintes et vitesses de chargement, ainsi qu'une validation de l'approche analytique de la section 2. Dans la section 4, l'approche analytique est élargie pour étudier de façon cohérente la réponse à long terme du béton sous divers modèles de charge, en proposant des équations de dimensionnement simples. Enfin, la section 5 traite de plusieurs cas de charge typiques de la pratique de l'ingénierie afin de proposer quelques recommandations de conception.

La deuxième partie de ce rapport est présentée dans les sections 6-7 et traite de la résistance au cisaillement des éléments sans armature transversale. La section 6 présente les résultats d'un programme expérimental sur la réponse des poutres en béton critiques à l'effort tranchant sous différentes charges. La section 7 présente une analyse détaillée des résultats et une discussion de la réponse du béton observée à court et à long terme.

La troisième partie du rapport (section 8) présente l'état actuel des clauses du code suisse du dimensionnement (SIA 262:2013) et de l'annexe nationale suisse à l'Eurocode 2 (EN 1992-1-1 CH NA:2014) qui ont fait l'objet des travaux de recherche des sections précédentes, et propose une discussion et des propositions d'amélioration de ces clauses.

Finalement, la section 9 présente les principales conclusions du rapport.

Effet de charges soutenues constantes

Le comportement différé du béton soumis à une compression uniaxiale est généralement étudié par des essais de fluage classiques où un niveau de contrainte constant est maintenu dans le temps. Dans le cadre de cette étude, deux nouvelles séries d'essais ont été réalisées pour étudier d'autres histoires de chargement à long terme.

La première série d'essais a été réalisée en faisant varier la vitesse de déformation. Pour avoir un béton assez mature et limiter l'influence de l'augmentation de la résistance avec le temps, l'âge du béton lors des essais variait entre 10 et 14 mois. Lors de cette série d'essais les vitesses de déformation allaient de $2 \cdot 10^{-3}$ s^{-1} à $2 \cdot 10^{-9}$ s^{-1} (durée jusqu'à la rupture de 1 seconde à environ 14 jours).

La deuxième série d'essais a été réalisée en faisant varier le taux de contrainte. L'âge du béton à l'essai variait entre 22 et 24 mois. Tout d'abord, une rampe de chargement initiale ($3{,}5 \cdot 10^{-1}$ MPa/s) était appliquée jusqu'à 80 % de la résistance de référence ($\dot{\varepsilon}$ = 0,02 ‰·s^{-1}) le jour du chargement. Ensuite, une deuxième rampe de chargement était appliquée de 5 MPa/s à $1{,}25 \cdot 10^{-5}$ MPa/s (durée jusqu'à la rupture 1 de seconde à environ 5 jours).

Les résultats de la première série d'essais confirment que la charge de rupture est plus faible lorsque la vitesse de déformation diminue (charge appliquée sur de plus longues périodes de temps), avec une variation de la résistance mesurée à la résistance de référence (vitesse de charge standard) au même âge comprise entre 1,10 (vitesses de déformation élevées) et 0,932 (faibles vitesses de déformation). De plus, on peut observer que les déformations longitudinales et transversales à la rupture augmentent habituellement avec la diminution de la vitesse de déformation. Les résultats de la deuxième série montrent également que la résistance est plus faible lorsque la vitesse de chargement diminue. Cette diminution s'accompagne de déformations plus importantes à la rupture dans les directions longitudinale et transversale.

Sur la base d'un modèle mécanique amélioré, qui a été validé par des séries d'essais supplémentaires sur des cylindres en béton non armés chargés en compression, il a été montré que la diminution de résistance, qui peut atteindre environ 20%, est plus déterminante dans le cas d'une charge soutenue que dans le cas de charges augmentant progressivement. De plus, puisque la réduction de résistance due au fluage est liée à un endommagement du matériau, l'âge de chargement joue un rôle important. La réduction de résistance se produit très rapidement si le béton est mis en charge à un très jeune âge (pour un âge du béton de 7 jours lors du chargement, la réduction de 20% est atteinte seulement quelques heures après l'application de la charge), mais très lentement pour de vieux bétons (plusieurs mois de charge soutenue sont nécessaires pour atteindre la réduction de 20% pour un vieux béton). Ces considérations montrent l'importance de l'augmentation de la résistance due à la poursuite de l'hydratation du ciment et de l'âge auquel la résistance du béton est déterminée.

Accumulation de l'endommagement

Bien que la plupart des recherches sur le comportement de fluage non linéaire aient été effectuées sur des éprouvettes soumises à une contrainte constante et maintenue dans le temps, les structures sont rarement soumises à ce type de charge. Les normes ne fournissent généralement pas de méthode générale pour évaluer la réponse des structures en tenant compte de la progression de l'endommagement dans le temps. Le rapport propose une méthodologie simple pour calculer la réponse d'une structure soumise à une histoire de chargement générale, sur la base de la règle de Palmgren-Miner. Cette approche, largement utilisée pour décrire la résistance à la fatigue (p. ex. pour la vérification détaillée à la fatigue selon SIA 262:2013) a pour hypothèse principale que, lorsqu'un matériau est soumis à une amplitude de contrainte donnée, l'incrément de l'endommagement est une fonction linéaire du rapport cyclique $D = (N/N_F)$, où N désigne le nombre de cycles pour une amplitude de contrainte donnée et N_F est le nombre de cycles qui conduit à une rupture pour cette amplitude. De manière analogue, la méthodologie proposée dans ce rapport est basée sur l'hypothèse que, lorsqu'un matériau est soumis à une vitesse de chargement donnée (ou à une quelconque histoire de chargement croissante), l'incrément de l'endommagement est une fonction linéaire du rapport $D = \Delta t(\sigma_i)/\Delta t_F(\sigma_i)$, où $\Delta t(\sigma_i)$ désigne la durée d'application du niveau i de contrainte soutenue σ_i et $\Delta t_F(\sigma_i)$ est la durée qui conduit sur une rupture pour le niveau σ_i de contrainte soutenue.

Histoires de chargement complexes

Pour la vérification de structures avec des histoires de chargement complexes, la méthodologie basée sur l'adaptation de la règle de cumul des dommages de Palmgren-Miner conduit à des prédictions très raisonnables du comportement. Quelques cas simplifiés typiques de la pratique ont été analysés :

(i) variation de contrainte ou de déformation spécifique constante
(ii) augmentation lente et graduelle des contraintes après une augmentation initiale rapide (typique de l'augmentation de contraintes lors de la construction, lorsque des charges permanentes non structurelles sont ajoutées au cours des mois qui suivent une construction rapide)
(iii) augmentation rapide des contraintes après une période de charges soutenues (pour simuler des charges variables rapides agissant en plus des charges permanentes)
(iv) influence de la durée des actions variables

En pratique, il faut se souvenir que l'effet d'un chargement graduel est partiellement déjà implicitement pris en compte dans les normes, car les équations de dimensionnement ont été calibrées sur des essais en laboratoires avec des durées typiques entre 20 minutes et quelques heures. Cela signifie qu'une diminution de la résistance d'environ 6% a déjà été prise en compte et que la diminution de résistance de 15% pour charges soutenues est totalement justifiée (au lieu des 20% observés en laboratoire sur des spécimens en compression uniaxiale). Cela permet aussi de réduire la période requise pour compenser l'effet défavorable des charges soutenues par la poursuite de l'hydratation du ciment (quelques semaines après 28 jours pour un béton avec une classe de résistance initiale basse, quelques mois pour un béton ordinaire, jusqu'à plusieurs années pour une classe de béton à haute résistance initiale).

Selon les simulations des histoires de chargement simplifiées, on peut admettre que pour les durées de chargement jusqu'à une heure, l'effet des charges variables peut être considéré comme suffisamment rapide pour négliger leur influence sur la résistance à la compression. La présente étude montre aussi que les provisions de la SIA 262:2013 pour le facteur de réduction de la résistance devraient être légèrement adaptées.

Capacité de déformation et redistribution des efforts internes

Etant donné que le développement de déformations de fluage non linéaires à des niveaux de contrainte élevés peut conduire à une rupture sous charge soutenue, ce phénomène a traditionnellement été considéré comme défavorable pour le béton. Il convient néanmoins de noter que le développement d'un fluage non linéaire augmente les déformations du matériau à une vitesse plus élevée que dans les régions où le fluage linéaire prévaut. Cette réponse non linéaire en termes de déformations permet des redistributions des efforts internes entre les régions qui se déforment davantage (celles soumises à un niveau élevé de contraintes et qui développent des déformations non linéaires) et celles qui se déforment moins (celles soumises à une réponse linéaire). Cette influence est potentiellement favorable car elle contribue à réduire le niveau de contrainte dans les régions les plus sollicitées.

Cette influence bénéfique peut être observée dans la zone comprimée des éléments en flexion, où les fibres extrêmes comprimées subissent une diminution de contrainte due au fluage non linéaire. Ce phénomène justifie pourquoi il est plus réaliste d'adopter une distribution des contraintes parabolique/constante dans la zone comprimée due à la flexion plutôt que d'adopter une distribution linéaire basée sur la réponse à court terme du matériau.

Cette influence est également significative dans la réponse des colonnes en béton armé avec des effets de second ordre limités. Dans ces cas, régis par la résistance à la compression du béton et par l'armature longitudinale, la déformation supplémentaire due au fluage permet d'augmenter la contribution de l'armature comprimée située à une certaine distance de la fibre la plus comprimée, où le béton s'écraserait dans des conditions de charge rapide. Ainsi, si des taux de charge lents ou des charges soutenues peuvent

être préjudiciables à la résistance des colonnes avec un faible taux d'armature longitudinal (faible contribution de l'armature à la résistance globale), ils peuvent être bénéfiques pour les colonnes dans lesquelles le taux d'armature est élevé (contribution supplémentaire de l'armature compensant la diminution de la contribution du béton).

Eléments critiques à l'effort tranchant

Deux séries d'essais avec des taux d'augmentation de la charge variables ont été conduits sur des éléments élancés et trapus dans le but de déterminer si une réduction de la résistance à l'effort tranchant sous charges soutenues est également nécessaire. Un total de 16 poutres ont été testées en deux séries, la première comprenant huit poutres élancées (rapport entre la portée de cisaillement et la hauteur utile a/d = 3,5) et la seconde comprenant huit poutres trapues (a/d = 1,0). Le processus de rupture et le développement de la fissuration ont été suivis en détail au moyen de mesures de corrélation numérique d'images (DIC, Digital Image Correlation).

Les poutres avaient une section rectangulaire ($b \times h$ = 250 × 600 mm) et un taux d'armature de flexion ρ = 1,33%. L'armature de flexion, dont la hauteur utile était de 556 mm était constituée de 3 barres Ø 28 mm à haute résistance (f_y = 713 MPa). Il n'y avait pas d'armature d'effort tranchant. Le béton avait une résistance moyenne à la compression à 28 jours $f_{c,28}$ = 29 MPa (mesurée sur cylindre $Ø \times h$ = 160 × 320 mm).

Les poutres élancées ont été testées en porte-à-faux alors que les poutres trapues ont été testées comme des poutres simples. Deux schémas de chargement ont été utilisés, le premier correspondait à une vitesse de déplacement constante du point d''introduction de la charge jusqu'à la rupture. Le deuxième consistait en un préchargement avec une vitesse de déplacement constante jusqu'à un certain niveau de charge, suivi d'une augmentation de la charge à vitesse constante par la suite. Pour les poutres élancées, le changement de condition de charge a été appliqué au moment où les fissures de flexion ont commencé à se développer de manière quasi horizontale au-dessus de l'axe neutre. Pour les poutres trapues, le changement de condition de charge a été appliqué dès que la fissure diagonale s'est développée. Pour des vitesses de chargement élevés, la rupture s'est produite en quelques secondes (temps de charge minimal 3,88 secondes). Bien que ce temps soit court, les forces d'inertie n'ont pas d'influence sur les résultats.

Les résultats de ces deux séries, ainsi que la comparaison avec d'autres séries trouvées dans la littérature scientifique, montrent qu'il n'y a pas de diminution marquée de la résistance à l'effort tranchant pour des durées d'application de la charge longues ni pour des vitesses de chargement plus faibles que celles habituellement utilisées lors des essais en laboratoire. Ceci peut s'expliquer par l'effet favorable des redistributions des efforts internes dues au fluage non linéaire lié aux charges soutenues ou aux vitesses de chargement lentes. De plus, des vitesses de chargement plus rapides qu'utilisées habituellement montrent une augmentation systématique de la résistance, potentiellement gouvernée par la géométrie favorable des fissures. Sur la base de la présente étude, pour l'évaluation de structures existantes qui sont critiques à l'effort tranchant, le facteur de réduction de la résistance η_t pour le calcul de la valeur de dimensionnement contrainte de cisaillement limite de la SIA 262:2013 peut être omis.

Conclusions

Les investigations effectuées dans ce rapport permettent de mieux comprendre le phénomène de résistance du béton en fonction du temps sous différentes histoires de chargement allant des actions rapides aux actions soutenues. Ce phénomène est étudié à la fois sur des spécimens en compression uniaxiale et sur des éléments en béton armé critiques à l'effort tranchant.

Compression uniaxiale

Sur la base d'une campagne expérimentale de compression uniaxiale avec des vitesses de déformation et de contrainte variables, les conclusions suivantes ont été tirées sur le comportement du béton en fonction du temps due à un haut niveau de charge soutenue :

1. La résistance à la compression du béton diminue sous l'effet d'une charge soutenue ou d'une faible vitesse de déformation ou de contrainte. Ceci est un effet préjudiciable pour les éléments soumis à un haut niveau de charge soutenue
2. La déformation à la rupture augmente pour de hauts niveaux de charge soutenue. Cela peut être un effet favorable pour les systèmes hyperstatiques, où des redistributions des efforts sont possibles et peuvent en outre activer l'armature en compression
3. La rupture sous charge soutenue est régie par la capacité de déformation inélastique du béton. Lorsque la déformation inélastique développée dans le béton est égale à la capacité de déformation inélastique, la rupture se produit par coalescence progressive des fissures
4. La capacité de déformation inélastique peut être estimée comme étant la différence entre les contraintes instantanées post-pic et pré-pic pour un niveau de contrainte donné. Cela permet de définir un critère de rupture pour la capacité de déformation inélastique disponible

Le développement de déformations de fluage linéaire et non linéaire pouvant conduire à une rupture sous charge soutenue a été étudié de manière analytique, en appliquant les modèles de fluage existants et un ensemble d'hypothèses inspirées du comportement mécanique du béton. Ce travail analytique a abouti aux conclusions suivantes :

5. L'hypothèse d'affinité entre les déformations de fluage linéaire et non linéaire permet de formuler une relation simple et efficace pour estimer l'évolution des déformations inélastiques dans le béton pour une histoire de chargement donné. Il explique en plus de manière explicite le développement des déformations de fluage tertiaire
6. Le calcul analytique de la rupture sous des scénarios de chargement soutenu à long terme peut être effectué par intersection entre la relation définissant le développement de déformations inélastiques pour une histoire de chargement donnée (basé sur l'hypothèse d'affinité) et le critère de rupture défini par la capacité de déformation inélastique de béton. Cette approche permet d'estimer de manière cohérente la résistance et la déformation associée pour différentes histoires de chargement, comme le confirment les résultats des tests sous charge soutenue ainsi que sous des vitesses de contrainte et de déformation variables
7. Sur la base du modèle théorique, certains effets peuvent être clairement reproduits et étudiés, comme par exemple :
    a. Des scénarios de chargement constant soutenu dans le temps conduisent plus rapidement à des ruptures avec des niveaux de contrainte plus faibles comparés à des vitesses de contrainte ou de déformation variables (le béton est soumis à des niveaux de contrainte plus élevés depuis le début du processus de chargement)
    b. Le vieillissement du béton (augmentation de la résistance du béton dans le temps) est un phénomène déterminant, car il compense l'endommagement du matériau. Pour les bétons soumis à une charge soutenue au jeune âge, la rupture ne peut se produire qu'après quelques heures ou quelques jours, car l'augmentation de la résistance dans le temps le compensera, alors que pour les bétons chargés à un âge plus avancé, une rupture à long terme peut se produire plusieurs années après (car il n'y a presque pas de réserve d'augmentation de résistance)

Effort tranchant

Sur la base d'une campagne expérimentale sur des éléments élancés et trapus critiques à l'effort tranchant et sans armature transversale soumises à des vitesses d'augmentation de la charge variables, il est possible de tirer les conclusions suivantes sur la résistance au cisaillement des éléments en béton armé en fonction du temps :

1. Les essais effectués ne montrent pas de diminution marquée de la résistance à l'effort tranchant pour des durées d'application plus longues de la charge ou pour de faibles vitesses d'augmentation de la charge par rapport aux essais d'effort tranchant typiques
2. Pour des vitesses d'augmentation de la charge supérieures aux essais d'effort tranchant typiques (associés à des ruptures au bout de quelques secondes), une augmentation relativement constante de la résistance peut être observée pour les échantillons élancés. Une analyse des modes de transmission de l'effort tranchant montre que cela peut être justifié par une géométrie plus favorable de la fissure critique en cas de vitesses d'augmentation de la charge élevées. Les résultats ne sont pas aussi clairs pour les éléments trapus, mais la réponse est similaire
3. Pour les éléments élancés, la résistance à l'effort tranchant relativement constante pour des niveaux de charge soutenue élevés peut être justifiée par la capacité potentielle de redistribution et de confinement du béton entourant la bielle de compression portant l'effort tranchant
4. Pour les éléments élancés, la sensibilité limitée de la résistance à l'effort tranchant aux faibles vitesses d'augmentation de la charge peut être justifiée par la forme et les ouvertures similaires de la fissure critique ainsi que par l'ouverture et le glissement relativement rapides (mais stables) de la fissure critique proche à la rupture. Cela permet d'engager de manière significative l'engrènement d'agrégats, le mode dominant de transmission d'effort tranchant dans ces éléments, d'une manière relativement rapide (cette contribution est donc peu influencée par la durée totale d'application de la charge).

Conception

Les travaux expérimentaux et analytiques de ce rapport conduisent à une approche simplifiée pour les ingénieurs de la pratique. Les points principaux sont :

1. Le phénomène de fluage du béton doit être pris en compte à la fois pour les états limites de service (ELS) et les états limites ultimes (ELU)
2. Des expressions simples peuvent être dérivées pour caractériser la charge de rupture du béton sous charge soutenue. La combinaison de ces expressions avec l'approche de Palmgren-Miner fournit un moyen pratique de quantifier l'accumulation de dommages et d'estimer la charge et le temps de rupture
3. Il a pu être confirmé que l'effet bénéfique d'une hydratation continue du ciment compense généralement l'effet défavorable d'une charge soutenue. Cela est vrai à condition que la résistance du béton soit déterminée à 28 jours et que l'ELU ait lieu après une période suffisamment longue. Si la résistance du béton est déterminée après 28 jours (particulièrement utile pour l'évaluation des structures existantes), une réduction de la résistance du béton tenant compte d'une charge élevée soutenue est nécessaire
4. Pour un niveau donné de contrainte totale, une combinaison d'actions permanentes et une action variable rapide est moins défavorable pour la résistance à la compression du béton qu'une action permanente complète. Ce phénomène peut être décrit par de simples expressions aboutissant à une interpolation linéaire entre la réponse d'un membre amené à la ruine sous une charge constante et le cas où des effets de charge permanents peuvent être négligés. En outre, dans les cas où l'action variable est maintenue sur une période donnée, une approche similaire peut être suivie
5. Bien que pour le comportement du matériau béton une diminution de la résistance ait été largement documentée et vérifiée, il semblerait qu'une réduction de la résistance à l'effort tranchant pour les membres critiques n'est pas nécessaire pour les charges élevées maintenues pendant de longues périodes.

Jusqu’ici, il y a eu très peu de recherche sur l’effet des charges soutenues sur la résistance au poinçonnement, qui ne faisait pas partie de ce projet de recherche. En conséquence, des considérations supplémentaires sont requises avant de pouvoir supprimer le facteur de réduction de la résistance pour le calcul de la valeur de dimensionnement de la contrainte limite de cisaillement de la SIA 262:2013.

Zusammenfassung

Dauerlastszenarien auf Stahlbetonkonstruktionen, die mit erhöhten Verformungen aufgrund von Kriecheffekten des Betons resultieren, werden traditionell im Zusammenhang mit dem Grenzzustand der Gebrauchstauglichkeit betrachtet; jedoch können sie sich auch im Grenzzustand der Tragfähigkeit auswirken. In diesem Bericht wird der Einfluss der Belastungsdauer und -geschwindigkeit auf den Widerstand von Betontragwerken untersucht.

Es ist allgemein bekannt, dass ein schnelles Aufbringen der Last sich auf die Betondruckfestigkeit eher günstig auswirkt. Andererseits, wenn die Betondruckspannung im Grenzzustand der Tragfähigkeit höher als etwa 80% der Nenndruckfestigkeit ist (in der Regel ermittelt mittels einachsigem Druckversuch mit einer Belastungsdauer von 1-2 Minuten), können Dauerbelastungen einen negativen Einfluss auf die Materialfestigkeit aufweisen (als Dauerbelastungen werden ständige Einwirkungen und veränderliche Einwirkungen mit einer Dauer länger als einige Stunden betrachtet). Dieser Festigkeitsabfall ist auf die Entwicklung des nichtlinearen Kriechens zurückzuführen, die mit einer Materialschädigung zusammenhängt (Öffnung und Fortpflanzung von Mikrorissen). Dies kann der Fall sein, weil das Betonspannungsniveau aufgrund der Dauerbelastung im Grenzzustand der Tragfähigkeit normalerweise höher ist als im Grenzzustand der Gebrauchstauglichkeit, da die Lasteinwirkungen erhöht werden und die Betondruckfestigkeit reduziert wird, um alle Unsicherheiten hinsichtlich Lasteinwirkungen, Materialfestigkeit, Abmessungen, Schnittgrössenberechnung und Berechnungsmodelle zu berücksichtigen.

Beim Entwurf neuer Tragwerke kann der Druckfestigkeitsabfall von Beton aufgrund der hohen Dauerbelastung meist vernachlässigt werden, da dieser negative Effekt durch die vorteilhafte Festigkeitszunahme infolge kontinuierlicher Zementhydratation kompensiert wird. Es ist bekannt, dass die Betonfestigkeit auch nach dem Bezugsalter von 28 Tagen weiter ansteigt und nach einigen Monaten / Jahren um zusätzliche 20% ansteigen kann. Die Vernachlässigung des Dauerlasteffekts kann jedoch auf der unsicheren Seite liegen, wenn:

(i) die Belastungssituation mit der maximalen Bemessungsdauerlast im relativ jungen Betonalter eintritt (bevor sich die Festigkeitszunahme infolge kontinuierlicher Zementhydratation entwickeln kann)
(ii) die Betondruckfestigkeit in einem Betonalter höher als 28 Tage ermittelt wird (dies ist insbesondere der Fall bei der Bewertung von bestehenden Bauwerken, bei denen die Druckfestigkeit des Betons oft in einem Alter von einigen Jahren / Jahrzehnten ermittelt wird und keine signifikante Zusatzsteigerung der Festigkeit aufgrund der kontinuierlichen Zementhydratation zu erwarten ist).

In den Normen (in der Schweiz SIA 262:2013 und EN 1992-1-1/CH-NA:2014) wird dieser Effekt durch eine Abminderung des Bemessungswertes der Betondruckfestigkeit um einen Faktor zwischen 0,85 und 1,0 berücksichtigt (oder sogar eine Erhöhung um 1,2 für sehr schnelle Lastaufbringung). Dieser Faktor wird in der Regel beim Entwurf von neuen Tragwerken gleich 1,0 gesetzt, da in diesem Fall zu erwarten ist, dass die massgebliche Belastungssituation erst in einem Alter eintritt, wo die Zementhydratation ausreichend fortgeschritten ist um den Festigkeitsabfall infolge Dauerbelastung zu kompensieren, oder wenn die Betonspannung infolge Dauerlast im Bemessungszustand den Wert von 85-90% der Druckfestigkeit nicht überschreitet. Der niedrigere Wert von 0,85 gilt im Extremfall, wo die Betonfestigkeit nach einigen Jahren / Jahrzehnten ermittelt wird und der Beitrag von kurzen veränderlichen Einwirkungen vernachlässigbar klein ist. Da diese Abminderung sich auf den Bemessungswert der Betondruckfestigkeit bezieht, trifft dieser Effekt in allen Fällen zu, wo der Widerstand direkt von der Betondruckfestigkeit abhängt (Druckglieder, Biegedruckzonen, obere Grenze des Querkraftwiderstands von Bauteilen mit Schubbewehrung, örtliche Pressung auf Bauteilen etc.).

Gemäss SIA 262:2013 und EN 1992-1-1/CH-NA:2014 (jedoch nicht EN 1992-1-1:2004)

trifft diese Abminderung auch auf den Querkraftwiderstand von Bauteilen ohne Schubbewehrung zu (die kritische Schubspannung ist um den gleichen Faktor wie die Betondruckfestigkeit abgemindert). Da die Betonfestigkeitszunahme infolge kontinuierlicher Zementhydratation einen geringeren Einfluss auf den Querkraftwiderstand hat (der Querkraftwiderstand ist näherungsweise proportional zu $f_{ck}^{1/3}$), ist diese Abminderung nach dem derzeitigen Ansatz bei der Bewertung von bestehenden Bauwerken besonders problematisch, da die Festigkeitszunahme nach einigen Jahrzehnten oft nicht ausreicht, um den Festigkeitsabfall infolge Dauerlast zu kompensieren.

Hauptziele

Im vorliegenden Forschungsprojekt wurden mehrere Ziele verfolgt:

(i) Untersuchung des Unterschieds zwischen konstanten Dauerlasten und langsamen Belastungsgeschwindingkeiten (Letztere sind typisch für den Bauprozess, wo die maximale Betonspannung infolge von ständigen Einwirkungen nach einigen Monaten erreicht werden kann)
(ii) Vorschlag eines Verifikationsverfahren für komplexe Belastungsgeschichten
(iii) Klarstellung ob veränderliche Einwirkungen mit einer Dauer von Stunden/Tagen die Betonfestigkeit beeinflussen
(iv) eventueller Vorschlag einer Verbesserung der geltenden Normen im Bezug auf die Bemessungsdruckfestigkeit
(v) Klarstellung ob eine Abminderung des Querkraftwiderstands infolge Dauerbelastung auch für Bauteile ohne Schubbewehrung erforderlich ist.

Auswirkung konstanter Dauerlasten

Anhand von einem verbesserten mechanischen Modell, das anhand mehrerer Testserien an einachsigen Druckproben validiert wurde, konnte gezeigt werden, dass der Festigkeitsabfall infolge konstanter Dauerbelastung stärker ist als bei einer Lastaufbringung mittels langsamen Belastungsraten (im ersten Fall beträgt der Langzeitfestigkeitsabfall etwa 20%). Da der Festigkeitsabfall mit Kriechen und Materialschädigung verbunden ist, spielt das Belastungsalter eine wichtige Rolle. Wenn der Beton im jungen Alter belastet wird, tritt der Festigkeitsabfall rasch auf, (Festigkeitsabfall von etwa 20% in nur wenigen Stunden bei einer Dauerlastaufbringung im Alter von 7 Tagen), während bei einer Lastaufbringung im späten Betonalter die Festigkeit eher langsam abfällt (für alte Betone, ist eine Dauerbelastung von mehreren Monaten erforderlich um einen Festigkeitsabfall von 20% zu erreichen). Die vorherigen Betrachtungen zeigen die grosse Bedeutung der Festigkeitszunahme aufgrund der kontinuierlichen Zementhydratation (die möglicherweise den Dauerlasteffekt kompensiert) sowie des Bezugsalters bei der Ermittlung der Betonfestigkeit.

Darüber hinaus zeigen sowohl das mechanische Modell als auch die Ergebnisse der durchgeführten Laborexperimente, dass der nachteilige Druckfestigkeitsabfall infolge Dauerbelastung bzw. langsamer Belastungsgeschwindingkeit mit einer grösseren Verformungsfähigkeit beim Versagen verbunden ist. Der letztere Effekt kann eher vorteilhaft sein und möglicherweise die obengenannten nachteiligen Effekte kompensieren, da eine bessere Umlagerung der inneren Kräfte ermöglicht wird, indem typischerweise Spannungskonzentrationen im Beton (zum Beispiel in der Biegedruckzone) reduziert werden und eine erhöhte Aktivierung der Druckbewehrung vor dem Versagen des Betons ermöglicht wird.

Komplexe Belastungsgeschichten

Für eine detaillierte Bewertung von Bauwerken mit komplexer Belastungsgeschichte wurde der Ansatz von Palmgren-Miner angepasst (diese Methode wird auch für einen detaillierten Ermüdungsnachweis nach SIA 262:2013 verwendet), was zu konsequenten Ergebnissen führt. Einige vereinfachte praktische Belastungsfälle wurden analysiert:

(i) Variation von konstanten Spannungsraten und konstanten Dehnungsraten
(ii) konstante langsame Spannungsrate nach einem schnellen anfänglichen Spannungsanstieg (typisch für eine langsame Erhöhung des Gewichts von nichttragenden Elementen im Laufe einiger Monate nach einem schnellen Bauprozess)
(iii) ein schneller Spannungsanstieg nach einer Dauerbelastung (typisch für schnelle Einwirkungen welche zusätzlich zu ständigen Einwirkungen agieren)
(iv) der Einfluss von veränderlichen Einwirkungen mit unterschiedlicher Belastungsdauer.

Beim Entwerfen von Bauwerken in der Praxis muss berücksichtigt werden, dass die Auswirkungen einer langsamen Belastungsgeschwindigkeit bereits implizit in den Normenbestimmungen teilweise berücksichtigt sind. Dies ist auf die Tatsache zurückzuführen, dass die Bemessungsgleichungen anhand von Labortests mit typischer Belastungsdauer zwischen etwa 20 Minuten und einigen Stunden kalibriert wurden. Dies bedeutet, dass eine Festigkeitsabminderung von etwa 6% bereits implizit berücksichtigt wurde und somit eine Festigkeitsabminderung von 15% für die dauerhafte Belastung der tragenden Bauteile gemäss aktueller Norm vollständig begründet ist (anstelle der 20%, die in Labortests auf uniaxialen Druckproben beobachtet wurden). Dies ermöglicht es auch, den Zeitraum zu verkürzen, während dem der nachteilige Dauerbelastungseffekt nicht vollständig durch die kontinuierliche Zementhydratation kompensiert wird (dieser Zeitraum beträgt einige Wochen nach den 28 Tagen bei einem Beton mit langsam erhärtendem Zement bis zu einigen Monaten bei einem Beton mit normal erhärtendem Zement, aber theoretisch mehrere Jahre bei einem Beton mit schnell erhärtendem Zement).

Gemäss einer Simulation mit vereinfachten Belastungsgeschichten kann davon ausgegangen werden, dass veränderliche Einwirkungen mit einer Belastungsdauer von bis zu einer Stunde als ausreichend schnell angesehen werden können um ihren Einfluss auf die Druckfestigkeit vernachlässigen zu können. Die vorliegende Arbeit zeigt auch, dass die Bemessungsbestimmungen für den Faktor für Druckfestigkeitsabminderung der SIA 262:2013 leicht angepasst werden sollten.

Querkraftkritische Bauteile

Um zu überprüfen, ob eine Abminderung des Querkraftwiderstands infolge Dauerbelastung auch für Bauteile ohne Schubbewehrung erforderlich ist, wurden zwei Versuchsserien an schlanken bzw. gedrungenen Bauteilen mit unterschiedlichen Belastungsraten durchgeführt. Die Ergebnisse beider Testserien sowie ein Vergleich mit anderen in der wissenschaftlichen Literatur gefundenen Versuchen zeigen, dass der Querkraftwiderstand bei höheren Belastungsdauern oder bei niedrigeren Belastungsraten im Vergleich zu typischen Querkraftversuchen nicht merklich abfällt. Dies lässt sich durch den günstigen Effekt der Spannungsumlagerung aufgrund des nichtlinearen Kriechens erklären, der mit Dauerbelastung oder langsamen Belastungsgeschwindigkeiten einhergeht. Darüber hinaus zeigen Querkraftversuche mit höheren Belastungsraten (mit Bezug auf typische Querkraftversuche) eine konsistente Widerstandserhöhung, möglicherweise bedingt durch die günstigere Geometrie der Rissbildung. Aufgrund der vorliegenden Arbeit kann davon ausgegangen werden, dass beim Nachweis bestehender querkraftkritischer Bauteile auf den η_t-Abminderungsfaktor der Schubspannungsgrenze nach SIA 262:2013 verzichtet werden kann.

Die Untersuchung des Einflusses einer Dauerbelastung auf den Durchstanzwiderstand war kein Gegenstand dieses Forschungsvorhabens. Darüber hinaus wurde auf diesem Gebiet bisher nur sehr wenig geforscht. Aus diesen Gründen sind zusätzliche Erwägungen erforderlich, bevor auf den Festigkeitsabminderungsfaktor zur Berechnung des Bemessungswerts der Schubspannungsgrenze nach SIA 262:2013 verzichtet werden kann.

1 Introduction

In the current state of knowledge, it is well established that concrete is a material sensitive to the loading rate and the duration of load application. While high levels of sustained loads may have detrimental influence on the compressive strength of concrete, rapid application of the load is shown to have a potentially beneficial influence. This fact is significant in the design and assessment of concrete structures, which may experience load actions of different duration throughout their lifetime. Typical load durations on civil engineering structures can vary from rapid loads typical for accidental actions, over short variable loads (typically live load on bridges) to permanent loads sustained over longer periods of time (possibly the case of dead loads on large bridges and soil pressure on retaining structures and cut-and-cover tunnels). Hence, understanding the influence of load actions of different nature and duration on the strength of the material is instrumental for practicing engineers.

1.1 Concrete strength under sustained loads

As already observed since the early developments of concrete, the compressive strength increases with time due to the continued cement hydration [1] (see red curve in *Fig. 1*a). For this reason, already the first standards for reinforced concrete defined a concrete age (t_{ref}) to characterize the compressive strength of concrete and its associated mechanical properties (for instance 28 days according to the Swiss Code of 1903 [2], 90 days according to the French Code of 1906 and 42 days according to the Austrian Code of 1907, refer to Mörsch [3]). The reference time was in these codes in accordance to the rules related to the age at which removal of the scaffolding was allowed (which were usually lower than t_{ref}, see for instance the Swiss Code of 1903 [2]). This approach already implicitly considered that additional permanent loads and variable actions are relevant for the structural performance in addition to self-weight, and that they are usually applied at a time larger than t_{ref}, see blue curve in *Fig. 1*a.

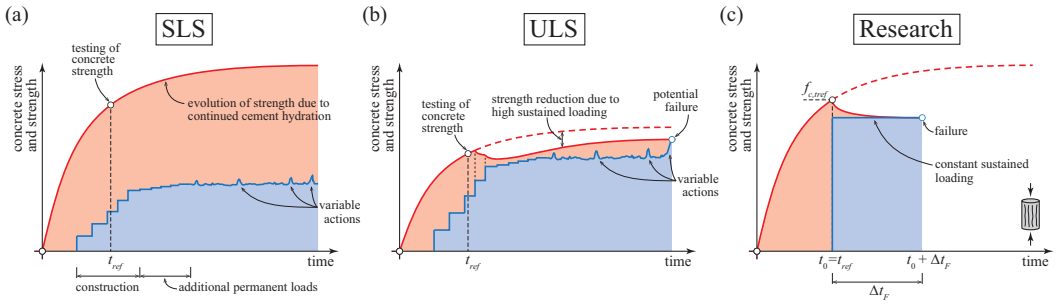

Fig. 1 Stress (blue) and strength (red) evolutions in time: (a) characteristic values for typical structures; (b) design values at Ultimate Limit State (ULS); and (c) typical tests investigating the effect of sustained load

When assessing the structural performance at ultimate limit state, the uncertainties related to actions (higher stresses than expected) and the uncertainties related to the concrete strength (including the difference between the strength of the specimens for concrete testing and the local in-situ strength) have to be accounted for. This can be done by considering characteristic values for the actions and material properties and by applying pertinent partial safety factors (as performed in *Fig. 1*b with respect to *Fig. 1*a). This means that the verification is performed using design values for the internal actions and resistances. It can be noted that, in this frame of ultimate limit state analysis (which is a potential real situation, although with a very small probability of occurrence) the acting stresses may be relatively high compared to the material resistance [4], which may be detrimental for the material strength [5].

This phenomenon (see *Fig. 1*b) was already observed in the 1950s by the pioneer works of Shank [6] and later investigated in detail by Rüsch [7]–[9]. According to Rüsch [8], when

a high level of stress is applied to the concrete at a certain age (t_0), the strength of the material does not necessarily increase with time (as for unloaded specimens due to the continued cement hydration), but it may reduce. This occurs normally for stress levels above approximately 75%-80% of the strength of the material at the time of loading ($f_{c,t0}$, tested under standard conditions leading to failure in about 1-2 minutes according for instance to ISO 1920-4:2005 [10]). This fact is sketched in *Fig. 1*c for a concrete specimen subjected to a constant level of high stress (but below the resistance of the concrete at the time of loading, $f_{c,t0}$), showing that failure occurs after some time of application of the action. According to these observations, Rüsch [8] established the concept of sustained load strength, that he defined as the maximum stress level at which concrete can be permanently loaded without failure.

For the case of actual structures, the detrimental influence of high levels of sustained load is only critical after a significant fraction of the permanent load has been applied to the structure. This can be seen in *Fig. 1*b, by the decay in the red curve (material resistance) for high levels of permanent load. Thereafter, the strength may increase again due to the continued cement hydration, but in any case, the strength is reduced with respect to that of an unloaded material (dashed red curve in *Fig. 1*b). Failure will eventually occur when the action equals the resistance, which may take place at different moments depending on the acting variable actions and material decay on the strength (as already observed by Rüsch [8] and others [11]–[13], see *Fig. 1*b).

Due to its practical relevance, the topic of the long-term strength of concrete structures has attracted many research efforts after the works of Rüsch, with a number of investigations conducted both for normal strength concrete [11], [13]–[22] and high strength concrete [22]–[27]. The same phenomenon has been also investigated for the tensile and flexural behaviour under sustained load (see for instance references [28]–[30]). Within this frame, most experimental evidence with respect to the effect of sustained loading on the compressive strength has been obtained by considering a constant stress level applied to the member (refer to the load pattern shown in *Fig. 1*c). However, some experimental programmes and researches have also reported this phenomenon for low loading rates [14], [31], [32]. Several authors have also investigated the origin of the phenomenon, relating the delayed failure of concrete to microcracking and to material damage development and progression [14], [19], [33], [34]. According to these research works, if the level of sustained stress is higher than the threshold at which microcrack propagation is likely to occur ($\sigma_c/f_c > 0.4$, typically associated to the development of nonlinear creep strains), delayed damage may develop in the material. At elevated sustained stress levels ($\sigma_c/f_c > 0.75$, corresponding to Rüsch's sustained load strength), a significant amount of delayed damage may develop, yielding to unstable crack propagation over time and potentially to material failure.

For moderate levels of permanent load (σ_c between approximately $0.4 \cdot f_c$ and $0.6 \cdot f_c$) applied to the material, a small beneficial influence of sustained levels of stress has been observed on the material strength[19]. This fact, confirmed experimentally [35], has been attributed to the internal stress redistributions occurring in the material [19] (reducing stress concentrations; alternative explanations of this phenomenon can be consulted elsewhere [36]), but is usually neglected in practice.

With respect to codes, the approach for the design of new structures usually considers that the detrimental effect of sustained loads on the concrete strength can be compensated by the increase of strength due to continued cement hydration after the reference time t_{ref}. This is for instance the approach followed by SIA 262:2013 [37], MC2010 [38] and EN 1992-1-1:2004 [39] when the reference strength is considered at a time t_{ref} equal to 28 days. However, when the reference time for evaluation of the compressive strength is higher ($t_{ref} > 28$ days), the uniaxial compressive strength has to be reduced accordingly to account for the effects of sustained loading (refer for instance to coefficient η_t in SIA 262:2013 [37] or k_t in EN 1992-1-1:2004 [39]). This is a typical situation for the assessment of existing structures, where the concrete strength can be further updated after long periods of service of the structure and almost no strength increase due to cement hydration can be expected (this also presumes that concrete has suffered no degradation processes such as alkali-aggregate reaction, sulphate attack or freeze-thaw cycles).

However, when a general loading case is considered (refer for instance to *Fig. 1*b) there is usually little or no guidance on how to determine in a simple and consistent manner the uniaxial compressive strength of concrete.

In this context, this report presents a simple analytical approach to evaluate the compressive strength of concrete when subjected to long-term actions and accounting for potentially high levels of stress. The topic is analysed by using the theoretical framework of Tasevski et al. [13], which provides a model to assess the material damage and its influence both in terms of strength and deformation capacity. The model is consistently verified with test results considering different loading patterns (sustained stress, stress rates and strain rates) and formulated in a design-friendly manner. On that basis, several practical design situations are analysed, deriving a number of practical recommendations.

1.2 Shear resistance of members without transverse reinforcement

Since the early developments of concrete, significant research efforts have been devoted to the topic of sustained loading and loading rates, mostly in terms of the compressive and tensile behaviour of concrete. Yet there exists still very little knowledge on the influence of these phenomena on the shear strength of concrete members. This situation might be explained by the fact that sustained loading has traditionally been associated to the serviceability limit state (SLS) of concrete structures, and thus mostly related to the linear response of the material [40], [41]. In terms of experimental evidence, the first comprehensive test series dedicated to this issue was performed by Sarkhosh et al. [42], [43]. This experimental programme was performed on shear critical slender beams (a/d = 3.0) under sustained loading, focusing on the investigation of the time-dependent crack growth. The study comprised 42 simply supported beams without shear reinforcement, with 18 specimens subjected to high levels of sustained loads (87% - 95% of the average short-term shear capacity). Two of these beams failed under sustained loading (one after 2.5 hours and another after 44 hours). The beams that did not fail under sustained loading were eventually reloaded to failure, and showed in general a higher resistance than the reference beams. The results of Sarkosh are presented in *Fig. 2*a-b and compared to the prediction of the Critical Shear Crack Theory (CSCT, basis of current SIA 262:2013 [37]) formulated according to [44] for reference loading rates (failures occurring for loads applied during a period of 5 minutes to 2 hours). For this analysis, the equivalent aggregate size d_g is calculated according to [45] and the material strength is considered at the time of failure (details on the fundamentals of the theory can be found elsewhere [46]). The results show no significant decay on the strength and most specimens required to be reloaded to reach failure (failing at higher load levels than the reference specimens).

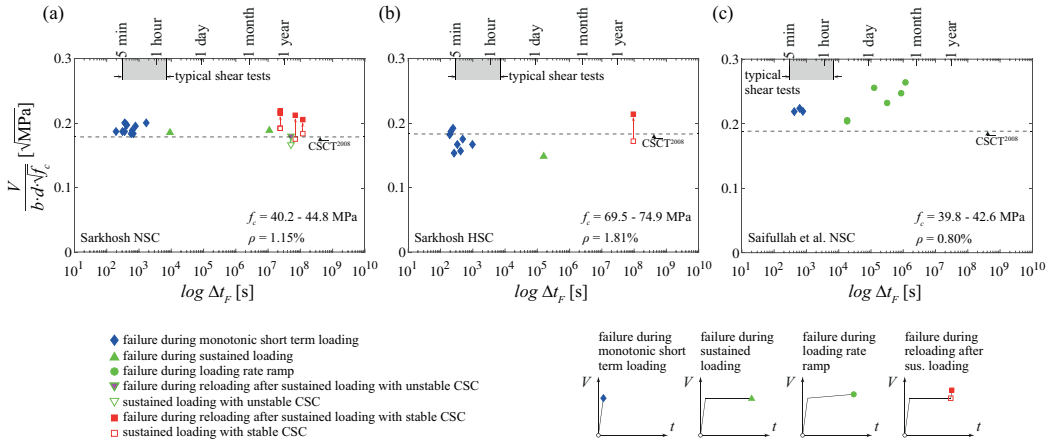

Fig. 2 Tests from literature on the influence of high levels of loading on the shear strength and comparison with the CSCT^{2008} [44]: (a-b) Sarkhosh [42]; and (c) Saifullah et al. [47]

Another recent study on the effects of sustained loading on the shear strength of slender concrete beams (a/d = 3.0) has been performed by Saifullah et al. [47]. In this series, the influence of low loading rates was investigated, comprising loading rates 100 to 1000 times lower than the reference loading rate (typically requiring about an hour to reach the shear failure). Three beams were tested under reference loading rate and 6 beams under low loading rates. A general increase of midspan deflection, crack opening and compressive strain at the top fibre with increasing time to failure was observed, as well as an overall increase in the ultimate shear capacity (yet the results were somewhat scattered, see *Fig. 2*c).

With respect to squat members, where arching action can be governing and thus a different shear response can be expected [48], [49], there is still a lack of experimental studies. It can however be cited the works of Maekawa et al. [50] to monitor the long-term deformation of underground box culverts, with the potential detection of a delayed shear failure under sustained soil pressure (confirmed by inspection of boreholes showing the existence of a well propagated diagonal shear crack). In a further numerical study on squat beams (a/d = 1.0 – 2.4), Bugalia and Maekawa [51] showed that arching action and direct strut action can potentially be influenced by sustained loading.

The scant knowledge in the field of shear under sustained loading is also reflected in codes of practice, where there is no clear consensus on the consideration of this effect. While ACI 318-14 [52], Eurocode 2 [39] and Model Code 2010 [38] acknowledge the effect of sustained loading on the compressive strength of concrete (which is considered in an implicit or explicit manner or explicitly neglected since it can be compensated by the strength increase due to continuous cement hydration [38]), no clear reference is provided in the shear section for slender members. However, for squat members verified with strut-and-tie models, this effect is normally implicitly accounted for in the strength of the struts. Other codes, as for instance the current Swiss code for concrete structures SIA 262:2013 [37], account for long-term effects both for slender and squat members when the concrete strength is evaluated at ages older than 28 days or for early loading times. According to SIA 262:2013, a reduction on shear strength for high levels of sustained loading shall be introduced, in a similar manner as for the compressive resistance of the concrete.

Within this context, this report presents new experimental data on concrete members without shear reinforcement subjected to high levels of sustained loading. The experimental programme consists of two series, one dedicated to slender members (a/d = 3.5) and the other to squat ones (a/d = 1.0) in order to understand the potential differences in the governing shear transfer actions. The phenomenon is investigated by means of low loading rates and by performing refined experimental measurements to track the cracking patterns and associated kinematics. On this basis, the contribution of the different shear transfer actions is investigated and a discussion is performed on the need for a reduction on the shear strength accounting for the duration of the loading. For comparison purposes, some specimens are also tested under relatively high loading rates and their results are also discussed.

1.3 Objectives

The present research project has two main objectives. The first one is to better understand the phenomenon of time-dependence of the uniaxial compressive strength of concrete under the influence of different load durations and rates. In scope of this objective, several points are addressed:

- To enrich the existing experimental results for sustained loads and strain rates and to introduce tests with stress rates at high stress levels
- To verify and to improve the existing models for non-linear creep strain prediction;
- To establish a general failure criterion for uniaxial compression of concrete under various loading patterns;
- To establish an analytical framework for the prediction of non-linear creep strain development at various loading histories and for delayed failure prediction;
- To verify the applicability of existing codes and to propose improvement if necessary.

The second objective is to investigate if the loading speed and duration have an influence on the strength of shear-critical reinforced concrete members without transverse reinforcement. Within this scope, the following points are addressed:

- To conduct experimental tests on one-way shear-critical members without shear reinforcement subjected to varying loading rates up to failure
- To investigate the time-dependent development of the failure mechanism and the crack pattern as well as the analogies with the uniaxial behaviour of concrete;
- To investigate the time-dependent contribution of different shear transfer actions and the redistribution of stresses;
- To validate the existing models for shear strength prediction (main focus on CSCT) for time-dependent effects and sustained load actions;
- To verify the applicability of existing codes and propose improvement if necessary.

1.4 Structure of this report

This report is structured in three main parts which address the different objectives. These three main parts are preceded by the current section 1, which presents an introduction to the report and a literature review.

The first main part is treated in sections 2-5 and deals with the uniaxial compressive strength of concrete. Section 2 presents an analytical approach allowing to consistently investigate the long-term response of concrete under constant sustained loading. Section 3 presents the results of an experimental campaign on the response of normal strength concrete under varying strain and stress rates, as well as a validation of the analytical approach of section 2. In section 4, the analytical approach is extended to consistently investigate the long-term response of concrete under various loading patterns, proposing simple code-like equations. Finally, section 5 deals with several typical loading cases of the engineering practice in order to propose some design recommendations.

The second part of this report is presented in sections 6-7 and deals with the shear strength of members without shear reinforcement. Section 6 presents the results of an experimental programme on the response of shear-critical concrete beams under varying loading rates. Section 7 presents a detailed analysis of the results and a discussion on the observed short- and long-term response of concrete.

The third part of the report (section 8) presents the current state of the clauses of the swiss design code (SIA 262:2013) and the swiss national annex to the Eurocode 2 (EN 1992-1-1 CH NA:2014) which have been concerned by the research work of the previous section, and proposes a pertinent discussion and an improvement of those clauses.

Finally, section 9 summarizes the main conclusions of the previous sections.

1.5 Publications in peer-reviewed academic journals

The contents of sections 1.1, 2-5 and 9.1 of this report have been published in two scientific publications:

> Tasevski, D., Fernández Ruiz, M. and Muttoni, A., (2018). "Compressive Strength and Deformation Capacity of Concrete under Sustained Loading and Low Stress Rates." Journal of Advanced Concrete Technology, 16(8), 396-415. (https://www.jstage.jst.go.jp/article/jact/16/8/16_396/_article/-char/en)
>
> Tasevski, D., Fernández Ruiz, M. and Muttoni, A., (2019). "Assessing the compressive strength of concrete under sustained actions: from refined models to simple design expressions." Structural Concrete, 2019, 1-15. (https://onlinelibrary.wiley.com/doi/full/10.1002/suco.201800303)

The contents of sections 1.2, 6, 1, 9.2 and appendix A of this report have been submitted for publication to a peer-reviewed journal:

> Tasevski, D., Fernández Ruiz, M. and Muttoni, A., (2019). "Influence of load duration on shear strength of reinforced concrete members.", *submitted for publication*.

2 Concrete strength in case of constant sustained loading

2.1 Nonlinear creep strains

A number of approaches on the modelling of nonlinear creep and associated damage as well as for prediction of delayed failure of concrete can be found in literature. Many of these approaches are based on material damage development [13], [14], [31], [53]–[57] and others are based on fracture mechanics [19], [58]–[61]. Within this work, the approach of Tasevski et al. [13] will be followed. This approach is based on the hypothesis of affinity between linear and nonlinear creep strains (proposed by Fernández Ruiz et al. [14]) and accounts for material damage development associated to nonlinear creep. This chapter gives a short review of this approach.

If concrete is subjected to a compressive stress lower than ~0.4·f_c, the correlation between the delayed creep strain and the instantaneous strain is almost linear (*Fig. 3*a) and thus governed by a linear creep phenomenon without development of any significant material damage. At higher stress levels ($\sigma_c/f_c > 0.4$), the linear correlation between the delayed creep strain and the instantaneous strain is lost and additional nonlinear creep strains develop [13]. This loss of linear correlation is due to the damage process in the material associated to concrete microcracking.

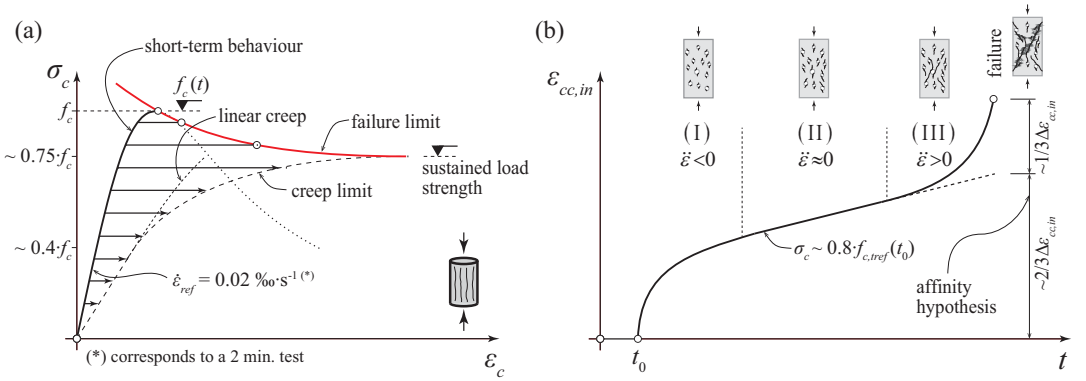

Fig. 3 Uniaxial compressive behaviour of concrete: (a) short- and long-term stress-strain response, adapted from Rüsch [8]; (b) stages of creep: primary, secondary and tertiary; definition of the affinity hypothesis

According to several authors [33], [56], [58], the development of inelastic strains associated to material damage can be separated into three phases (*Fig. 3*b). In the primary creep phase (immediately after load application), the strains develop at a high initial rate and stabilize with time. In the following (secondary creep) phase, the rate is fairly constant. At high load levels, the microcrack propagation becomes unstable and leads to failure of the specimen (see *Fig. 3*), corresponding to the tertiary creep phase. This latter phase is characterized by an increasing rate of strains, resulting in an uncontrolled process of crack coalescence.

2.2 Failure criterion

Following the approach of Fernández Ruiz et al. [14], the inelastic strain capacity $\varepsilon_{cc,in,av}$ for a given stress level defined as the difference between the instantaneous post- and pre-peak strains for that level of stress (*Fig. 4*a) can be assumed as the governing parameter for the failure criterion. This value can be directly calculated by using the monotonic stress-strain curve of concrete in compression, as further verified experimentally by Tasevski et al. [13]. The monotonic response is considered to be obtained at a reference strain rate of

$\dot{\varepsilon} = 0.02$ ‰·s^{-1} (approximately 2 minutes to reach the maximum strength). Failure is considered to occur when the total inelastic strain developed by the material (accounting for secondary and tertiary creep strains) equals the inelastic deformation capacity (see *Fig. 4*b).

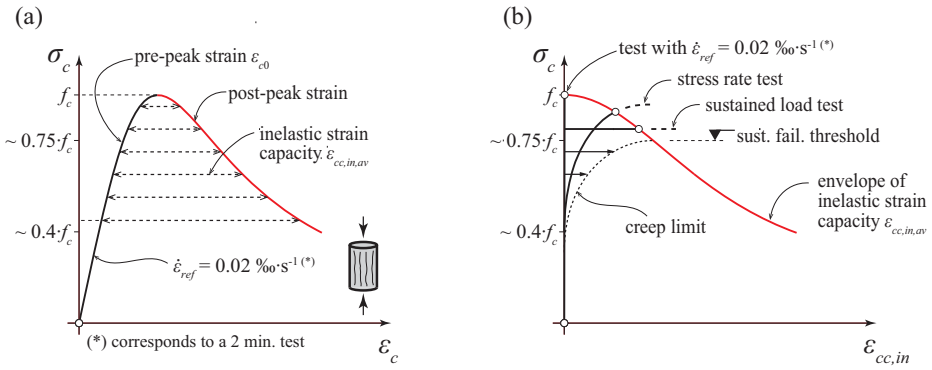

Fig. 4 Inelastic strain capacity $\varepsilon_{cc,in,av}$ according to Fernández Ruiz et al.[14]: (a) definition of $\varepsilon_{cc,in,av}$ as the difference between post- and pre-peak strains of the monotonic curve; (b) definition of failure as intersection of the stress – inelastic strain curve and the failure envelope of $\varepsilon_{cc,in,av}$ (Tasevski et al. [13])

Similar approaches by other authors have been reported, where the monotonic stress-strain curve is used as a failure criterion for fatigue life [5], [62], [63]. Details on the development of inelastic strain related to material damage and on the calculation of failure can be found in Tasevski et al. [13] and are summarized in the following section.

2.3 Development of inelastic strain by concrete at high stress levels

According to Tasevski et al. [13], the strains developed for a concrete loaded at time t_0 can be described in a general manner by the following expression:

$$\boldsymbol{\varepsilon_c\left(t,\frac{\sigma_c}{f_c}\right) = \varepsilon_{c0}\left(t_0,\frac{\sigma_c}{f_c}\right) + \Delta\varepsilon_{cs}(t,t_0) + \Delta\varepsilon_{cc}\left(t,t_0,\frac{\sigma_c}{f_c}\right)} \tag{1}$$

where the first term on the right side of the equation ($\varepsilon_{c0}\left(t_0,\frac{\sigma_c}{f_c}\right)$) corresponds to the instantaneous pre-peak strain (including elastic and inelastic components, refer to the short-term behaviour in *Fig. 3*a), the second ($\Delta\varepsilon_{cs}(t,t_0)$) to the shrinkage strains (assumed not to be associated to any material damage) and the third ($\Delta\varepsilon_{cc}\left(t,t_0,\frac{\sigma_c}{f_c}\right)$) to the creep strains [13].

The creep strains can be divided into primary, secondary and tertiary creep in the following manner:

$$\boldsymbol{\varepsilon_{cc}\left(t,t_0,\frac{\sigma_c}{f_c}\right) = \varepsilon_{cc,1}(t,t_0) + \varepsilon_{cc,2}\left(t,t_0,\frac{\sigma_c}{f_c}\right) + \varepsilon_{cc,3}\left(t,t_0,\frac{\sigma_c}{f_c},\frac{\varepsilon_{in}}{\varepsilon_{in,av}}\right)} \tag{2}$$

where the primary creep strains are calculated by means of the linear creep coefficient (and are not associated to material damage):

$$\boldsymbol{\varepsilon_{cc,1}(t,t_0) = \varphi_{lin}\cdot\varepsilon_{c0}} \tag{3}$$

The secondary creep strains (due to micro-cracking development and thus associated to material damage) are evaluated as [14]:

$$\boldsymbol{\varepsilon_{cc,2}\left(t,t_0,\frac{\sigma_c}{f_c}\right)=(\eta-1)\cdot\varepsilon_{cc,1}(t,t_0)} \tag{4}$$

where the coefficient η is expressed as follows [13], [14]:

$$\boldsymbol{\eta\left(\frac{\sigma_c}{f_c},t,t_0\right)=\left(1+2\cdot\eta_\tau(t,t_0)\left(\frac{\sigma_c}{f_c(t)}\right)^4\right)} \tag{5}$$

and coefficient η_τ takes into account the development of the nonlinear creep strains with time [13]:

$$\boldsymbol{\eta_\tau(t,t_0)=\left(1-\log\left(\frac{t-t_0}{t_m+t-t_0}\right)\right)^n} \tag{6}$$

where constant values t_m = 100 days and n = 0.75 can be generally assumed [13]. It can be noted that when $t \to \infty$, then $\eta_\tau \to 1$ and consequently Eq. (**5**) takes the form originally suggested by Fernández Ruiz et al. [14] for nonlinear creep strains after a long time.

The development of tertiary creep strains (associated to micro-crack coalescence and thus also to material damage) can be evaluated by taking into accounting the ratio of developed-to-available inelastic strains ($\varepsilon_{cc,in}/\varepsilon_{cc,in,av}$) and the level of stress, calculated by means of the following equation [13]:

$$\boldsymbol{\varepsilon_{cc,3}\left(t,t_0,\frac{\sigma_c}{f_c},\frac{\varepsilon_{cc,in}}{\varepsilon_{cc,in,av}}\right)=\gamma\left(\frac{\sigma_c}{f_c},\frac{\varepsilon_{cc,in}}{\varepsilon_{cc,in,av}}\right)\cdot\varepsilon_{cc,2}\left(t,t_0,\frac{\sigma_c}{f_c}\right)} \tag{7}$$

In the ratio $\varepsilon_{cc,in}/\varepsilon_{cc,in,av}$, the term $\varepsilon_{cc,in,av}$ corresponds to the total available inelastic strain and is characterised by the short-term monotonic response of concrete (*Fig. 4*a). The term $\varepsilon_{cc,in}$ corresponds to the developed nonlinear creep strain (total strain minus shrinkage, instantaneous and linear creep strains).

For low values of the ratio $\varepsilon_{cc,in}/\varepsilon_{cc,in,av}$, tertiary creep strains have a negligible contribution, whereas they increase at a growing rate when failure approaches. As suggested by Tasevski et al. [13], the parameter γ can be calculated with help of the following expression:

$$\boldsymbol{\gamma=\frac{1}{2}\cdot\left(\frac{\varepsilon_{cc,in}}{\varepsilon_{cc,in,av}(t)}\right)^\alpha} \quad \text{for } \sigma_c/f_c(t) \geq 0.75 \tag{8}$$

According to this assumption, γ is zero for stress levels below the threshold of possible tertiary creep development (σ_c/f_c = 0.75). The shape of the tertiary creep curve is governed by the parameter α, which can be considered equal to 4, based on the analysis of experimental results by Tasevski et al. [13]. At failure, $\varepsilon_{cc,in} = \varepsilon_{cc,in,av}$ which results $\varepsilon_{cc,3} = ½\varepsilon_{cc,2}$. This formula is in addition consistent with the affinity hypothesis originally formulated by Fernández Ruiz et al. [14] that considers $\varepsilon_{cc,2} = ⅔\varepsilon_{cc,in,av}$ and $\varepsilon_{cc,3} = ⅓\varepsilon_{cc,in,av}$ (*Fig. 3*b).

A significant advantage of the presented model is the fact that it is strain-based and allows thus tracking the amount of material damage for any loading history, and to calculate both the strength and deformation capacity of concrete for any potential loading pattern.

3 Experimental programme for concrete compressive strength under sustained load and model validation

3.1 Experimental programme

The aim of this experimental programme is to study the response of normal strength concrete at high stress levels both at varying strain and stress rates.

3.1.1 Materials and testing methods

The uniaxial compressive behaviour of concrete under different strain and stress rates has been investigated by means of cylindrical specimens with dimensions $Ø \times h$ = 160 × 320 mm. The concrete was produced with a CEM-II 42.5R cement (w/c = 0.56) and Rhone river aggregates. The specimens were kept moulded (with the top face sealed) until the age of 21 days. Thereafter, the specimens were unmoulded and stored under standard laboratory conditions (temperature of 21 °C and relative humidity of 65 %) until testing. The tests were performed using a Schenck Hydroplus servo-hydraulic testing machine (*Fig. 5*a) with capacity of 2.5 MN (noise level ±5 kN) and a custom-made steel frame which enhances the stiffness of the test setup [14]. The climatic room where the tests were performed has controlled temperature (21±0.5 °C) and relative humidity (65±3 %, some minor deviations are commented later). The longitudinal strain of the specimens $\varepsilon_{c,long}$ was measured with three surface displacement transducers (omega gauges, relative noise level 0.04 ‰) arranged radially on two steel rings at a distance of 250 mm (see *Fig. 5*b). The signal of the three transducers was acquired at high frequency (1200 Hz) and it was used to control the strain rate (in the strain rate test series) directly on the specimen. The transverse strain $\varepsilon_{c,trans}$ was measured with a steel ribbon dilatometer (*Fig. 5*b) equipped with a linear variable differential transformer (LVDT).

The reference compressive strength was tested at a strain rate of 0.02 ‰·s^{-1}, corresponding to approximately 100 seconds before maximum strength is reached. Its development with concrete age has been compared to the Model Code 2010 [38] formula:

$$f_{c,ref}(t_0) = f_{c,28} \cdot e^{s\cdot\left[1-\sqrt{\frac{28}{t}}\right]} \tag{9}$$

where $f_{c,28}$ = 29.0 MPa and t refers to the concrete age in days. The coefficient s was adapted by means of least square fitting and returns the value s = 0.316. The resulting development curve is given in *Fig. 6*a.

With respect to the shrinkage strains, a shrinkage rig with three cylindrical specimens was installed after unmoulding of the specimens (at 21 days), see *Fig. 5*c. The shrinkage measurements were performed during two years. Then, the standard shrinkage model from Model Code 2010 was used to reproduce the measured shrinkage strains (with α_{as}=600, α_{ds1}=6 and α_{ds2}=0.012 corresponding to a cement class 42.5 R). The resulting expression (Eq. (10)) is compared in *Fig. 6*b to the test results:

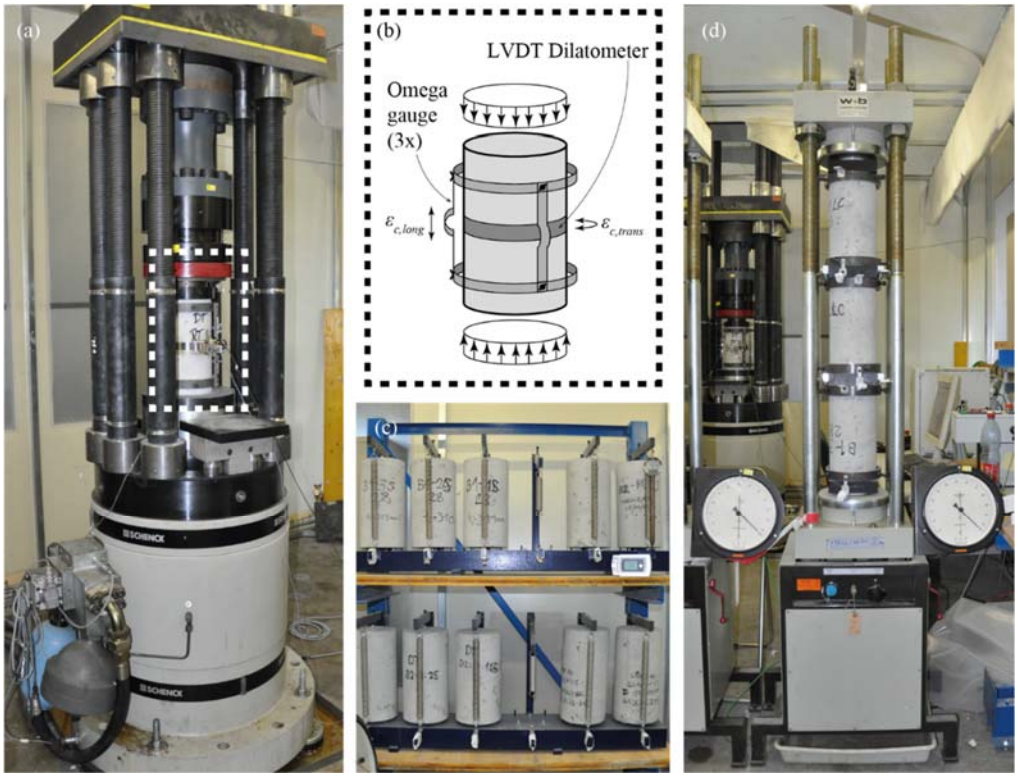

Fig. 5 Test setup: (a) testing frame for stress and strain rate long-term testing; (b) details of measurement devices; (c) shrinkage rigs; and (d) linear creep rigs

$$\varepsilon_{cs}(t,t_s) = -36.4\cdot 10^{-6}\cdot\left(1-e^{-0.2\cdot\sqrt{t}}\right) - 699\cdot 10^{-6}\cdot\frac{1}{\sqrt{\frac{224}{t-t_s}+1}} \tag{10}$$

where t_s is the concrete age at demoulding in days. Measurements on linear creep were also performed during two years in a standard creep rig with three cylindrical specimens loaded at a stress level $\sigma_c/f_c \approx 0.35$ at an age of 28 days (*Fig. 5*d). The creep strains were calculated by removing from the increase of strains with time the value corresponding to the measured shrinkage strains. Then, the standard creep law from Model Code 2010 was adapted by fitting the parameters to reproduce the measured curve (*Fig. 6*c):

$$\varphi(t,t_0) = 3.24\cdot\frac{1}{0.1+{t_0}^{0.2}}\cdot\left[\frac{t-t_0}{682+t-t_0}\right]^{\frac{1}{2.3+\frac{3.5}{\sqrt{t_0}}}} + 3.00\cdot\frac{1}{0.1+{t_0}^{0.2}}\cdot\left[\frac{t-t_0}{395+t-t_0}\right]^{\frac{1}{2.3+\frac{3.5}{\sqrt{t_0}}}} \tag{11}$$

where t_0 is the age of concrete at loading. It can be noted that the results obtained with the Model Code 2010 formulae slightly underestimate the linear creep strains and slightly overestimate the shrinkage strains up to the age of approximately 400 days, being fairly accurate thereafter. In any case, the delayed strains (linear creep and shrinkage) are reasonably well estimated by this model. The linear creep law for other loading ages was also calculated according to the Model Code 2010 expression for the creep coefficient (the two grey lines in *Fig. 6*c represent the calculated linear creep coefficients for the average loading ages of the two experimental series).

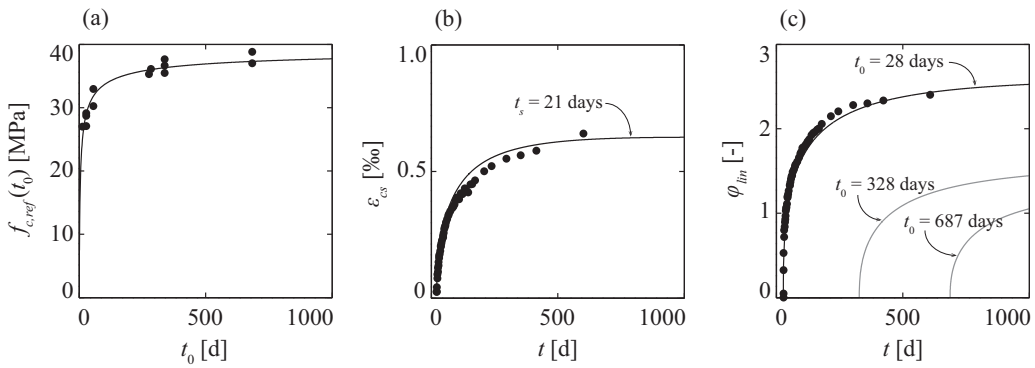

Fig. 6 Time-dependent concrete properties: (a) development of compressive strength with time (tests performed at reference strain rate of 0.02 ‰·s^{-1}, average of 28-day strength $f_{c,ref,28}$ = 29 MPa), (b) longitudinal shrinkage strains and (c) longitudinal linear creep strains ($\sigma/f_c \approx 0.35$)

It shall be commented that the relative humidity was kept as constant as possible. However, there have been some variations (±10 %) over very limited periods of time during the two years, mainly due to maintenance operations of the climate regulation system. These variations have been taken into account for the shrinkage and linear creep calculations presented in *Fig. 6*b and *Fig. 6*c according to Model Code 2010.

3.1.2 Types of loading

The delayed behaviour of concrete under uniaxial compression has so far been usually investigated with classical creep tests where a constant stress level is sustained over time [8], [14]. To investigate other long-term loading patterns, two new test series were performed in this study.

The first test series was performed by varying the strain rate (see *Fig. 7*). To have a fairly mature concrete and to limit the influence of strength increase with time, the concrete age at testing varied between 10 and 14 months (for more details on the evolution of concrete strength with time refer to *Fig. 6*a and *Table 1*). This test series covered strain rates ranging from 2.00·10^{-3} s^{-1} to 2.00·10^{-9} s^{-1} (time to failure from 1 second to ca. 14 days).

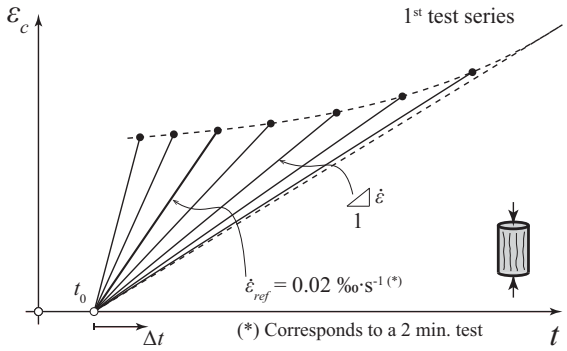

Fig. 7 Loading paths of 1st test series (DR tests): varying longitudinal strain rate

The second test series of uniaxial compression was performed by varying the stress rate. The concrete age at testing varied between 22 and 24 months (refer again to *Fig. 6*a and *Table 2*). First, an initial loading ramp (3.50·10^{-1} MPa·s^{-1}) was applied up to 80 % of the reference strength ($\dot{\sigma} = 0.02$ ‰·s^{-1}) at the day of loading (see *Fig. 8*). Then, a second loading ramp was applied from 5.00·10^{0} MPa·s^{-1} to 1.25·10^{-5} MPa·s^{-1} (time to failure from 1 second to ca. 5 days).

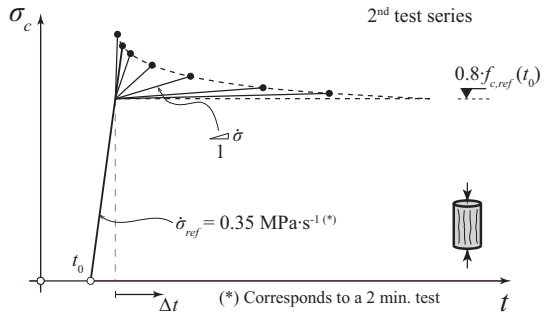

Fig. 8 Loading paths of 2nd test series (LR tests): varying stress rates at high stress levels

Despite the fact that the test series of this programme were aimed at investigating the influence of low stress and strain rates on the compressive strength of concrete, some tests with relatively high stress and strain rates were also conducted (tests DR1, DR2 and LR0). The results of these tests are presented in the following, but they will not be investigated in detail thereafter.

3.1.3 Results for strain rate tests (1st test series)

Table 1 presents an overview of the results of the test series performed with varying strain rate. The second column indicates the control strain rate, the third and fourth column give the age of concrete and the reference strength at load application respectively, and columns 5-9 give the main results (the average of every strain rate is written in bold font). The stress–strain diagrams are presented and compared to the reference test with $\dot{\varepsilon} = 0.02$ ‰·s^{-1} in *Fig. 9*. The evolution of the stress and of the strains versus time in logarithmic scale is also presented in *Fig. 10*a-c. It is worth noting that the specimen DR7_1 was tested with a very low strain rate and thus a preload had to be applied in order not to lose contact between the specimen and the loading plate (this explains the shape for stresses lower than $0.2 \cdot f_{c,ref}(t_0)$ in *Fig. 10*).

These tests confirm that the failure load is lower as the strain rate decreases (load applied over longer periods of time), with a variation of the measured strength to the reference strength (standard loading speed) at the same age ranging from 1.10 (high strain rates) to 0.932 (low strain rates). Also, it can be observed that the longitudinal and transverse strains at failure usually increase with decreasing strain rates. In terms of effective Poisson's ratio ($\nu_{eff} = \varepsilon_{c,trans}/\varepsilon_{c,long}$), an increasing trend could be observed with average values from 0.223 for higher strain rates (standard value for concrete tested in displacement control) up to 0.375 for the lower strain rates. It shall be noted that the low value of $\varepsilon_{c,trans}$ for the specimen DR7_1 may possibly be related to a measurement device malfunction (the contact grease may have dried and the device may have got stuck during the long test duration).

Table 1 Overview of the results of the 1st test series performed with varying strain rate ("Avg." indicating average of specimens with same loading rate)

Test Name	$\dot{\varepsilon}$	t_0	$f_{c,ref}(t_0)$	Δt	$f_{c,\Delta t}$	$f_{c,\Delta t} / f_{c,ref}(t_0)$	$\varepsilon_{c,long}$	$\varepsilon_{c,trans}$
	[s^{-1}]	[d]	[MPa]	[s]	[MPa]	[-]	[‰]	[‰]
DR1_1	**2.00E-03**	**340**	**36.3**	**1.00E+00**	**40.1**	**1.10**	**2.16**	**0.548**
DR2_1	2.00E-04	340	36.3	9.20E+00	37.9	1.04	2.21	0.562
DR2_1	2.00E-04	340	36.3	9.40E+00	38.6	1.06	2.29	0.440
Avg. DR2	**2.00E-04**	**340**	**36.3**	**9.30E+00**	**38.3**	**1.05**	**2.25**	**0.501**
DR3_1 (ref.)	2.00E-05	339	36.3	9.40E+01	36.7	1.01	2.28	0.543
DR3_2 (ref.)	2.00E-05	339	36.3	9.78E+01	35.5	0.977	2.38	0.763
DR3_3 (ref.)	2.00E-05	339	36.3	9.74E+01	37.7	1.04	2.37	0.608
Avg. DR3	**2.00E-05**	**339**	**36.3**	**9.64E+01**	**36.6**	**1.01**	**2.34**	**0.638**
DR4_1	2.00E-06	284	36.0	1.02E+03	33.8	0.939	2.49	0.726
DR4_2	2.00E-06	280	36.0	1.09E+03	35.9	0.999	2.62	0.998
Avg. DR4	**2.00E-06**	**282**	**36.0**	**1.06E+03**	**34.9**	**0.969**	**2.56**	**0.862**
DR5_1	2.00E-07	276	36.0	1.16E+04	34.7	0.966	2.81	0.813
DR5_2	2.00E-07	278	36.0	1.21E+04	34.5	0.959	2.95	1.34
Avg. DR5	**2.00E-07**	**277**	**36.0**	**1.19E+04**	**34.6**	**0.962**	**2.88**	**1.08**
DR6_1	**2.00E-08**	**343**	**36.3**	**1.26E+05**	**34.1**	**0.939**	**3.09**	**0.956**
DR7_1	**2.00E-09**	**440**	**36.7**	**1.21E+06**	**34.2**	**0.932**	**2.94**	**0.396**

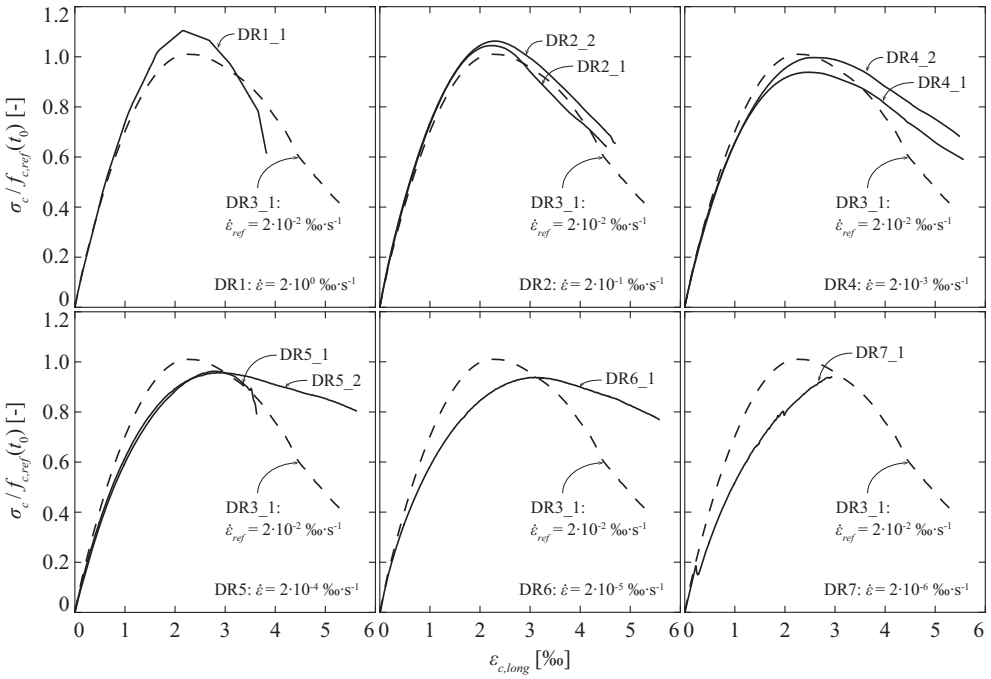

Fig. 9 Stress–strain diagrams of the 1st test series (tests with varying strain rate, refer to Table 1)

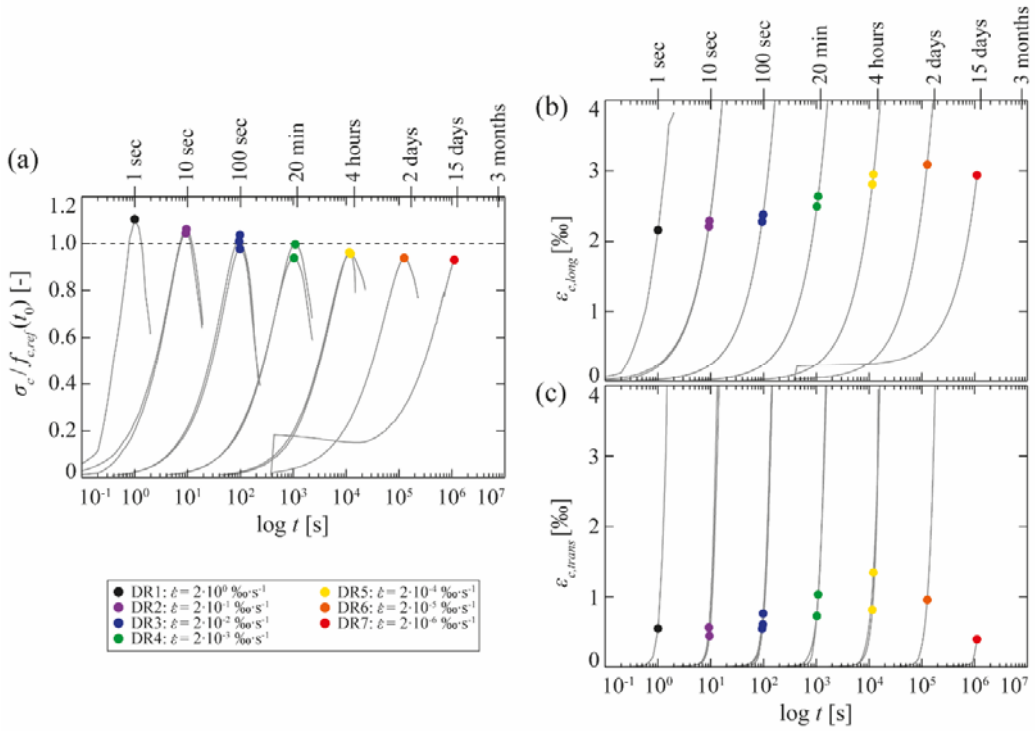

Fig. 10 Results of the 1st test series (tests with varying strain rate): (a) longitudinal stress; (b) longitudinal strain; and (c) transverse strain versus time

3.1.4 Results for stress rate tests (2nd test series)

Table 2 presents an overview of the results of the test series performed with varying stress rate. The second column indicates the control stress rate after the initial loading ramp, the third and fourth column give the age of concrete and the reference strength at load application respectively, and columns 5-9 give the main results (the average of every stress rate is written in bold font). The stress–strain diagrams are presented and compared to the reference test with $\dot{\varepsilon} = 0.02$ ‰·s^{-1} in *Fig. 11*. The evolution of the stress or the strains versus time in logarithmic scale is additionally presented in *Fig. 12*a-c.

As for the 1st series, it can be observed that the failure load is lower as the stress rate decreases (corresponding to longer times of application of the load, consistently to the strain rate tests). This decrease of the strength is accompanied by larger strains at failure in the longitudinal and transverse directions. Some fluctuations in the results can be observed, probably related to the load control of the test, where the failure occurs in a brittle manner and with no post-peak branch.

In terms of the influence of the stress rate in the measured compressive strength of the material, it varies between 1.07 (high stress rates) and 0.914 (low stress rates) when it is normalized by the reference material strength (obtained with a standard loading speed). The effective Poisson's ratio ($v_{eff} = \varepsilon_{c,trans}/\varepsilon_{c,long}$), varies also from 0.402 for higher stress rates up to 0.617 for lower stress rates. These latter values (load control) are higher than those observed for strain rates (deformation control).

Table 2 Overview of the results of the 2nd test series performed with varying stress rate ("Avg." indicating average of specimens with same loading rate)

Test Name	$\dot{\sigma}$	t_0	$f_{c,ref}(t_0)$	Δt	$f_{c,\Delta t}$	$f_{c,\Delta t} / f_{c,ref}(t_0)$	$\varepsilon_{c,long}$	$\varepsilon_{c,trans}$
	[MPa·s^{-1}]	[d]	[MPa]	[s]	[MPa]	[-]	[‰]	[‰]
LR0_1	**5.00E+00**	**728**	**37.4**	**5.00E-01**	**38.9**	**1.04**	**2.27**	**-**
LR1_1	5.00E-01	684	37.3	3.19E+01	39.8	1.07	2.36	0.918
LR1_2	5.00E-01	684	37.3	2.89E+01	38.8	1.04	2.53	0.984
LR1_3	5.00E-01	684	37.3	2.39E+01	37.0	0.992	2.52	1.08
Avg. LR1	**5.00E-01**	**684**	**37.3**	**2.82E+01**	**38.5**	**1.03**	**2.47**	**0.994**
LR2_1	5.00E-02	678	37.3	1.27E+02	35.3	0.948	2.72	1.69
LR2_2	5.00E-02	679	37.3	2.28E+02	40.0	1.07	2.69	1.19
LR2_3	5.00E-02	679	37.3	1.87E+02	38.1	1.02	2.67	1.40
Avg. LR2	**5.00E-02**	**679**	**37.3**	**1.81E+02**	**37.8**	**1.01**	**2.69**	**1.43**
LR3_1	5.00E-03	678	37.3	1.38E+03	35.6	0.954	2.96	1.46
LR3_2	5.00E-03	682	37.3	1.71E+03	37.3	1.00	2.85	1.75
LR3_3	5.00E-03	682	37.3	1.53E+03	36.1	0.968	2.99	2.21
Avg. LR3	**5.00E-03**	**682**	**37.3**	**1.54E+03**	**36.4**	**0.974**	**2.93**	**1.81**
LR4_1	**1.50E-03**	**650**	**37.2**	**4.08E+03**	**34.7**	**0.933**	**2.94**	**2.27**
LR5_1	5.00E-04	682	37.3	1.33E+04	35.4	0.949	2.90	1.88
LR5_2	5.00E-04	683	37.3	1.60E+04	36.6	0.981	3.41	2.02
Avg. LR5	**5.00E-04**	**683**	**37.3**	**1.47E+04**	**36.1**	**0.965**	**3.16**	**1.95**
LR6_1	5.00E-05	684	37.3	1.43E+05	36.4	0.977	3.60	2.06
LR6_2	5.00E-05	707	37.3	1.82E+05	37.6	1.01	2.95	1.05
Avg. LR6	**5.00E-05**	**696**	**37.3**	**1.63E+05**	**37.0**	**0.992**	**3.28**	**1.56**
LR7_1	**1.25E-05**	**742**	**37.4**	**4.48E+05**	**34.2**	**0.914**	**3.28**	**1.35**

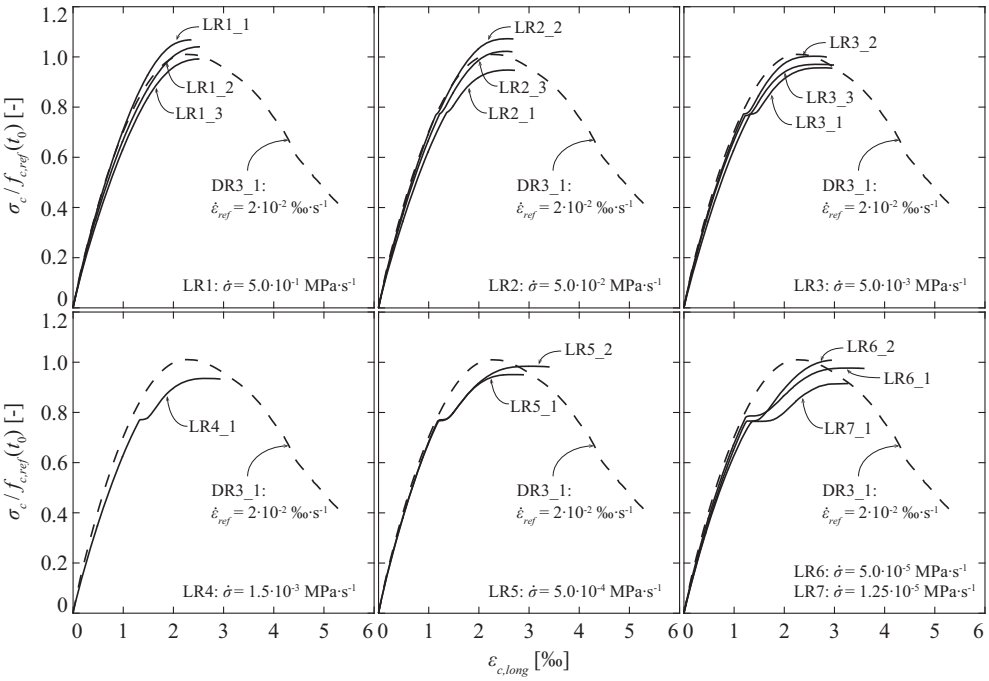

Fig. 11 Stress–strain diagrams of the 2nd test series (tests with varying stress rate, refer to *Table 2*)

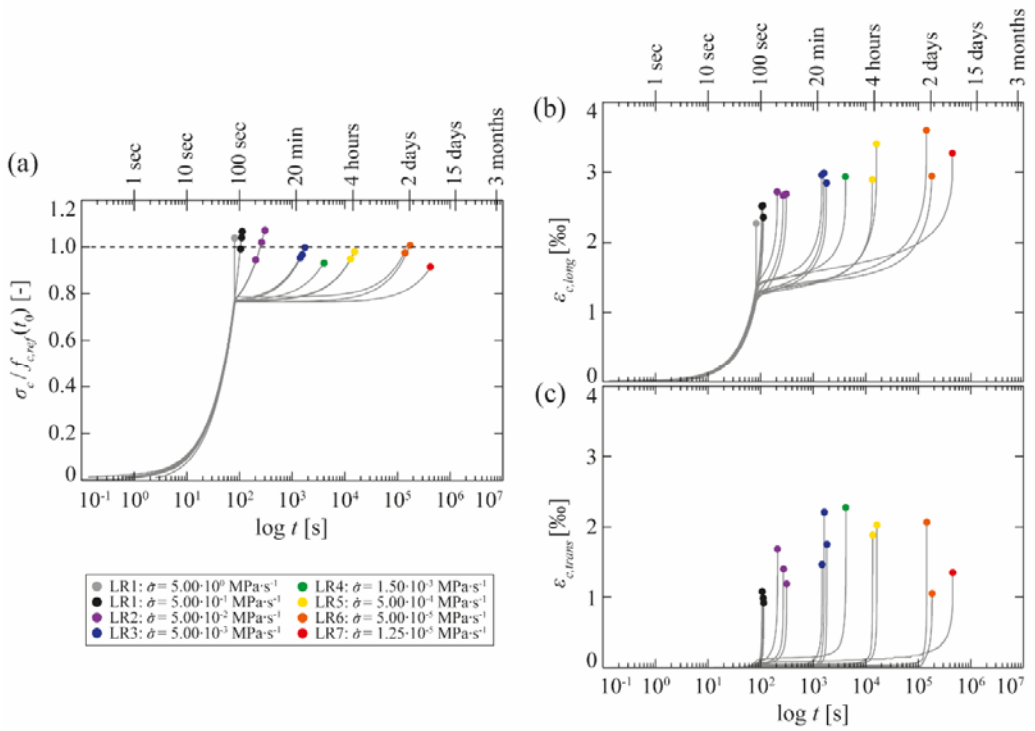

Fig. 12 Results of the 2nd test series (tests with varying stress rate): (a) longitudinal stress; (b) longitudinal strain; and (c) transverse strain versus time

3.1.5 Discussion of inelastic strains developed at failure

Strain rate tests

As described in Section 2.2, it has been observed for tests under constant sustained stress that when the developed nonlinear (inelastic) creep strain equals the inelastic strain capacity of the material for that level of stress, failure occurs ([14], refer to *Fig. 4*b). To evaluate the validity of this failure criterion for the investigated load patterns, the contributions of the instantaneous pre-peak strain (ε_{c0}), the linear creep strain ($\varepsilon_{cc,1}$) and the shrinkage strain (ε_{cs}) have been calculated and removed from the total strain:

$$\varepsilon_{cc,in} = \varepsilon_{tot} - \varepsilon_{c0} - \varepsilon_{cc,1} - \varepsilon_{cs} \tag{12}$$

To estimate the instantaneous pre-peak strains (ε_{c0}), the concrete model of [14] was used as a suitable stress-strain relationship reproducing the response of the reference tests (refer to [13]). As for the linear creep and shrinkage strains, the adapted laws from Model Code 2010 as defined in Section 3.1.1 were used. The calculation of the creep strains due to variable stresses has been performed by suitably adapting the superposition principle described in [13]. Finally, the estimated nonlinear (inelastic) creep strains were compared to the inelastic strain capacity, as presented in Fig. 13a. The figure shows a consistent trend between the developed inelastic strain at failure and the inelastic strain capacity (difference between post- and pre-peak strains obtained as an average of three reference test curves with $\dot{\varepsilon} = 0.02$ ‰·s^{-1} or the analytical expression curve presented in [13]). This confirms the validity of the assumptions by [14] also for this loading pattern.

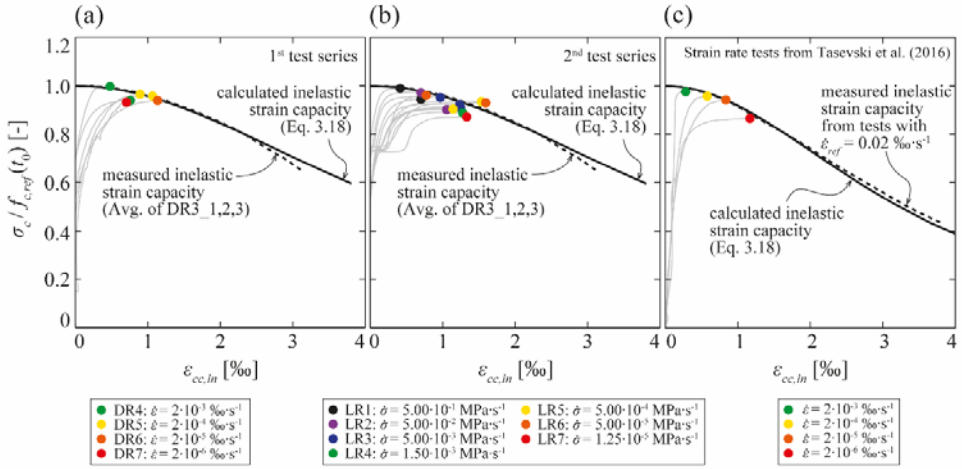

Fig. 13 Inelastic strains and corresponding inelastic strain capacity for: (a) 1st test series with constant strain rate, (b) 2nd test series with constant stress rate and (c) strain rate tests from [64]

A similar analysis has been performed for the results of a previous test series performed by the authors [64], [65] by using the same loading pattern (variable strain rate). The comparison is presented in *Fig. 13*c and shows also an excellent agreement.

Stress rate tests

In a similar manner as for the strain rate tests, the contributions of the instantaneous pre-peak strains, linear creep strains and shrinkage strains have been estimated and removed from the total strain recorded in the 2nd test series (refer to Eq. (12)). On that basis, the estimated nonlinear (inelastic) creep strain is compared to the inelastic strain capacity, as presented in *Fig. 13*b.

As for the strain rate tests, an excellent agreement is found at failure between the inelastic strain capacity predicted by the reference curve and the nonlinear creep strain developed by the specimen for the various load patterns investigated, validating again the pertinence of this assumption.

3.2 Comparison of the developed model to the *fib* MC2010 approach and proposal of an analytical expression

According to *fib* MC2010 [38] (Eq. (5.1-53)), the compressive concrete strength in case of a constant sustained loading starting at time t_0 and for a duration Δt_F can be expressed by (Eq. (5.1-53) of *fib* MC2010 [38], notation adapted consistently to the one of this report):

$$\boldsymbol{f_c(t_0 + \Delta t_F) = f_{c,28} \cdot \beta_{cc}(t_0 + \Delta t_F) \cdot \beta_{c,sus}(\Delta t_F)} \tag{13}$$

In this expression, the influence of two effects is considered: the increase of strength due to continued cement hydration ($\beta_{cc}(t_0+\Delta t_F)$) which depends on the age at failure $t_0+\Delta t_F$ and the strength reduction due to sustained loading ($\beta_{c,sus}(\Delta t_F)$) which depends on the load duration Δt_F. The parameter $\beta_{cc}(t_0+\Delta t_F)$ can be calculated for t_{ref} = 28 days with Eq. (5.1-51) of *fib* MC2010 [38] (notation adapted consistently to the one of this report):

$$\boldsymbol{\beta_{cc}(t_0 + \Delta t_F) = e^{s\cdot\left(1-\sqrt{\frac{28}{t_0+\Delta t_F}}\right)}} \tag{14}$$

where s is a coefficient that depends on the cement type. For t_{ref} different to 28 days, Eq. (**14**) has to be replaced by:

$$\boldsymbol{\beta_{cc}(t_0 + \Delta t_F) = e^{s\cdot\left(1-\sqrt{\frac{t_{ref}}{t_0+\Delta t_F}}\right)\cdot\sqrt{\frac{28}{t_{ref}}}}} \tag{15}$$

With respect to the parameter $\beta_{c,sus}(\Delta t_F)$ in Eq. (**13**), it accounts for the strength reduction due to sustained loading, and is evaluated by means of the following expression (Eq. (5.1-54) from *fib* MC2010 [38], notation adapted consistently to the one of this report):

$$\boldsymbol{\beta_{c,sus}(\Delta t_F) = 0.96 - 0.12 \cdot \left(\ln(72 \cdot \Delta t_F)\right)^{1/4}} \tag{16}$$

where Δt_F is measured in days. This expression has been obtained as a best fit of test results by the research group of Rüsch [8], [9]. It can be noted that, since the evaluation of the test data was made adding the initial loading time (20 minutes for those tests) to the sustained loading duration, the expression is in principle only applicable for Δt_F > 0.015 days (= 20 minutes). In addition, the coefficient 0.96 in this expression covers the difference of a test loaded in 20 minutes and a standard test loaded in approximately 2 minutes [66].

Fig. 14 presents a comparison of these expressions with the model described in the previous section and the test data gathered in Tasevski et al. [13] collected from several research groups [6], [9], [17], [22], [26]. The sustained loading duration has been corrected to account consistently for the duration of the initial loading phase. It can be seen in that figure that the *fib* MC2010 [38] expressions (green lines in *Fig. 14*a-c) provide a lower limit of the measured strength under sustained loading. Furthermore, the formula is only valid for times of application of the load larger than 20 minutes, which makes the expression rather sensitive (strong drop on the strength after 20 minutes) and limits its field of application. In addition, the coefficient $\beta_{c,sus}(\Delta t)$ according to MC2010 does not depend on the concrete age at loading (t_0), but only on the time duration for which the load is applied (Δt). However, according to the test results and the theoretical model [13], the age of concrete at loading is a significant parameter.

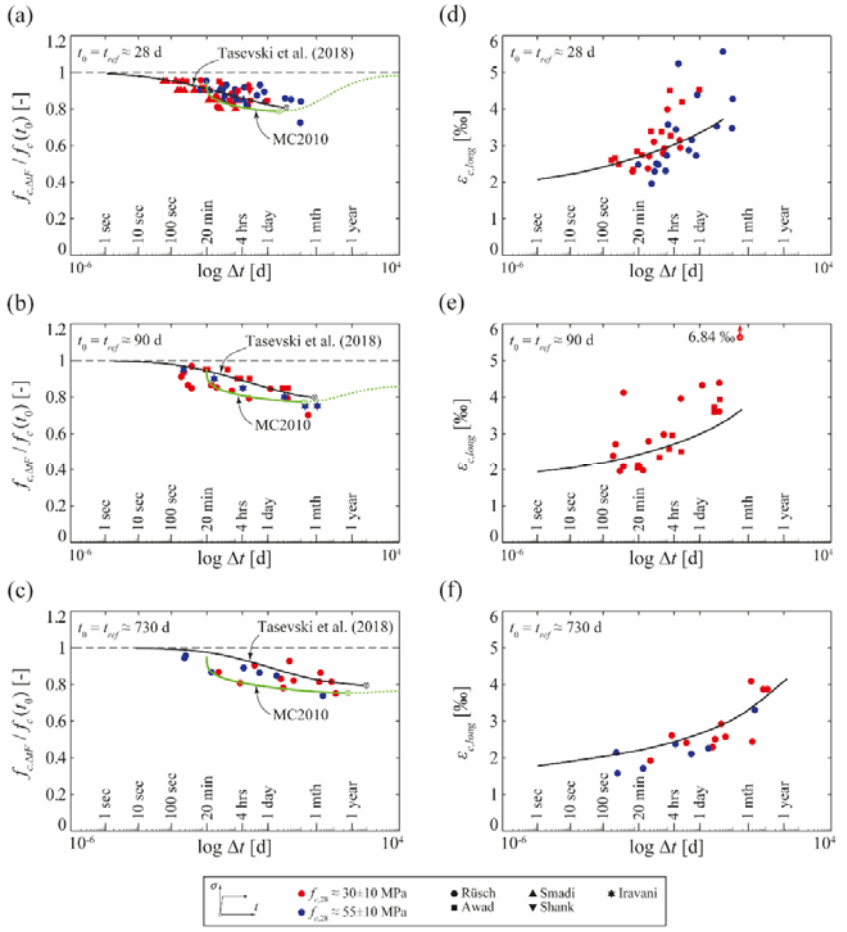

Fig. 14 Comparison of experimental data points with the theoretical model [13] (solid black lines, Tasevski et al. [13]) and *fib* MC2010 (Eq. (**13**)), solid green lines) for constant sustained stress (s = 0.25 chosen as an average for all test results of this comparison)

Fig. 14 also plots the results of the model by Tasevski et al. [13] (black solid curves in *Fig. 14*). This approach yields to a smooth and gradual reduction of the strength with increasing times of application of the load.

Accounting for these facts, it is considered that current *fib*'s MC2010 formula can be improved to yield to more consistent predictions of the behaviour and to expand its range of validity to short-time applications of the load (lower than 20 minutes). On the basis of the results presented in section 3.1 and *Fig. 14* and by analysis of the results, the following analytical expression is proposed for the phenomenon of strength reduction due to high levels of sustained loading:

$$\boldsymbol{\beta_{c,sus}(t_0,\Delta t_F) = \lambda(t_0) + \frac{1-\lambda(t_0)}{\left(1+k_2\frac{\Delta t_F}{t_0}\right)^{1/k_1}}} \tag{17}$$

This expression is derived by fitting of the numerical predictions of the general model by Tasevski et al. [13] with a simple analytical equation depending both on t_0 and Δt_F. It can be noted that Eq. (**17**), differently to Eq. (**16**), shows an explicit dependence on t_0 as: (1) the inelastic strain development is based on a creep model that depends on t_0 and Δt_F, and a monotonic response that depends on t_0; (2) the failure envelope depends on the monotonic response which is calculated at $t_0+\Delta t_F$.

With respect to the parameters of Eq. (**17**), the values $k_1 = 10$; $k_2 = 10^4$ and $\lambda(t_0) = 0.64 + 0.01\cdot\ln(t_0)$ (with t_0 in days) can be adopted yielding to overall accurate and

consistent results. A comparison of the results of the model by Tasevski et al. [13] and those of Eq. (**17**) can be seen in *Fig. 15*. A nice agreement is found, yielding in addition to a good approximation of the sustained load strength (values about 80% of the reference strength, indicated with a circle in *Fig. 14*). It shall be noted that *Fig. 15* presents the failure of concrete under constant levels of stress. Cases where the material does not fail and additional loading can be applied will be discussed in section 4.

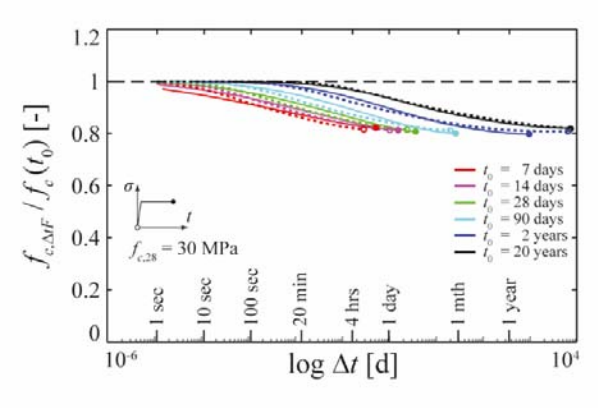

Fig. 15 Comparison of theoretical model [13] (solid lines) and analytical Eq. (**17**) (dashed lines) for a constant sustained stress ($f_{c,28}$ = 30 MPa and s = 0.25)

4 Concrete strength for different loading patterns

4.1 Introduction

Despite the fact that most research on the topic of nonlinear creep behaviour has been performed on specimens loaded under a constant sustained stress (*Fig. 1*c), structures are seldom subjected to such type of loading. On the contrary, refer for instance *Fig. 1*b, most structures are subjected to other loading patterns. With this respect, three loading patterns can be identified as particularly relevant for practice: approximately monotonic stress rates (*Fig. 16*a, typically referring to the construction sequence); approximately monotonic stress rates after application of a first loading ramp (*Fig. 16*b, typically referring to the application of dead loads after construction) or loading patterns with a rapid increase of load after a period of quasi-sustained loading (*Fig. 16*c, typically referring to live loads in addition to permanent loads).

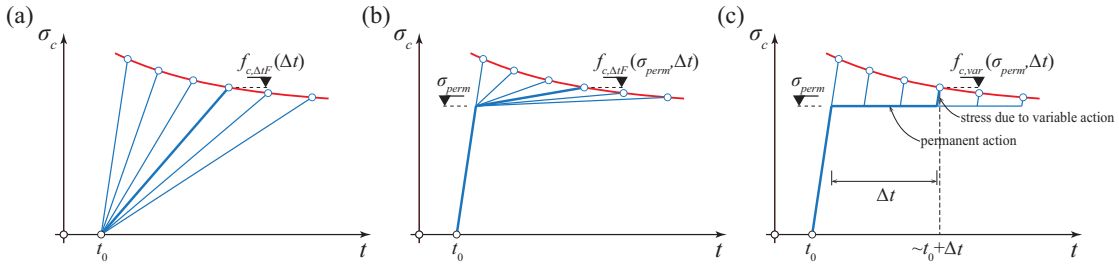

Fig. 16 Investigated loading patterns: (a) stress rate without initial loading; (b) stress rate with initial rapid loading; and (c) additional loading after a period of sustained loading

With reference to these patterns, design codes usually provide no general method to assess their structural response accounting for the progression of material damage with time. In addition, refined and general approaches (as the one of Tasevski et al. [13]) may be too complex for their application in practice. In the following, a simple methodology to calculate the response of a structure subjected to a general loading pattern will thus be presented. The approach is based on the Palmgren-Miner's rule, whose pertinence will be justified from a theoretical perspective and by comparison to test results. By making use of this tool, the various loading patterns relevant for practice shown in *Fig. 16* will be investigated (cases (a-b) in section 4.3 and case (c) in section 4.4).

4.2 The Palmgren-Miner's rule for linear damage accumulation

The concept of linear damage theory was initially developed by Palmgren [67] in 1924 and extended later by Miner [68] in 1945, being widely used thereafter to describe the fatigue life of engineering materials [69]. Its main assumption considers that, when a material is subjected to a given stress amplitude, the damage accumulation is in linear correlation with the cycle ratio, i.e. $D = (N/N_F)$, where N refers to the number of cycles elapsed with a given stress amplitude and N_F is the number of cycles that leads to failure for that stress amplitude. For variable amplitude fatigue loads, the total accumulation of damage D would thus read:

$$\boldsymbol{D = \sum_{i=1}^{n} \frac{N(\sigma_i)}{N_F(\sigma_i)}} \tag{18}$$

where i is the index of the i-th amplitude (stress level σ_i), and the occurrence of failure would be given when $D = 1$.

It is worth noting that Palmgren-Miner's formulation of damage does not account for the order in which the different stress levels are applied, which has been reported as a drawback of this rule [69]. Also, there is actually no thoroughly mechanical justification grounding it. Another reported drawback is the linearity assumption of damage accumulation for all stress levels [70]. Hence, some authors have contested the applicability of the Palmgren-Miner's rule for concrete, especially in the case of variable amplitude loadings and complex loading patterns [63], [69], [71]–[73]. Despite these drawbacks, the Palmgren-Miner's rule has still been widely used due to its simplicity and reasonable fitting to test results, and is for instance acknowledged in *fib* Model Code 2010 [38] for detailed fatigue verifications.

With respect to the failure of concrete under variable sustained stress (low stress and strain rates), the Palmgren-Miner's rule can be applied by analogy to the case of fatigue life estimation under variable stress amplitudes, reading:

$$\boldsymbol{D = \sum_{i=1}^{n} \frac{\Delta t(\sigma_i)}{\Delta t_F(\sigma_i)} \; (= 1 \;\; \text{at failure})} \tag{19}$$

where $\Delta t(\sigma_i)$ is the duration of the i-th level of sustained stress σ_i and $\Delta t_F(\sigma_i)$ is the associated failure time for the same constant level of sustained stress (normally only occurring for stress levels above $\sigma_c/f_c = 0.75$). The sum can also be written in an integral form in the following manner:

$$\sum_{i=1}^{n} \frac{\Delta t(\sigma_i)}{\Delta t_F(\sigma_i)} = \int_0^{\Delta t} \frac{dt(\sigma)}{\Delta t_F(\sigma)} \tag{20}$$

In the following sections, the Palmgren-Miner's rule will be used in combination with Eq. (17) proposed in Section 3.2 for calculation of the time to failure (Δt_F) for a given level of sustained load.

4.3 Application to a constant stress rate with and without initial stress level

To apply the Palmgren-Miner's rule presented in section 4.2, the accumulation of damage can be integrated by means of a discretization of the loading history in time steps. *Fig. 17* shows for instance the case of a constant stress rate without and with an initial stress level (σ_{perm}, refer to *Fig. 17*a and *Fig. 17*b respectively). According to the Palmgren-Miner's rule, the first load steps generate low or no damage in the material. The stress level at failure for a given duration of the loading pattern is consequently higher than the one corresponding to a sustained loading pattern (refer to the solid and dashed lines in *Fig. 17*). When an initial stress level is applied (*Fig. 17*b), the first load steps generate more material damage and the failure stress is consequently closer to that of a constant sustained loading.

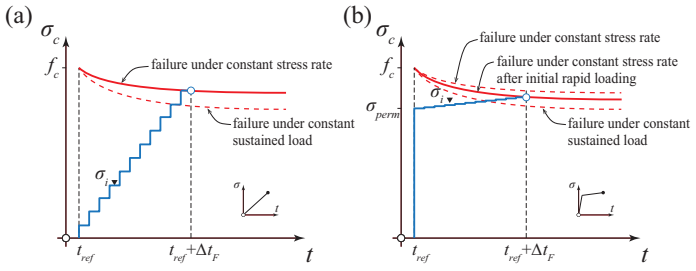

Fig. 17 Example of a numerical discretisation scheme for the Palmgren-Miner's rule for loading case of a constant stress rate: (a) no initial preload; (b) with initial preload

The results for these loading cases are investigated in *Fig. 18*a and *Fig. 18*b (case without rapid preloading and with a rapid preloading $\sigma_{perm} = 0.5 \cdot f_c$), comparing the numerical predictions of the mechanical model from Tasevski et al. [13] (solid lines) and the integration of Eq. (**17**) by means of the Palmgren-Miner's rule (dashed lines). The results show fine agreement for the different regimes: when the strength decays (damage governing, higher strain rates) and when the strength increases (continued cement hydration governing, lower strain rates). Values above one are also possible for significant strength increase due to continued cement hydration (typically associated to rather low strain rates). A comparison to the test results on variable stress rates from Tasevski et al. [13] (with and without rapid preloading) is also plotted in *Fig. 18*c and *Fig. 18*d, showing sound agreement for the different cases investigated. It can be noted that the results of the model are in good agreement with the test results even for very low times of application of the load, despite the fact that the creep model used [13] (*fib*'s MC2010) has not been calibrated to precisely describe these cases.

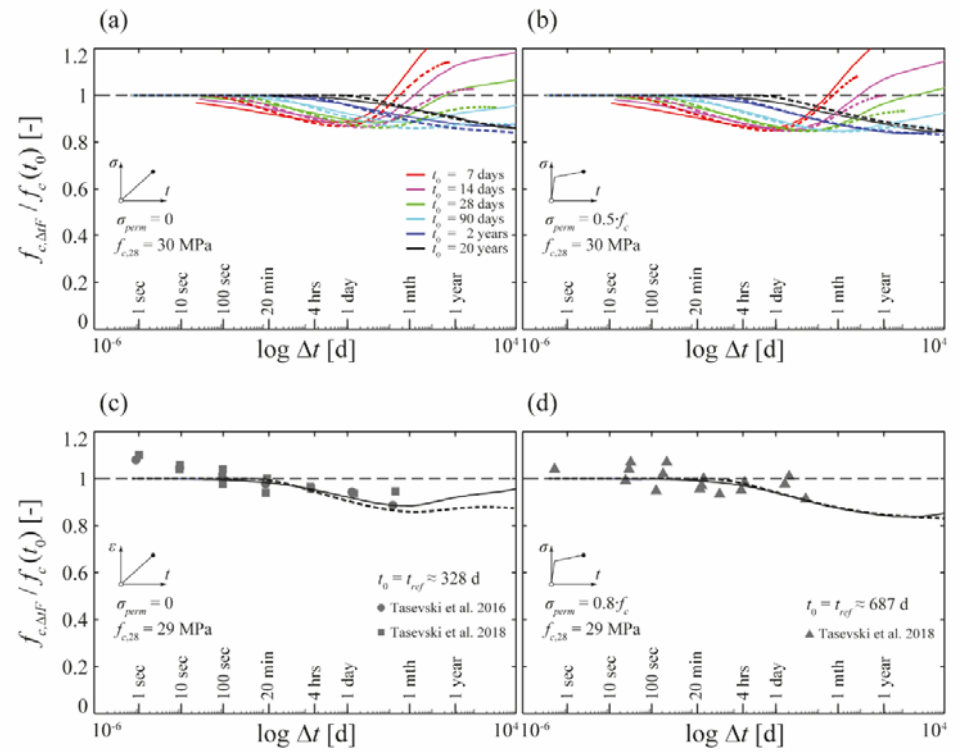

Fig. 18 Comparison of the theoretical model [13] (solid lines) and the analytical approach based on the Palmgren-Miner's rule (dashed lines) for constant stress rate with (a) no preload and (b) a preload of $\sigma_{perm} = 0.5 \cdot f_c$; comparison to test results from Tasevski et al. [13] for: (c) no preload and (d) a preload of $\sigma_{perm} = 0.8 \cdot f_c$. ($s = 0.25$)

4.4 Application of a rapid additional loading after a period of sustained load

Another loading pattern of practical relevance corresponds to the case when additional rapid loading is applied after a period of permanent sustained loading (*Fig. 16*c). When the levels of permanent load are high (*Fig. 19*a-c), material damage ($\varepsilon_{cc,in}$ in *Fig. 19*b) develops and the strength reduces accordingly [14] (see *Fig. 19*b), with reducing strength for increasing levels of damage. At failure, the total applied stress (σ_{tot}, comprising the effect of permanent and variable actions) equals the compressive strength accounting for the detrimental effect of sustained loading and the beneficial effect of continued cement hydration.

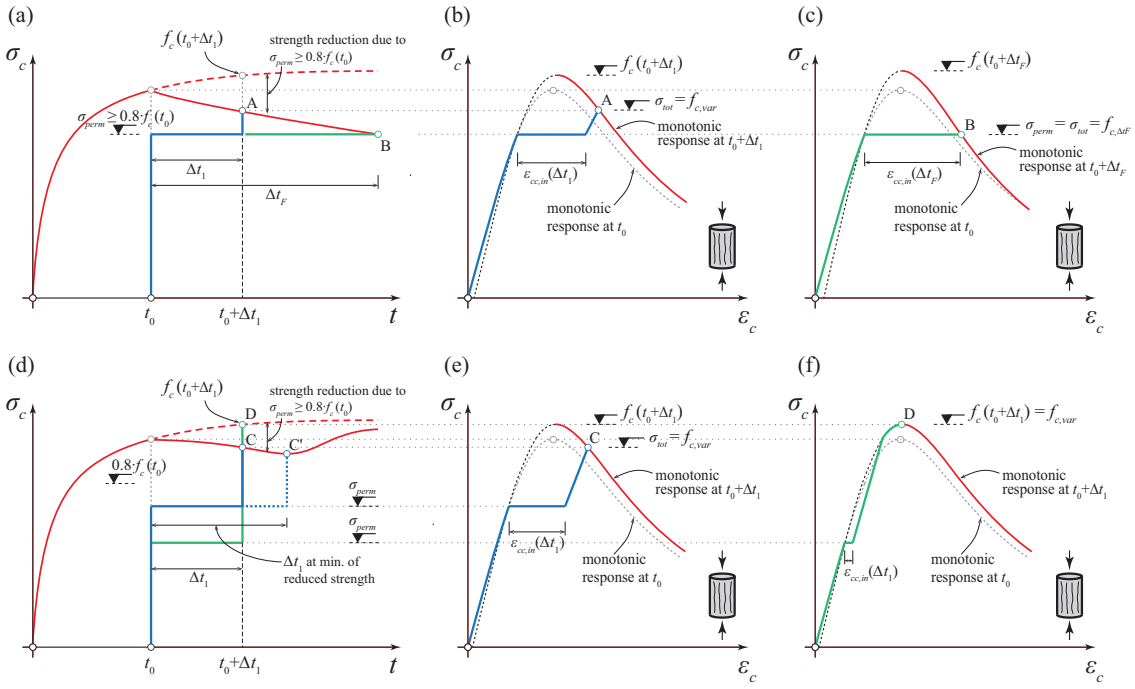

Fig. 19 Response of concrete for the application of a variable action after a period of sustained load: (a) loading patterns for σ_{perm} levels above the sustained load strength; (b-c) corresponding stress-strain responses; (d) loading patterns for σ_{perm} levels below the sustained load strength; (e-f) corresponding stress-strain responses

For practical purposes, two situations may be relevant with respect to this loading pattern:

Application of the variable action after a permanent stress level (σ_{perm} in *Fig. 19*a) above the threshold of failure under sustained load. In this case (point A in *Fig. 19*a), large material damage occurs associated to reductions of the material strength (resulting in $\sigma_{tot} < f_c(t_0+\Delta t_1)$, see *Fig. 19*b). In any case, if the permanent action were applied for a sufficiently long period of time, a delayed failure of the material would occur even without the application of the variable action (point B in Fig. 19a and c).

Application of the variable action after a permanent stress level (σ_{perm} in *Fig. 19*d) below the threshold of failure under sustained load. In this case, if the stress level is sufficiently low, the material will suffer no (or very limited) damage and no strength reduction will be apparent ($\sigma_{tot} = f_c(t_0+\Delta t_1)$, point D in *Fig. 19*f). However, in some cases (for permanent stress levels close to the sustained load strength, Fig. 19e), a certain material damage can occur and this can potentially lead to a reduction of the material strength when the variable action is applied (point C in *Fig. 19*d-e). In this case, as the continued cement hydration eventually compensates for the material damage due to the sustained loading, a minimum value to the strength can be found (represented as point C' in *Fig. 19*d).

For the former situation (*Fig. 19*a-c), the envelopes of the reduction of strength (points A) for a constant level of permanent stress (σ_{perm}) are plotted in *Fig. 20*a. The case corresponding to the permanent stress level equal to the sustained load strength is represented by the green curve, while cases with higher levels of permanent load are plotted as grey curves. The dark grey area in the top right corner of *Fig. 20*b denotes thus the area where a failure under permanent load is possible even if no variable actions were applied.

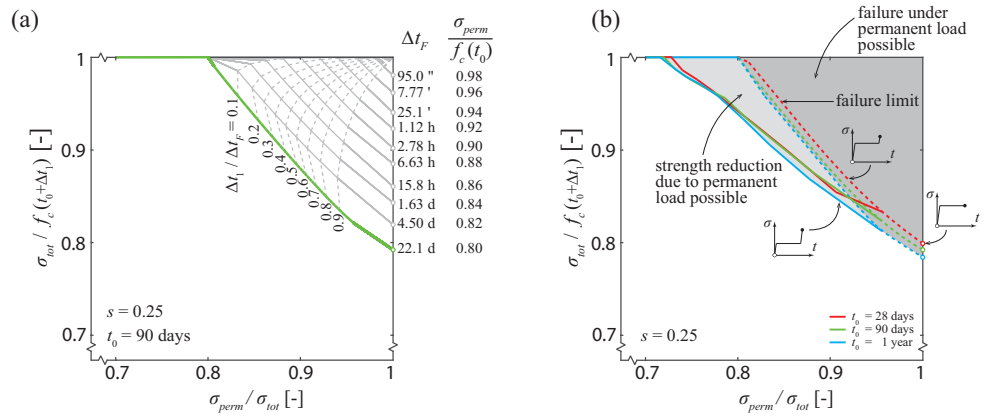

Fig. 20 Response of concrete for the application of variable action after a period of sustained load: (a) envelopes of the reduction of strength for σ_{perm} level above the sustained load strength; (b) areas of danger of strength reduction with and without failure danger.

It is interesting to note that similar shapes of the curves (almost linear) and strength reductions are found for other times of application of the permanent load (t_0, refer to the red and blue dashed curves in *Fig. 20*b).

For the case of permanent stress levels below the sustained load strength of concrete (no delayed failure under only permanent load), the solid curves in *Fig. 20*b represent the envelopes of minimum material resistance after application of the variable action (points C' in *Fig. 19*d). The shape of these curves can again be reasonably approximated by a linear segment, defining the region where a reduction on the concrete strength can potentially happen due to the damage developed during the application of the permanent stress level (refer to the area shaded in light grey in *Fig. 20*b). It is interesting to note that for ratios $\sigma_{perm} / \sigma_{tot} < 0.75$ no strength reduction is to be accounted for. Above this threshold, safe design can be performed by considering a linear reduction (up to 20%) of the uniaxial compressive strength. This can be considered in the format of a simplified expression for practical application as follows (a design approach consistent with SIA 262:2013 format is presented in Chapter 8):

$$\frac{\sigma_{tot}}{f_c(t_0+\Delta t_1)} = 1.0 \quad \text{if } \frac{\sigma_{perm}}{\sigma_{tot}} \leq 0.75$$

$$\frac{\sigma_{tot}}{f_c(t_0+\Delta t_1)} = 1.6 - 0.8\frac{\sigma_{perm}}{\sigma_{tot}} \quad \text{if } \frac{\sigma_{perm}}{\sigma_{tot}} > 0.75 \tag{21}$$

It can be noted that for total levels of stress $\sigma_{tot} \leq 0.75 \cdot f_c(t_0+\Delta t_1)$, there is no strength reduction.

4.5 Deformation capacity and redistribution of internal forces

Due to the fact that the development of nonlinear creep strains at high stress levels may potentially lead to failure under sustained load, this phenomenon has traditionally been considered as a detrimental effect for concrete. With this respect, it shall nevertheless be noted that the development of nonlinear creep increases the deformations of the material at a non-proportional rate with respect to regions where linear creep governs. This phenomenon can be observed in *Fig. 3*a, where the curve defining the creep limit (deformations of the material accounting for instantaneous and creep strains) loses the proportionality for stress levels above 40% of the (short-term) compressive strength of the material. Some test results as well as the predictions of the theoretical model by Tasevski et al. [13] with respect to this phenomenon can also be seen in *Fig. 14*d-f, where the deformation capacity at peak load is plotted as a function of the load duration.

As a consequence of this nonlinear response in terms of strains, redistributions of stresses can occur between regions deforming more (those subjected to high level of stresses and developing nonlinear creep strains) and those deforming less (those subjected to a linear creep response). This is a potentially beneficial influence of the development of nonlinear creep strains as it contributes reducing the stress level at the most stressed regions.

One clear example of this beneficial influence can be observed in the compression zone of members in bending, where the outermost compressed fibres reduce relatively their stress due to nonlinear creep. As experimentally observed [8], [74], this phenomenon justifies why adopting a parabolic/constant stress distribution in the compression zone due to bending is more realistic than adopting one based on the short-term material response and considering a linear profile of strains [75], see *Fig. 21*.

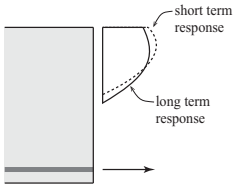

Fig. 21 Compression zone of a member in bending with stress distribution under short-term and long-term loading

Another example where this phenomenon is significant refers to the response of reinforced concrete columns with limited 2nd order effects. In these cases, governed by the compressive strength of concrete and by the presence of the longitudinal reinforcement steel, the additional deformation due to creep allows to increase the contribution of the compression reinforcement located at some distance from the most compressed fibre (which is potentially not yielded when concrete crushes under rapid loading conditions). Thus, while slow loading rates or sustained loading may be detrimental for the strength of columns with low longitudinal reinforcement ratios (low contribution of the reinforcement to the overall strength), it may be beneficial for columns with large reinforcement ratios (additional contribution of the reinforcement compensating for the decrease of the concrete contribution).

5 Practical design considerations for the concrete strength

5.1 Implications for codes of practice

In codes of practice, the design compressive strength of concrete is used in a number of situations such as (i) the resistance of axially-loaded members (e.g. columns), (ii) the compression zone due to bending, (iii) the compression field due to shear in webs of girders and beams, (iv) the strut resistance when designing using strut-and-tie models or stress fields and (v) partially loaded areas (e.g. introduction of bearing or prestressing forces). For all these cases, design equations used in codes of practice have been validated and calibrated on the basis of laboratory tests. Since these tests are usually conducted in a period varying between approximately 20 minutes and some hours, it can be stated that the structural design formulas for verification at ultimate limit state already partially account in an implicit manner for the detrimental influence of low stress or strain rates. *Fig. 22* shows for instance that for typical test durations and typical specimen ages, it can be assumed a compressive concrete strength decrease between 4% - 8% compared to a material test duration of approximately 2 minutes (according to ISO 1920-4:2005 [10]). For this reason, the strength ratio at failure previously discussed ($\sigma_{tot} / f_c(t_0+\Delta t_1)$) may be corrected by increasing it by approximately 6% when formulas for design of structural elements are used. Thus, in the previous Eq. (21), this effect can be accounted for by shifting the curve in the following manner:

$$\frac{\sigma_{tot}}{f_c(t_0+\Delta t_1)} = 1.0 \quad \text{if } \frac{\sigma_{perm}}{\sigma_{tot}} \leq 0.85$$

$$\frac{\sigma_{tot}}{f_c(t_0+\Delta t_1)} = 1.85 - \frac{\sigma_{perm}}{\sigma_{tot}} \quad \text{if } \frac{\sigma_{perm}}{\sigma_{tot}} > 0.85 \tag{22}$$

where design values for the stress and material strength shall be considered (reduction of red line and increase of blue line in *Fig. 1*b). As a consequence, for the case $\sigma_{perm} / \sigma_{tot} = 1$, the limit stress value shifts from 0.80 (Eq. (21)) to 0.85 (Eq. (22)). It can also be noted that, for practical purposes, the stresses indicated in Eq. (22) are normally replaced by a generalized stress (internal forces).

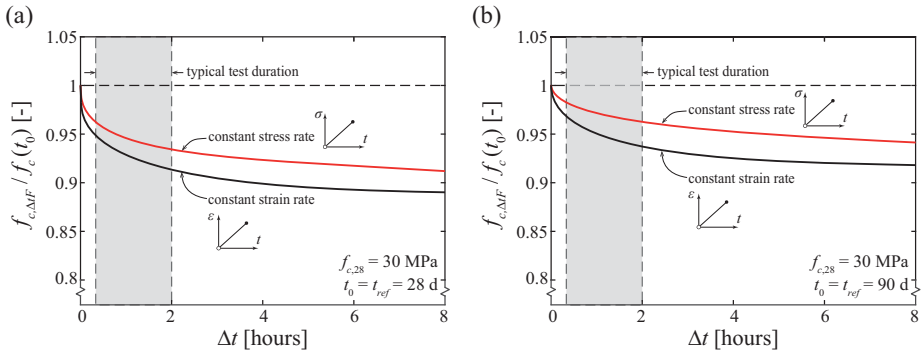

Fig. 22 Influence of test duration on the compressive strength of concrete for constant stress and strain rates for: (a) t_0 = 28 days; (b) t_0 = 90 days (calculated according to the approach of Tasevski et al. [13])

5.2 Design versus assessment

As already introduced, for design of new structures, codes of practice usually assume that the detrimental effect of sustained loading is compensated by the strength increase due to

continued cement hydration. This fact is investigated in *Fig. 23* for the most critical loading case ($\sigma_{perm} / \sigma_{tot} = 1$) and with reference to different types of cement (defined by the parameter s characterizing the rheology of cement hydration and thus the increase of concrete strength with time [38]). The results are calculated on the basis of the refined rheological approach by Tasevski et al. [13] and assuming Eq. (14) for calculation of the continued cement hydration (refer to black curves in the diagrams for the material compressive strength for rapid loading). In the figures, several cases are presented corresponding to the application of a sustained load at different ages. It can be observed that, for a given t_0, the strength decreases as the time of application of the sustained load increases, reaching an envelope curve (red curves in *Fig. 23*) at approximately 80% of the rapid loading strength.

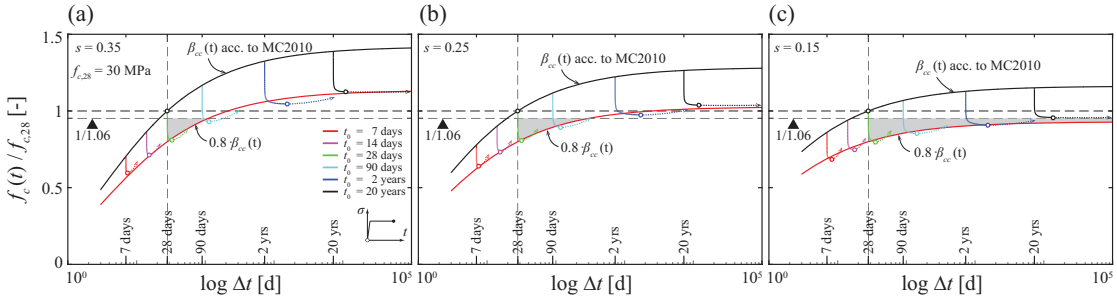

Fig. 23 Influence of the age of loading on the delayed failure under sustained load ($f_{c,28}$ = 30 MPa): (a) s = 0.35 (low early strength class concrete); (b) s = 0.25 (ordinary early strength class concrete); and (c) s = 0.15 (high early strength class concrete)

It can be noted that the assumption that the detrimental effect of the sustained load on the compressive strength is compensated by the continued cement hydration is valid only when the time of load application t_0 is sufficiently large (refer to the construction sequence in *Fig. 1*b). With this respect, the areas shaded in light grey in *Fig. 23* refer to the period when the sustained loading effect is not fully compensated by the continued cement hydration. In addition, the time when the concrete strength is not fully compensated depends significantly on the value of parameter s. For instance, considering a t_{ref} = 28 days (see *Fig. 23*), the full compensation of the strength occurs after 4 months for s = 0.35 (low early strength class concrete) and two years for s = 0.25 (ordinary early strength class concrete). For the case of s = 0.15 (very high early strength class concrete), the continued cement hydration does not even appear to fully compensate for the effects of sustained loading.

With this respect, and as previously discussed, it shall be noted that for design of structural members (columns, bending, shear in webs…) the detrimental effect of sustained loading is already partially accounted for in the design equations. This implies that, for design of structural members, the period where the continued cement hydration does not fully compensate for the sustained loading effect can in fact be assumed shorter than for the material response. This can be seen in *Fig. 23*, where the corrected ratio between the failure under sustained load strength (1/1.06 discussed in Section 5.1) is also plotted.

For assessment of existing structures, the approach to be followed is very different to that for design. The concrete strength is in this case usually updated by means for instance of core samples extracted from the actual structure at a time t_{ref} much larger than 28 days (normally some years or decades after construction). Consequently, the concrete strength increase due to continued cement hydration can be reasonably neglected and, if the sustained loading is governing ($\sigma_{perm} \approx \sigma_{tot}$), then a conservative value $\sigma_{tot} / f_c(t_0+\Delta t_1) = 0.85$ (≈0.8·1.06) should be assumed. This assumption is obviously safe and when variable (rapid) actions may have significant relevance, a more refined estimate of the strength can be obtained by means of Eq. (21) and Eq. (22) (material and structural levels respectively).

For more complex loading patterns or when more accurate estimates of the strength reduction shall be obtained (both for design and for assessment), the general approaches

described in this report (using the Palmgren-Miner rule or the general rheological approach by Tasevski et al.[13]) can for instance be used.

5.3 Influence of time of application of variable loads on the strength of concrete

The case of application of a variable action after a period of sustained load was investigated in Section 4.4 by considering the variable action as instantaneous. However, this might not be the case in many design situations, where the variable actions might be applied during some minutes, hours or even days (refer to point E in *Fig. 24*a).

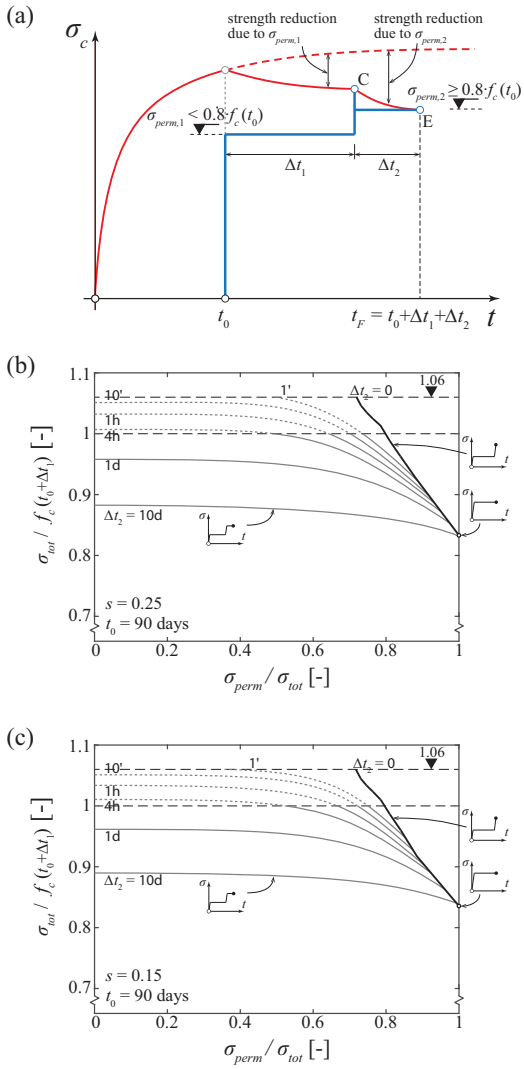

Fig. 24 Influence of the duration of the application of the variable load: (a) load pattern; (b-c) strength reductions (for structural design) as a function of the duration of the variable action

In a general manner, the influence of the duration of the application of the variable load on the concrete strength can be addressed by using the general procedures presented in this report. *Fig. 24*b-c show for instance the results calculated by using the refined model of Tasevski et al. [13] with reference to two values of parameter *s* (0.25 and 0.15 respectively, values for *s* = 0.35 being almost identical to those of *s* = 0.25). In those figures, the factor increasing the strength by 6% has already been considered, in order to be consistent with

the application of these results to design formulas (referring normally to generalized stresses or internal forces). The results show that a reduction on the strength can already be noted for relatively low times of application of the variable load and that it can clearly be appreciated for durations of the variable load of some days. The ratio $\sigma_{perm} / \sigma_{tot}$ also plays a significant role, by reducing notably the strength for ratios $\sigma_{perm} / \sigma_{tot}$ above 0.6.

6 Experimental programme on shear in members without transverse reinforcement

6.1 Aims of the programme

As stated in section 1.2, there are scanty experimental data on the shear strength of reinforced concrete members subjected to high levels of sustained load. In order to investigate the phenomenon in a comprehensive manner, a specific testing programme has been designed and performed.

Sixteen beams have been tested in total, divided in two series, the first one comprising eight slender beams (shear span to effective depth ratio a/d = 3.5) and the second one comprising eight squat beams (a/d = 1.0). The failure process and the development of the corresponding cracking patterns have been observed in detail by means of Digital Image Correlation (DIC) measurements.

6.2 Materials and specimens

The specimens investigated were reinforced concrete beams with a rectangular cross section ($b \times h$ = 250 × 600 mm) and a flexural reinforcement ratio ρ = 1.33%. The flexural reinforcement was composed of 3 bars diameter 28 mm placed at an effective flexural depth of 556 mm. The reinforcement was made of high-strength cold worked steel with an average yield strength f_y = 713 MPa (corresponding to the 0.2% proof stress [39]). Neither shear nor compressive reinforcement were used.

Normal-strength concrete was used for all specimens. The average compressive strength at 28 days (measured in cylinder $Ø \times h$ = 160 × 320 mm) resulted $f_{c,28}$ = 29 MPa. It was produced with a CEM-II 42.5R cement (w/c = 0.56) and river aggregates (maximum aggregate size d_g = 32 mm). The beams were cured during 18 days and stored under controlled-ambient laboratory conditions until the day of testing (temperature of 21±0.5 °C and relative humidity of 65±3 %).

The concrete strength at the time of testing for each series and specimen can be consulted in *Table 3* and *Table 4*. The development of concrete strength, shrinkage strains and linear creep coefficient with time can be consulted in section 3.1.1 (the beams have been produced from the same concrete batch as the cylinders).

6.3 Test setups

The test setups are shown in *Fig. 25*. The slender beams were tested as cantilevers where the test specimens were clamped to the testing frame by prestressing four vertical bars diameter 50 mm (see *Fig. 25*b) whereas the squat beams were tested as simply supported members. In both cases, the load was applied at the end support of the beams with a servo-hydraulic jack (capacity 2000 kN) pushing upwards. In the case of the squat members, the beams were retained in the middle by four bars diameter 50 mm.

The shear force was measured at the load introduction between the jack and the beam by means of a load cell (capacity of 500 kN, 0.1% noise level). Additional measurements were conducted with load cells at the vertical prestressing/retaining bars and between the beam and the testing frame in the case of the slender members. Both measurements were compared with consistent agreement (differences lower than 4%). In the following, the measurements of the shear force will be given between the jack and the beam at the end support. All tests were performed under controlled-ambient laboratory conditions (same conditions than before testing).

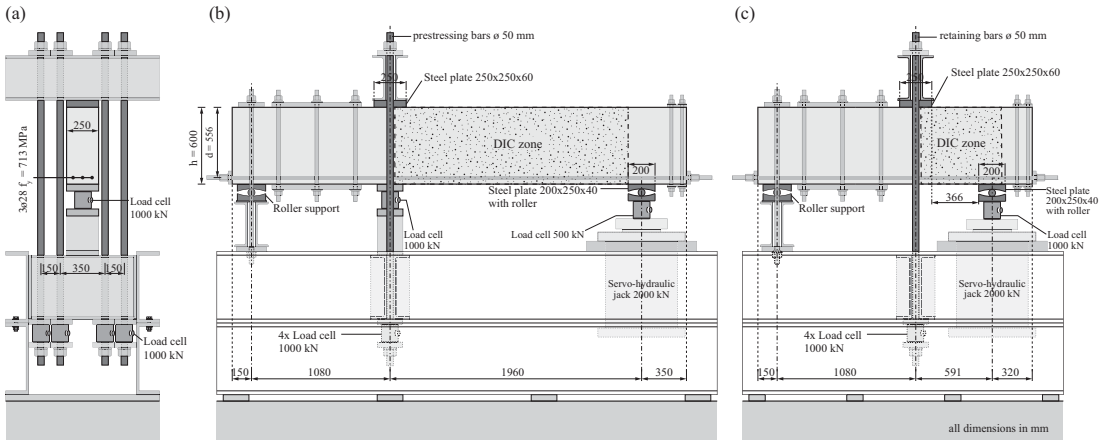

Fig. 25 Test setup: (a) section; (b) side view for slender beams; and (c) side view for squat beams

Photogrammetric (DIC) measurements setup

The development of the cracking pattern in the shear critical zone was tracked by means of 3D DIC (*Fig. 25*). The DIC hardware consisted of a pair of CMOS sensor cameras (model jAi SP-20000-USB, 20 Mpix), which, in combination with green lighting, had low sensitivity to day-night luminosity changes for the long-term tests.

The image acquisition was performed every 2 kN (ca. 1/100 of the failure load) for the slender beam series and 4 kN (ca. 1/250 of the failure load) for the squat beam series. Close to failure, the acquisition of images was increased to a frequency of 8 Hz.

A random speckle pattern with an approximately constant density was applied on the beam surface by means of spray painting. Depending on the camera distance, the size of the speckles was 1.5±0.5 mm for the slender beam series and 0.8±0.3 mm for the squat beam series (the physical pixel size was of approximately 0.36 mm and 0.25 mm respectively). The deformation analysis was performed with the Vic3D software (Correlated Solutions [76]), using a subset size of 23 × 23 pixels and 21 × 21 pixels for the slender and squat beam series respectively. The stable ambient control and the consistent calibration procedure helped to keep the error of displacement measurements below 1/75 of a pixel.

Loading patterns

Two loading patterns were used. The first one corresponds to a constant displacement rate at the load introduction at the end support up to failure, applied on specimens RT1.05 - RT5.01 of the slender beam series and specimens RT11.24 – RT15.17 of the squat beam series (for specimen RT15.17 the deflection rate was however changed to a lower one at V_{exp} = 250 kN).

The second type of loading pattern consisted of a preloading at a constant displacement rate up to a certain load level, followed by a constant load rate afterwards. For the slender beams, the change of the loading condition was applied at the moment when the flexural cracks started to develop in a quasi-horizontal manner above the neutral axis (120 kN for RT6.06 and RT8.18 and 100 kN for RT7.19). For the squat beams (RT16.15 – RT18.25), the change of the loading condition was applied at V_{exp} = 800 kN, which was the level at which the diagonal cracking developed. Details on the actual loading path in terms of applied shear force with time and corresponding deflection at the load introduction are provided in the following sections.

With respect to the high loading rates, failure occurred after some seconds of application of load (3.88 seconds as minimum loading time). Although such time was short, it allows neglecting any significant inertial effect in the results.

6.4 Results for slender beams (*a*/*d* = 3.5)

The time to failure and the measured shear strength of the slender beams are presented in *Table 3*. *Fig. 26* plots the normalized measured shear force versus the logarithm of time (*Fig. 26*a) and the deflection at the load introduction at the edge support (*Fig. 26*b). For low loading rates, a roughly constant normalized strength was observed. For higher loading rates, an increase on the shear strength was rather consistently observed. Overall, a reduction on the normalized shear strength of approximately 16% was measured between the highest (t_F = 3.88 s) and the lowest (t_F = 73.8 days) loading rates.

Table 3 Overview of the results of the slender beam series (round bracket value corresponds to first peak of specimen RT1.05, t_0 is the age of concrete at load application and t_F is the loading time at failure)

Beam	t_0	$f_c(t_0)$	t_F	$t_{F,100kN}$	V_{exp} / ($b \cdot d \cdot \sqrt{f_c}$)	V_{exp}
	[days]	[MPa]	[-]	[-]	[√MPa]	[kN]
RT1.05	359	36.4	3.88 (2.41) s	2.87 (1.40) s	0.262 (0.232)	219 (194)
RT2.04	352	36.4	11.4 s	6.87 s	0.240	200
RT3.03	327	36.3	104 s	60.2 s	0.222	186
RT4.02	283	36.0	19.5 m	12.0 m	0.238	200
RT5.01	268	35.9	5.70 h	3.08 h	0.213	179
RT6.06	460	36.8	1.01 d	0.88 d	0.195	165
RT7.19	494	36.9	13.8 d	13.7 d	0.207	175
RT8.18	1004	37.7	73.8 d	73.6 d	0.201	171

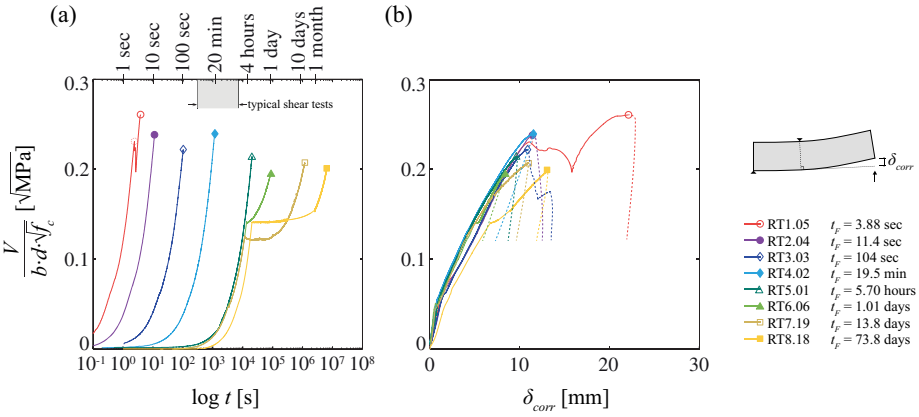

Fig. 26 Results of the slender beam series (*a*/*d* = 3.5): (a) normalized shear force vs. time in logarithmic scale; and (b) normalized shear force vs. deflection at the load introduction (corrected by removing the contribution to the deformation of the clamping device)

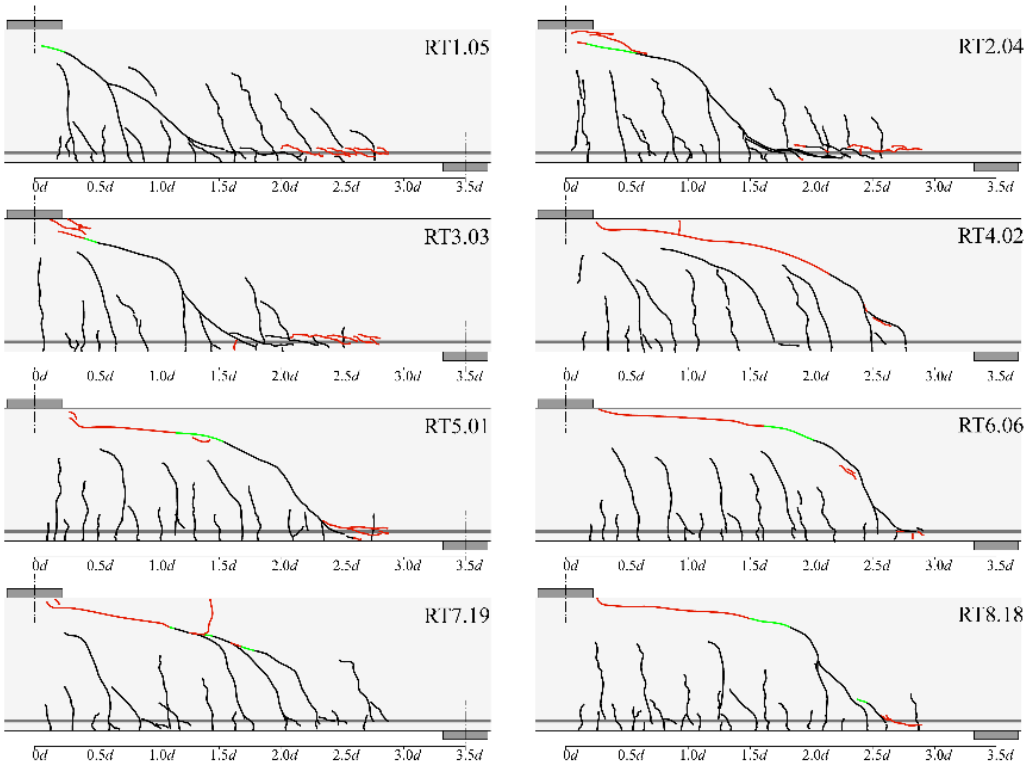

Fig. 27 Crack patterns of the slender beam series (a/d = 3.5). Green segments indicate stable post-peak development, red segments indicate unstable development.

Fig. 27 and *Fig. 28* present the cracking patterns and kinematics observed at different load levels using the DIC technique. The kinematics shown in *Fig. 28* refer to the crack opening and the relative tangential displacement between the two lips of a crack and is plotted as a vector for selected load levels (details on how the crack opening and displacements have been calculated can be found in [77]). These measurements allow calculating the shear transfer contributions due to residual tensile strength and aggregate interlocking as will be discussed later in this report. Two trends can clearly be observed depending mostly on the loading rate:

- For high loading rates (specimens RT1.05 – RT3.03), the critical shear crack (CSC) was located close to the mid-support region (between 1.0d – 1.3d from the mid-support axis). It started as a flexural crack and its length increased progressively for higher load levels. When the load was close to 90%–94% of the maximum strength (or first significant drop in the strength for beam RT1.05) other flexural cracks started to merge with it. Yet, an uncracked portion of concrete remained above the CSC and allowed the load to be partly carried by arching action. Failure of specimens RT2.04 and RT3.03 occurred by a crack developing diagonally through the inclined concrete strut near the load introduction region at the mid-support. The response of specimen RT1.05 was a bit different, as it experienced a first drop of load (sudden opening of the CSC probably associated to a loss of aggregate interlock capacity), but it could be reloaded and eventually failed at a higher load by the development of a delamination crack at the level of the flexural reinforcement.

- For both reference and low loading rates (specimens RT4.02 – RT8.18), the critical shear crack (CSC) was located at distances between 2.2d – 2.6d from the mid-support axis. After cracking of the beam, the CSC propagated to a certain length, where it almost stabilized (consistently to the observations of Cavagnis et al. [78]). Thereafter, the opening of the CSC increased for higher load levels. Close to the maximum load level, flexural cracks (and sometimes delamination cracks at the level of the flexural

reinforcement) merged with the CSC. After reaching the maximum load, the propagation of the CSC continued, becoming eventually unstable.

Fig. 29 plots the measured horizontal opening of the CSC at two different levels, namely at the level of the flexural reinforcement (sum of the horizontal openings of all cracks in the tributary length l_b, *Fig. 29*b) and at the distance of 0.4*d* from the upper edge (*Fig. 29*c). In agreement to the observations of Cavagnis [79] an almost linear profile can be observed for the development of the horizontal component of the crack opening, *Fig. 29*a. It can be observed that the total horizontal crack widths at the reinforcement level (opening u_A in *Fig. 29*b) increase for increasing moments (abscissa in *Fig. 29*b) in a similar manner as the experimental observations of Cavagnis [79] (refer to dashed straight line in *Fig. 29*b). As shown in [79], at failure, the horizontal component of the total crack opening (u_A) can be estimated by multiplying the reinforcement strain ($M_A/(A_s \cdot E_s)$) by a tributary length (l_b) that can be estimated as $l_b = d - c$ (where c refers to the thickness of the compression zone).

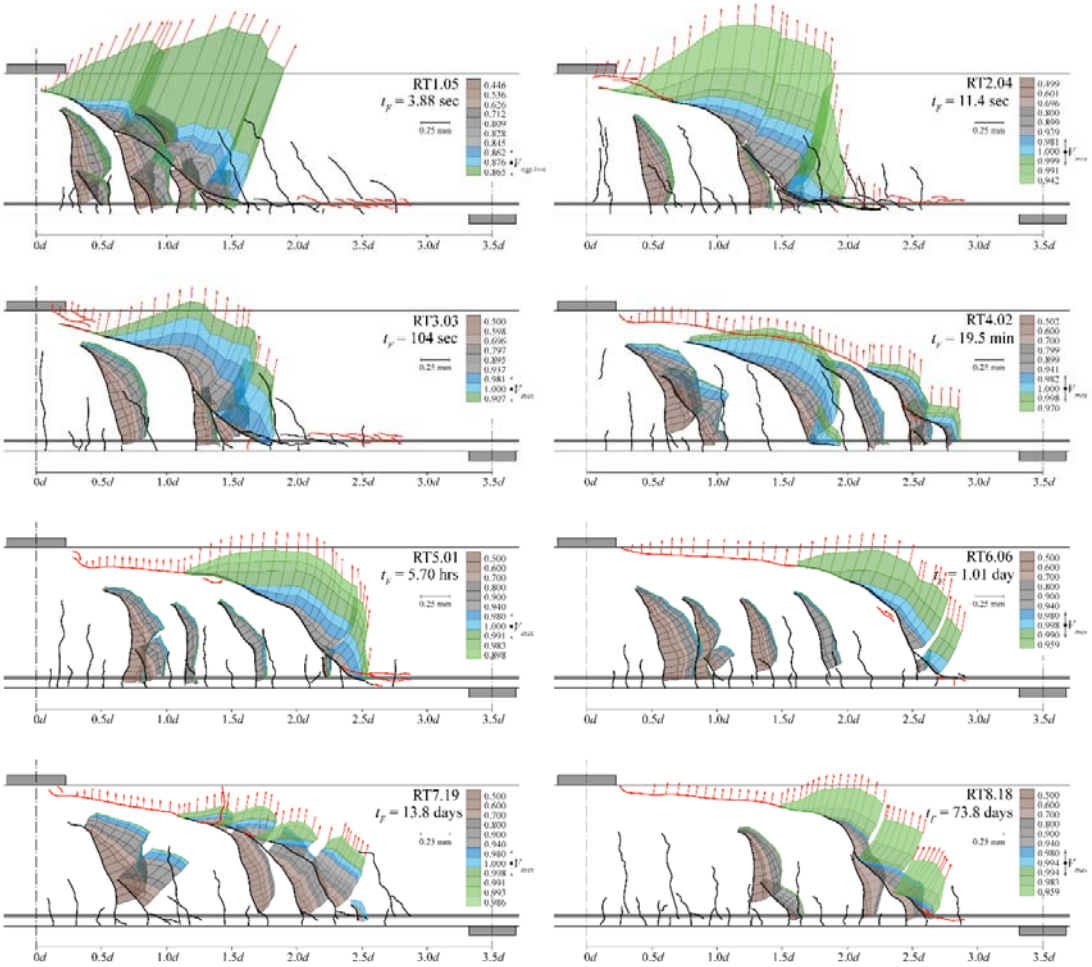

Fig. 28 Crack kinematics patterns of the slender beam series (*a*/*d* = 3.5). Green vectors indicate stable post-peak displacements, red cracks and red vectors indicate unstable behaviour.

When the analysis of the crack opening is performed at the level of the reinforcement (*Fig. 29*b) the results at failure are mostly dependent on the acting moment, but some influence of the crack opening is also observed with respect to the duration of the test, with low loading rates associated to larger crack openings (dots above the dashed line in *Fig. 29*b). With respect to specimen RT1.05 (plotted as a dashed line in *Fig. 29*b), the results are not strictly comparable to the others as two potential critical shear cracks developed and merged at the moment of failure. When such analysis of crack openings is performed in

the region where aggregate interlock is governing (approximately at 0.4*d* of the outermost compression fibre [48], see *Fig. 29*c), only a clear dependence of the crack width with the level of the acting moment is observed at failure, with no significant influence of the duration of the test. The fact that crack widths are relatively insensitive in this region to the duration of the test can be justified by the fact that two phenomena compensate due to concrete creep: the increase of the sectional curvature (increasing the strains) and the lowering of the neutral axis (decreasing the strains at that region).

With respect to the development of the cracks with time, it is important to note that the opening of the CSC was progressing in a rather stable manner until high levels of load (close to failure). This fact can be clearly observed in *Fig. 28*, where the opening until approximately 94% of the failure load is shaded in grey, between 94% and 100% in blue and after reaching the peak load in green (softening phase, unstable failure indicated with vectors in red). As it can be noted in that figure, aggregate interlock was significantly engaged in the last phases of loading (between 94% and 100% of the failure load, blue shaded areas in *Fig. 28*) when a rapid but stable opening and sliding of the CSC occurred. As a consequence, the transfer capacity due to aggregate interlock can be considered to have been significantly engaged when the specimen were close to failure, and its contribution shall thus be less influenced by large periods of sustained loading (similar conclusions on non-proportional activation of the various potential shear-transfer actions have been reported and verified elsewhere [48]).

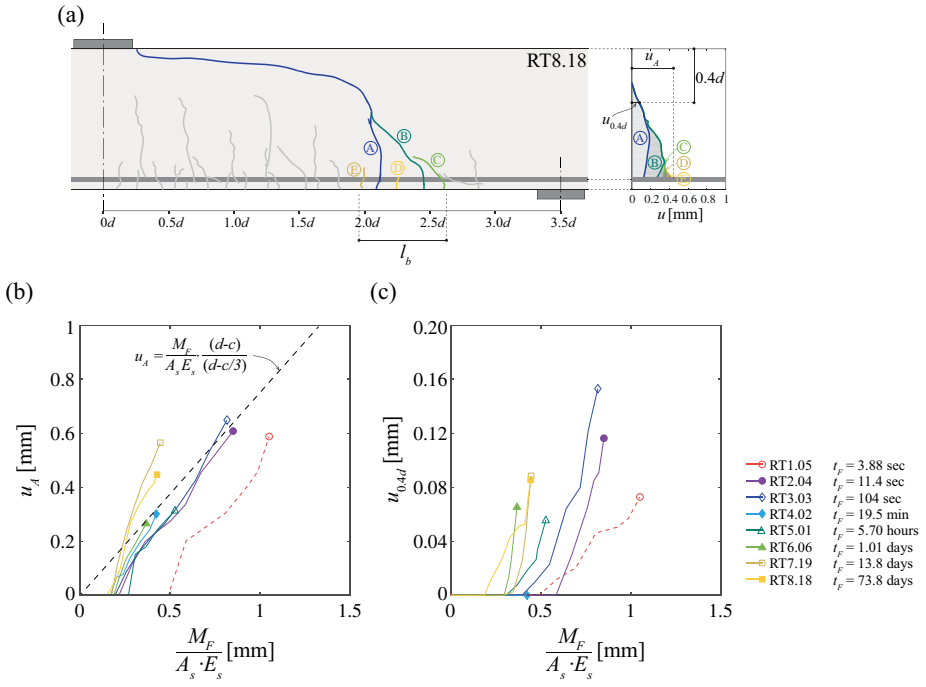

Fig. 29 Crack opening in the horizontal axis direction of the beam at different load levels of the slender beam series (*a*/*d* = 3.5): (a) definition of horizontal crack opening u_A and $u_{0.4d}$;(b) sum of horizontal openings at the level of the flexural reinforcement over the length l_b; and (c) horizontal openings at 0.4*d* from the outermost compression fibre

6.5 Results for squat beams (*a*/*d* = 1.0)

Fig. 30 gives an overview of the results of the squat beam series (*a*/*d* = 1.0) representing the measured normalized shear force versus the logarithm of time (*Fig. 30*a) and the deflection at the load introduction at the end support (*Fig. 30*b). With respect to the varying loading rate, particularly for low loading rates, no clear influence can be drawn on the measured shear strength. However, an overall increase of deflection due to creep effects

could be observed (almost 100% between the highest (t_F = 9.20 s) and the lowest (t_F = 5.70 days) loading rates).

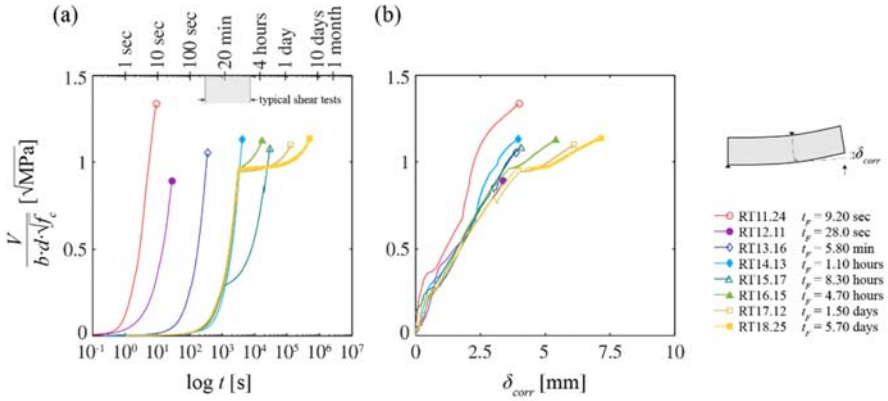

Fig. 30 Results of the squat beam series (a/d = 1.0): (a) normalized shear force vs. time in logarithmic scale; and (b) normalized shear force vs. deflection (corrected accounting for the deformation of the test setup and the specimen's rotation at middle section)

Table 4 Overview of the results of the squat beam series (t_0 is the age of concrete at load application and t_F is the loading time at failure)

Beam	t_0	$f_c(t_0)$	t_F	$t_{F,250kN}$	$V_{exp} / (b \cdot d \cdot \sqrt{f_c})$	V_{exp}
	[days]	[MPa]	[-]	[-]	[√MPa]	[kN]
RT11.24	718	37.4	9.20 s	7.40 s	1.34	1'136
RT12.11	697	37.3	28.0 s	19.7 s	0.890	756
RT13.16	613	37.2	5.80 m	4.00 m	1.05	893
RT14.13	683	37.3	1.10 h	47.1 m	1.13	959
RT15.17	696	37.3	8.30 h	7.90 h	1.08	918
RT16.15	640	37.2	4.70 h	4.40 h	1.13	956
RT17.12	646	37.2	1.50 d	1.50 d	1.10	933
RT18.25	750	37.4	5.70 d	5.70 d	1.13	964

Contrary to the slender beams, governed by the development of a single CSC, for the squat beams, a smeared cracking was consistently observed in the upper region of the inclined compression strut carrying shear (where it meets the flexural compression zone). *Fig. 31* shows the development of the cracking patterns for three representative specimens (RT11.24, RT12.11 and RT17.12), with several cracks developing in many cases in a quasi-parallel manner (the crack patterns of the other specimens are shown in appendix A). The direction and intensity of the measured principal compressive strains (blue vectors) and the crack openings (red vectors) are also presented in the same figures. According to the strain measurements, it can be noted that the strains are concentrated in a band between the load introduction plate and the support plate, associated to the development of an inclined compression strut carrying shear by direct strut action.

Fig. 32 plots additionally the profiles of the longitudinal strain in the direction of the theoretical compression strut for specimens RT11.24 and RT17.12 (similar plots of other specimens are shown in appendix A). The base length for the strain calculation was 100 mm (the discontinuities of the plot are due to the presence of localized cracks). An overall increase of the strain in the strut direction can be observed for lower loading rates, mostly pronounced in the zones of the load introduction plates (particularly the one close to the compression zone). It can also be observed that the smeared nature of cracking in the upper part of the strut leads to rather regular strain profiles in this zone. More details

can be also seen in *Fig. 33*, presenting the integral response of the strut region. With respect to the evolution of the strains in time, it can be observed a gradual activation of the concrete in the region where the compression strut develops, not only in its central part but also at its sides (*Fig. 32*). It can be noted that large compressive strains were measured (more than 4‰ for low loading rates) and relatively high transverse strains (more than 8‰) indicating the presence of wide cracks (actual crack openings up to 5 mm).

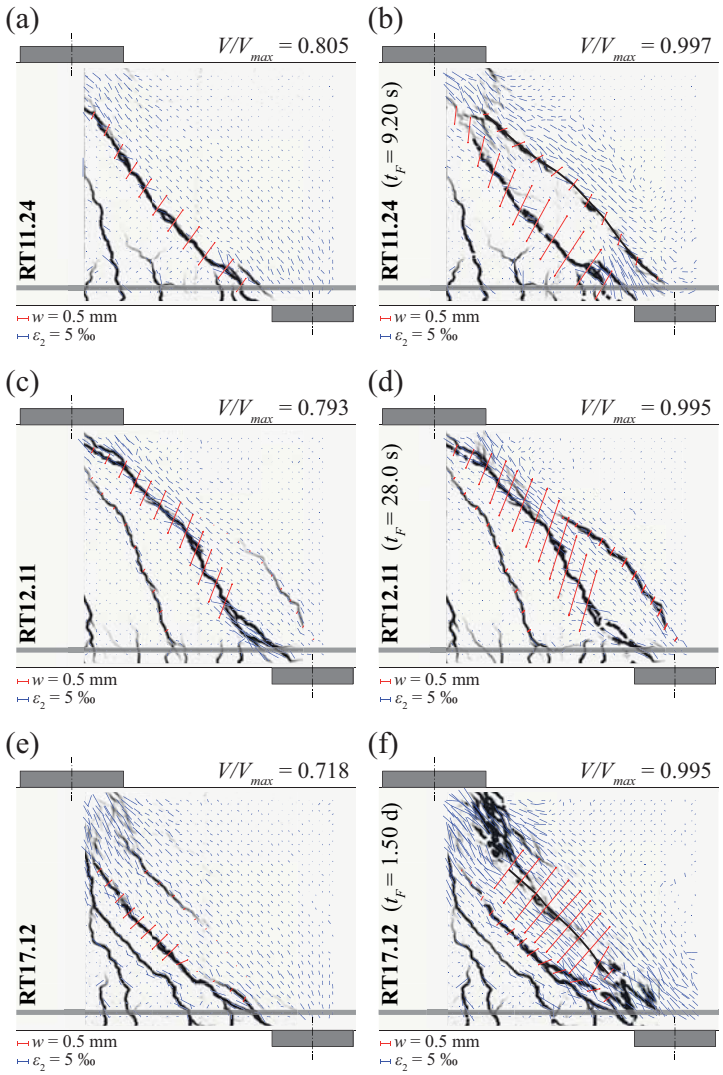

Fig. 31 Crack kinematics patterns and principal compressive strain (ε_2) vectors for specimens (a-b) RT11.24; (c-d) RT12.11; and (e-f) RT17.12. The left ones represent a load level of approximately 0.72-0.8·V_{max} and the right ones represent the last available DIC image before V_{max}.

Failure occurred in the specimens by crushing of the concrete in the upper part of the strut. Particularly for the low loading rates, failure was associated to an extensive smeared cracking of this region, see *Fig. 31*e-f and appendix A (such progression of microcracking under high levels of sustained stress is consistent with the material response observed by Tasevski et al. [13]). For the high loading rates, it is worth noting that the higher strength observed in specimen RT11.24 can be related to the fact that the inclined compression strut was not disturbed by any wide crack (*Fig. 31*a). When the diagonal crack appeared (*Fig. 31*b), failure followed instantly. On the contrary, the lower strength in specimen RT12.11 was due to the fact that a diagonal crack, disturbing the strut, already formed at 50% of the maximum strength (*Fig. 31*c-d).

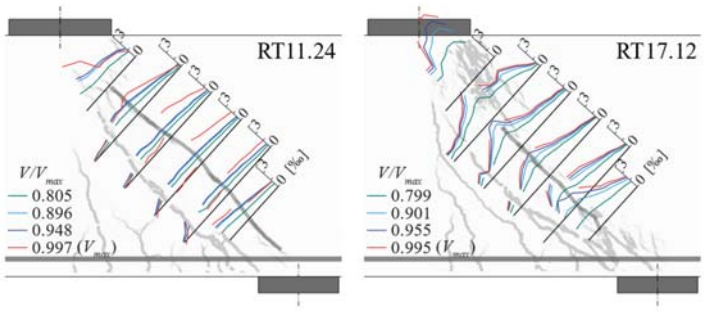

Fig. 32 Longitudinal strain profiles in the compression strut for specimens (a) RT11.24; and (b) RT17.12

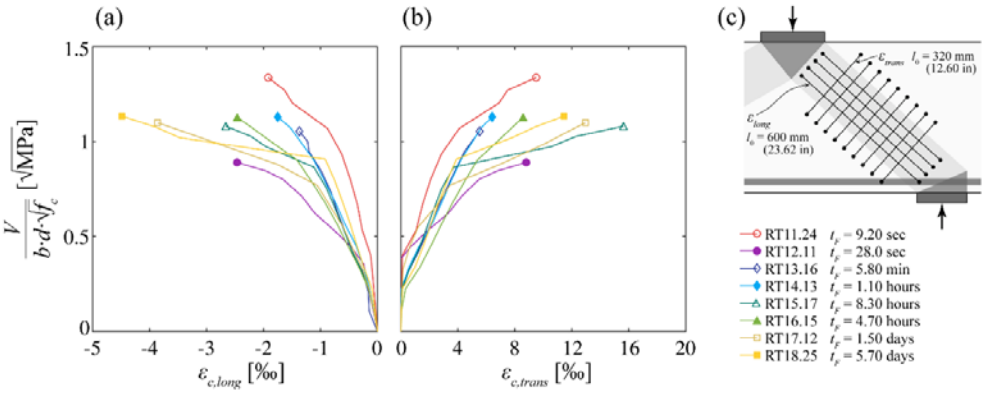

Fig. 33 (a) Longitudinal ($\varepsilon_{c,long}$) and (b) transverse ($\varepsilon_{c,trans}$) strain of the direct strut of the squat beams (a/d = 1.0); and (c) base for the measurement of the strains (extraction from DIC data)

7 Interpretation of shear tests

7.1 Slender beam series

Fig. 34 compares the normalized measured shear strength of the slender beam series to the CSCT shear strength prediction ([44] where the aggregate size d_g was corrected according to [48] similarly to the plots shown in *Fig. 2* for other test series). For higher loading rates, an increase in the strength was rather consistently observed in the tests (in agreement to other results from the scientific literature [80]). For low loading rates, however, no marked decrease of the shear strength compared to typical shear test durations was observed (in agreement to the series previously discussed [42],[47], see *Fig. 2*).

As shown by Campana et al. [77], Fernández Ruiz et al. [46] and Cavagnis et al. [48], the shear resistance can be calculated as the sum of the contribution of all potential shear transfer actions (the procedure is explained in detail in FEDRO-Report of Project AGB 2011-015). For that purpose, the contribution of aggregate interlock can be calculated on the basis of the measured crack opening and sliding together with an aggregate interlock law. In a similar manner, the shear force carried by the residual concrete tensile strength at the crack can be calculated based on of the measured crack opening and considering a constitutive law for the tensile response of concrete. For dowelling action of the flexural reinforcement, the contribution of the reinforcing bars is determined based on the deflected shape of the bars (assumed to behave elastically). Finally, for the shear force carried by the compression zone (arching action), high-resolution DIC measurements were used, being accurate enough to determine the concrete principal strains and to integrate the associated shear stresses [48]. The results of such analysis are presented in *Fig. 35* where the aforementioned shear transfer actions are calculated consistently with [48] and the total shear strength (addition of all components) is compared to the measured one. As it can be noted, the shape of the CSC and its kinematics significantly influences the various contributions of the shear transfer actions as well as the total shear strength. Some variability is observed with this respect. For instance, the higher strength of specimen RT1.05 (highest loading rate) can be explained by the favourable position of the critical shear crack allowing a significant shear force to be carried by an inclined compression strut. Specimen RT4.02 gave a relatively high strength due to the favourable shape of the crack to the engagement of aggregate interlock. It can also be seen in the analysis that the shear force carried by the compression zone has a relatively larger significance for higher loading rates, while its significance decreases for decreasing loading rates (where aggregate interlock becomes governing).

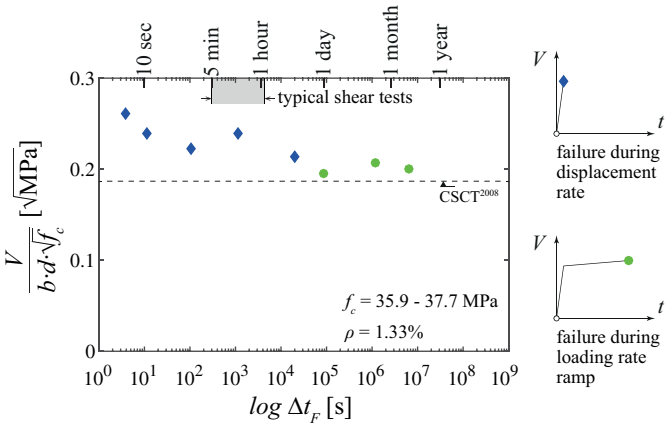

Fig. 34 Comparison of the slender beam series (a/d = 3.5) with CSCT[2008] [44]

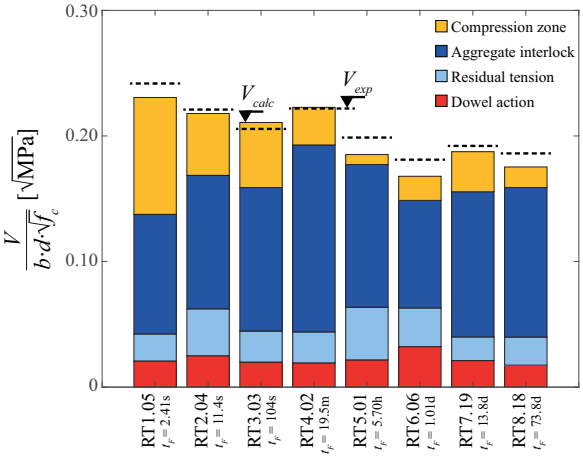

Fig. 35 Contribution of different shear transfer actions at maximum load for the slender beam series (a/d = 3.5)

Overall, a fairly good estimate of the shear strength is obtained following this approach (average measured-to-calculated strength of 1.03 with a coefficient of variation of only 3.6%). The more favourable shape of the crack developed for high loading rates allowed for larger capacities than for specimens loaded at reference or low loading rates.

It is important to note that the resistance of the shear transfer actions does not seem to need any correction with respect to the potential softening due to sustained loading effects on the material behaviour (all members have been analysed using the same constitutive laws and without accounting for potential short- or long-term influences). This observation can be considered consistent for the aggregate interlock contribution (dominant shear-transfer action in the slender beams subjected to low loading rates). This is justified by the fact that a comparable shape of the CSC developed (*Fig. 28*), with similar crack openings in the critical region for aggregate interlock transfer (*Fig. 29*c), and by the fact that the aggregate interlocking was significantly engaged in a relatively rapid manner when the specimens were close to failure (blue areas in *Fig. 28*). These aspects allow to consider that the contribution of aggregate interlock was little sensitive to low loading rates (similar crack shape, opening and significant engagement of the shear-transfer action in a rapid manner close to failure). A similar consideration can also be performed for the residual tension contribution and dowelling action (associated to the rapid opening of the CSC close to failure). With respect to the contribution of the compression zone, this action can potentially be more influenced by high levels of sustained load [13]. However, its overall contribution to the shear strength was limited for low loading rates and slender members and with the possibility to develop stress redistributions (this aspect is commented in detail in the next section with reference to the arching action in squat members).

7.2 Squat beam series

In the squat beam series, a larger scatter in terms of strength was observed for higher loading rates. For reference or low loading rates, almost no variation on the shear strength was observed. This fact is shown in *Fig. 36*, where the measured shear strength is compared to that of a rigid-plastic stress field (lower bound according to limit analysis) [81]. This stress field was derived assuming an effective concrete strength $f_{ce} = 0.75 \cdot f_c$ in the strut. The efficiency factor (constant $\nu = 0.75$) accounts for concrete brittleness (factor η_{fc} in SIA 262:2013) and for the influence of transverse cracking (factor k_c in SIA 262:2013 [82], the value 0.75 is intermediate of those generally accepted for concrete cracked in a direction parallel or inclined with respect to the strut direction and without significant redistribution of internal forces [82]). It can be noted that in the nodal regions of the stress field shown in *Fig. 36,* non-hydrostatic stress states were considered (despite the fact that the third principal stress can potentially be higher than the uniaxial concrete compressive strength, detailed verification of the nodal zone is not governing in this case accounting for the Kupfer's effect and in agreement to experimental failure modes observed).

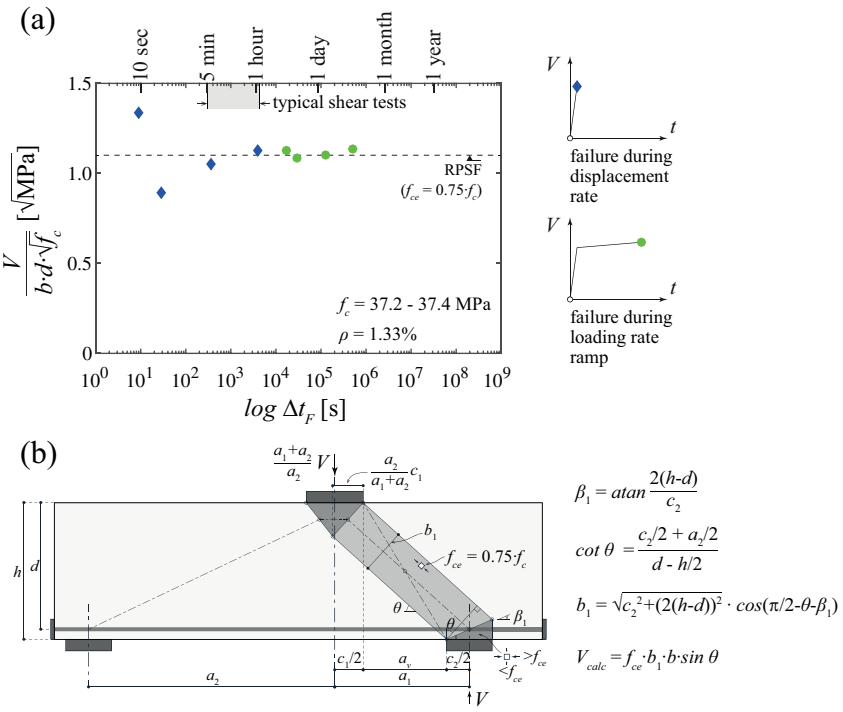

Fig. 36 (a) Comparison of the squat beam series (*a*/*d* = 1.0) with a rigid-plastic stress field solution (effective concrete strength $f_{ce} = 0.75 \cdot f_c$); and (b) detail of the stress field

With respect to this relatively insensitive response to the duration of the load, one could expect that the concrete strut may reduce its strength when subjected to high levels of sustained stress during long periods [8], [13]. This phenomenon, however, appeared to be compensated by the potential confinement of the strut by the surrounding concrete (restraining the transversal deformation of the strut) and the influence of the surrounding concrete due to the activation of additional concrete at the sides of the strut (increase of the area of the strut). The development of a confinement of the strut by the surrounding concrete can be supported by the measurements of *Fig. 37*. The crack below the compression strut (crack characterized by point A) opens at early stages of loading (*Fig. 37*a,c, blue lines), but it closes completely or partly for higher load levels after the crack in the inclined strut develops (crack with point B in *Fig. 37*b,c, refer to green lines). Such closure was particularly notable at its upper part where the crack lips were again in contact (thus allowing to transfer compressive stresses). As a consequence of this crack closure and potential confining stresses, larger portions of concrete could be activated and the opening of crack B was controlled. This is shown in a schematic manner in *Fig. 37*d and can also be observed in *Fig. 31* and Appendix A. These effects allowed for an enhanced performance of the strut, thus leading to relatively high calculated values of the efficiency factor of the strut. It can additionally be noted that the strut cannot be confined in the upper region since no longitudinal reinforcement is available to ensure the equilibrium of the deviation forces. A similar effect has been demonstrated for the case of footings with concentrated loading where the reinforcement in the compression zone can increase the load-carrying capacity [83].

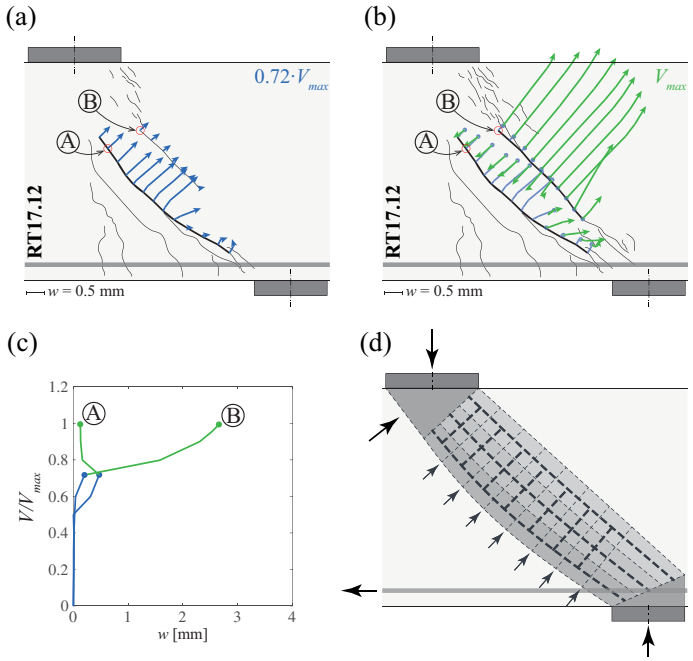

Fig. 37 Crack kinematics for specimen RT17.12: (a) Crack opening at 0.72·V_{max}; (b) crack closure at V_{max} for lower crack; (c) plot of crack evolution at locations A and B; and (d) potential confinement of the strut.

7.3 Practical design recommendations

As previously discussed, codes of practice show no consensus on the consideration of the effect of long-term actions on the shear strength. On the basis of the test results and the considerations discussed in this manuscript, there seems to be no need to consider a strength reduction for shear critical members without transverse reinforcement subjected to high levels of sustained load with respect to members loaded at a reference loading rate (failure in 5 minutes - 2 hours). This conclusion shall be understood valid for the duration of the loading, member slenderness and material property ranges investigated in this report and is supported on the following considerations:

- For slender beams, the shape of the CSC seems to be governing for the strength. For high loading rates (higher than the reference one), a more favourable shape of the CSC may develop, but no significant modification in the shape of the crack or shear strength is observed for lower loading rates compared to typical shear tests. This limited sensitivity of the shear strength for low loading rates can be justified by the similar shape and openings of the CSC and by the relatively rapid (yet stable) opening and sliding of the CSC close to failure.

- For squat beams, the capacity of stress redistribution and potential confinement by the concrete surrounding the direct strut region seems to compensate for the potential decrease of material strength under sustained loading during long periods of time.

8 Practical design recommendations

The investigations summarized in the previous chapters of this report have resulted in a number of design recommendations. In this chapter we address the sections of current design codes SIA 262:2013 [37] and National Annex of Eurocode 2 (EN 1992-1-1 CH NA:2014 [84]) that can potentially be improved according to the findings of this research. The clauses are stated and proposals for their improvement are presented.

8.1 SIA 262:2013

8.1.1 Clause 2.3.2.3

1) Current text

2.3.2.3 The design value of the concrete compressive strength is:

$$f_{cd} = \frac{\eta_{fc} \cdot \eta_t \cdot f_{ck}}{\gamma_c} \tag{2}$$

The factors η_{fc} and η_t shall be determined according to sections 4.2.1.2 and 4.2.1.3.

2) Comments and proposed improvement

The clause is pertinent according to the results of this report, refer to section 3-5. The value for factor η_t can however be improved, refer to the comment of §4.2.1.3 below.

3) Proposal

- Keep current clause
- Improve factor η_t (see improvement proposed for §4.2.1.3 below)

8.1.2 Clause 2.3.2.4

1) Current text

2.3.2.4 The design value of the shear stress limit is:

$$\tau_{cd} = \frac{0,3 \cdot \eta_t \cdot \sqrt{f_{ck}}}{\gamma_c} \tag{3a}$$

2) Comments and proposed improvement

According to the findings in sections 6 and 7, both for shear-critical slender and squat members, the activation of redistribution capacities for high sustained loading levels can occur. Furthermore, no clear decrease of the shear strength was observed under sustained loading. On the other hand, an increase on the shear strength was observed for high loading rates. This effect, for practical purposes, can however be neglected as a safe assumption. These findings can be implemented to enhance the consistency of the current clause.

3) Proposal

The design value of the shear stress limit is:

$$\tau_{cd} = \frac{0,3 \cdot \sqrt{f_{ck}}}{\gamma_c} \tag{3b}$$

Nevertheless, before this proposal is implemented in the code SIA 262, the effect of sustained loading on the punching shear resistance of slabs needs to be studied in detail (this study was not part of the present research project).

8.1.3 Clause 4.2.1.3

1) Current text

4.2.1.3 The factor η_t in equations (2) and (3) takes in account the effect of the duration of the action on the strength of concrete. The strength reduction due to permanent actions is normally compensated by the strength increase related to the age of concrete, which generally allows to admit $\eta_t = 1{,}0$**.** In other cases:

- $\eta_t = 0{,}85$ for permanent actions in case the effect of the permanent action at the design level exceeds 90% of the total effect
- $\eta_t = 1{,}0$ for load actions of duration < 1 hour and for permanent actions in case the effect of the permanent action at the design level does not exceed 90% of the total effect
- $\eta_t = 1{,}2$ for impact loads, like for example collision and explosion.

If in any case the concrete strength is determined for a $t_P > 28$, or if the permanent action is applied already at early age of concrete, the factor η_t is:

$$\boldsymbol{\eta_t = 0{,}85 \frac{f_{cm}(t_L)}{f_{cm}(t_P)} \leq 1{,}0} \tag{27}$$

The evolution in time of the concrete compressive strength $\boldsymbol{f_{cm}}(\mathrm{t})$ can be estimated according to figure 1.

2) Comments and proposed improvement

According to the findings in section 3, the strength reduction due to high permanent actions is fully compensated by the strength increase related to the continued cement hydration only after a period of some months (normally 3-12 months, depending on the early strength class of concrete). For design of new structures, in case the concrete strength is measured at 28 days, this means that no reduction of the strength is necessary if the permanent action is applied after such period (which is very often the case). However, when high permanent loads are applied at earlier age, the reduction would apply for safe design.

For the assessment of existing structures, when the concrete strength is updated some years after construction by means of core samples, very limited increase of the strength can be expected due to cement hydration. In these cases, if a high level of permanent load is to be applied, a reduction of the concrete strength is thus reasonable.

The maximal possible reduction can be estimated as 15% (see section 5) which is the case when the permanent action represents 100% of the total action, whereas for permanent actions lower than 85% of the total action, no reduction is necessary. Intermediary cases may be considered by a linear interpolation between the two extreme cases.

With respect to the definition of permanent loading, according to section 5.3, durations of the loading lower than 1-2 hours can be considered as non-permanent actions.

3) Proposal

The factor η_t in equation (2) takes in account the effect of the duration of the action on the strength of concrete. The strength reduction due to permanent actions is normally compensated by the strength increase related to concrete ageing, provided that the full permanent actions are applied at a concrete age higher than 3 months. In this case, it can be assumed a value $\eta_t = 1{,}0$. Otherwise, or in situations where the concrete strength f_{ck} is determined at an age greater than 28 days, η_t can be calculated as follows:

- $\eta_t = 0{,}85$ in case the effect of the permanent action (or variable actions of a duration > 1 hour) represents 100% of the total effect at design level
- $\eta_t = 1{,}0$ when rapid variable actions (actions of duration < 1 hour) represent at least 15% of the total effect at design level

- For intermediate cases (effect of rapid actions between 0 and 15% of the total load effect at design level), η_t may be determined by linear interpolation between the previous values

For members subjected to impulsive loading (blast, impact or other), a value $\eta_t = 1{,}2$ applies.

8.1.4 Clause 3.1.2.6.3

1) Current text

3.1.2.6.3 The influence of the stress level on creep has to be taken into account for concrete stresses $\sigma_c > 0{,}45 f_{ck}$. This is done by increasing the creep coefficient by the factor:

$$\boldsymbol{\beta_{c\sigma} = e^{1{,}5(\sigma_c/f_{ck}-0{,}45)}} \tag{14a}$$

2) Comments and proposed improvement

The existing formula is adapted from Eurocode 2:2004. It however represents a too steep change in the slope of the phenomenon. As presented in this document (section 2.3) an improved (smooth) formula was proposed by Fernández Ruiz et al. [14] (see *Fig. 54*), which could be written for design purposes as:

$$\boldsymbol{\beta_{c\sigma} = 1.0 + 2(\sigma_c/f_{cm})^4} \tag{14b}$$

It can be noted that since this expression is used at serviceability limit state, it is expressed as a function of f_{cm} and not of f_{ck} (also, following the change in prEN 1992-1-1:2018 with respect to EN 1992-1-1:2004). The formula, however, if applied only above the value $\sigma_c > 0.4 f_{cm}$, would yield to a (small) discontinuity. Thus, it is adapted, for design purposes, to the following format:

$$\boldsymbol{\beta_{c\sigma} = 0.95 + 2(\sigma_c/f_{cm})^4} \tag{14c}$$

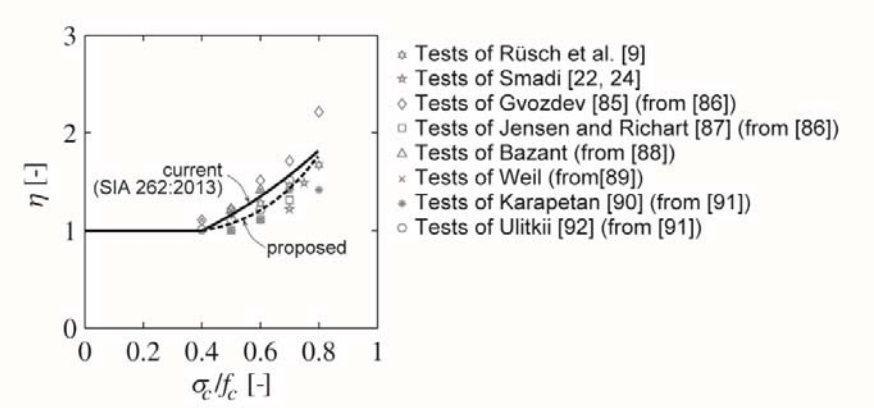

Fig. 54 Comparison of equations for calculating the correction factor for nonlinear creep

3) Proposal

3.1.2.6.3 The influence of the stress level on creep at serviceability limit state shall be taken into account for concrete stresses $0{,}4 f_{cm} < \sigma_c < 0{,}8 f_{cm}$. This is done by increasing the creep coefficient by the factor:

$$\boldsymbol{\beta_{c\sigma} = 0.95 + 2(\sigma_c/f_{cm})^4} \tag{14d}$$

8.2 Design compressive strength according to EN 1992-1-1 CH NA:2014

8.2.1 Clause 3.1.6(1)

1) Current text

Eurocode original text:

(1)P The value of the design compressive strength is defined as

$$f_{cd} = \alpha_{cc} f_{ck} / \gamma_C \qquad (3.15)$$

where:

γ_C is the partial safety factor for concrete, see 2.4.2.4, and

α_{cc} is the coefficient taking account of long term effects on the compressive strength and of unfavourable effects resulting from the way the load is applied.

Note: The value of α_{cc} for use in a Country should lie between 0,8 and 1,0 and may be found in its National Annex. The recommended value is 1.

Choice of National Determined Parameters:

The value of coefficient α_{cc} can be taken as:

- α_{cc} = 0,85 if the effect of permanent loads represent 100% of the total effect
- α_{cc} = 1,0 if the effect of permanent loads represent 85% or less of the total effect
- α_{cc} can be obtained by means of a linear interpolation between the previous values for intermediate cases

- α_{cc} = 1,.20 for members subjected to impulsive loading (blast, impact or others)

When assessing the strength of existing structures, concrete can be characterized by its compressive strength at 28 days or it can be updated. In the first case (f_{ck}(28 days)), after a period of some years, the increase on the compressive strength of concrete due to the hydration of the cement paste compensates the potential reduction due to propagation of microcracking under sustained loading. In this case it can be assumed α_{cc} = 1,0 (independently of the level of permanent loading).

2) Comments and proposed improvement

Same as for SIA 262:2013 §4.2.1.3.

3) Proposal

Choice of National Determined Parameters:

The value of coefficient α_{cc} can be taken as $\alpha_{cc} = 1$, if the permanent actions are applied at a concrete age higher than 3 months. Otherwise, or in situations where the concrete strength f_{ck} is determined at an age later than 28 days, α_{cc} can be admitted as follows:

- $\alpha_{cc} = 0{,}85$ in case the effect of the permanent action (or variable actions of a duration > 1 hour) represents 100% of the total effect at design level
- $\alpha_{cc} = 1{,}0$ when rapid variable actions (actions of duration < 1 hour) represent at least 15% of the total effect at design level
- For intermediate cases (effect of rapid actions between 0 and 15% of the total load effect at design level), α_{cc} shall be determined by linear interpolation between the previous values

For members subjected to impulsive loading (blast, impact or other), a value $\alpha_{cc} = 1{,}2$ applies.

9 Conclusions (EN)

The investigations performed in this report contribute to better understand the phenomenon of time-dependent strength of concrete under various loading patterns ranging from rapid to sustained actions. This phenomenon is investigated on both uniaxial compression specimens and shear-critical reinforced concrete members.

9.1 Uniaxial compressive strength

Based on an experimental campaign of uniaxial compression with varying strain and stress rates, the following conclusions on the time-dependent behaviour of concrete under high levels of sustained load can be drawn:

1. The compressive strength of concrete reduces due to sustained loading or low strain or stress rates. This is a detrimental effect in members subjected to high levels of stress
2. The corresponding strain at failure increases for high levels of sustained stress. This may be a positive effect for statically redundant systems, where redistributions of stresses are possible and may increasingly activate compression reinforcement
3. Failure under sustained load is governed by the inelastic strain capacity of concrete. When the developed inelastic strain of concrete equals the inelastic strain capacity, failure occurs by progressive coalescence of cracks
4. The inelastic strain capacity can be estimated as the difference between the instantaneous post- and pre-peak strains for a given stress level. This allows defining a failure criterion for the available inelastic strain capacity

Furthermore, the development of linear and nonlinear creep strains potentially leading to failure under high levels of load has been investigated in an analytical manner, by applying existing creep models and a set of assumptions inspired from the mechanical behaviour of concrete. This analytical work has resulted in a consistent approach, whose results draw the following conclusions:

5. The affinity assumption between linear and nonlinear creep strains allows to formulate a simple and efficient relation to estimate the development of inelastic strains in concrete for a given loading history. It accounts in an explicit manner for the development of tertiary creep strains
6. Analytical calculation of failures under long-term loading patterns can be performed as the intersection between the relationship defining the development of inelastic strains for a given loading pattern (based on the affinity assumption) and the failure criterion defined by the inelastic strain capacity of concrete. This approach allows to consistently estimate the strength and the associated strain for different loading patterns, as confirmed by test results on both sustained load and stress and strain rates
7. On the basis of the theoretical model, some effects can be clearly reproduced and investigated, for instance:
    a. Constant sustained stress patterns lead to failures at lower stress levels and more rapidly than for stress or strain rates (concrete is subjected to higher stress levels since the beginning of the loading process)
    b. Ageing of the concrete (increase of concrete strength with time) is observed to be an instrumental phenomenon as it compensates for the material damage. For concretes loaded at early ages, failure can only occur after some hours or days, while for concretes loaded at older ages, failures under long-term load can occur several years after (as there is almost no increase of strength due to ageing)

9.2 Shear strength of reinforced concrete members

Based on an experimental campaign on shear-critical slender and squat beams without shear reinforcement subjected to varying loading rates, the following conclusions on the time-dependent shear strength of reinforced concrete members can be drawn:

6. The performed tests do not show any marked decrease on the shear strength for higher durations of application of the load or for low loading rates compared to typical shear tests
7. For loading rates higher than typical shear tests (associated to failures after some seconds), a relatively consistent increase on the strength can be observed for slender specimens. An analysis of the shear transfer actions shows that this can be justified by a more favourable geometry of the critical shear crack in case of high loading rates. The results are not so clear for squat members but indicate a similar response
8. For squat members, the relatively constant shear strength for high levels of sustained load can be justified by the potential redistribution and confinement capacity of the concrete surrounding the strut carrying shear
9. For slender members, the limited sensitivity of the shear strength to low loading rates can be justified by the similar shape and openings of the critical shear crack (CSC) and by the relatively rapid (yet stable) opening and sliding of the CSC close to failure. This allows to significantly engage aggregate interlocking (the dominant shear-transfer action in these members) in a relatively rapid manner (this contribution is thus little influenced by the total duration of the loading process).

9.3 Design considerations

Based on the experimental and analytical work of this report, a simplified code-like approach could be developed for engineering practice. Some important aspects are:

1. The phenomenon of concrete creep shall be accounted for both for Serviceability Limit States (SLS) and Ultimate Limit States (ULS)
2. Simple expressions can be derived to characterize the failure load of concrete under sustained load. Combining these expressions with the Palmgren-Miner's rule provides a practical manner to account for damage accumulation and to estimate the failure load and time
3. It could be confirmed that the beneficial effect of continued cement hydration usually compensates for the detrimental effect of sustained loading. This holds true provided that the concrete strength is determined at 28 days and the ULS occurs after a sufficiently long period of time. In case the concrete strength is determined later than 28 days (particularly relevant for assessment of existing structures), the reduction of concrete strength accounting for long-term and high sustained loading is justified
4. For a given level of total stress, a combination of permanent actions and a rapid variable action is less detrimental for the concrete compressive strength than a full permanent action. This phenomenon can be described by simple, code-like expressions resulting in a linear interpolation between the response of a member failing under constant sustained load and the case where permanent load effects can be neglected. Also, for cases where the variable action is maintained over a period of time, a similar approach can be followed
5. Despite the fact that for the pure material response a decrease on the strength has been largely documented and verified, for members in shear, it seems that there is no need for a reduction in the shear resistance for high levels of sustained loads during long periods of time.

So far, very little research has been conducted on the effect of sustained loading on the punching shear resistance, which was not part of this research project. As a consequence, additional considerations are needed before the strength reduction factor for calculating the design value of the shear stress limit in SIA 262:2013 can be removed.

9.4 Proposal for future research

Following the advancement of knowledge presented in this investigation, a number of topics have been identified as aspects that will require future research efforts:

1. With respect to the uniaxial response of concrete in compression and the long-term response of compression zones of members in bending:
    a. The effect of confined conditions, potentially influencing the inelastic strain capacity and thus the failure criterion of concrete
    b. The activation of compression reinforcement in columns and compression zones of members in bending due to nonlinear creep
2. With respect to the shear response under sustained actions:
    c. To perform a more comprehensive experimental investigation, both on full-scale specimens and on small samples allowing to characterize the material response
    d. To study the response for failures in punching

10 Conclusions (FR)

Les investigations effectuées dans ce rapport permettent de mieux comprendre le phénomène de résistance du béton en fonction du temps sous différentes histoires de chargement allant des actions rapides aux actions soutenues. Ce phénomène est étudié à la fois sur des spécimens en compression uniaxiale et sur des éléments en béton armé critiques à l'effort tranchant.

10.1 Résistance à la compression uniaxiale

Sur la base d'une campagne expérimentale de compression uniaxiale avec des vitesses de déformation et de contrainte variables, les conclusions suivantes ont été tirées sur le comportement du béton en fonction du temps due à un haut niveau de charge soutenue :

8. La résistance à la compression du béton diminue sous l'effet d'une charge soutenue ou d'une faible vitesse de déformation ou de contrainte. Ceci est un effet préjudiciable pour les éléments soumis à un haut niveau de charge soutenue
9. La déformation à la rupture augmente pour de hauts niveaux de charge soutenue. Cela peut être un effet favorable pour les systèmes hyperstatiques, où des redistributions des efforts sont possibles et peuvent activer l'armature en compression
10. La rupture sous charge soutenue est régie par la capacité de déformation inélastique du béton. Lorsque la déformation inélastique développée dans le béton est égale à la capacité de déformation inélastique, la rupture se produit par coalescence progressive des fissures
11. La capacité de déformation inélastique peut être estimée comme étant la différence entre les contraintes instantanées post-pic et pré-pic pour un niveau de contrainte donné. Cela permet de définir un critère de rupture pour la capacité de déformation inélastique disponible

En outre, le développement de déformations de fluage linéaire et non linéaire pouvant conduire à une rupture sous charge soutenue a été étudié de manière analytique, en appliquant les modèles de fluage existants et un ensemble d'hypothèses inspirées du comportement mécanique du béton. Ce travail analytique a abouti à une approche cohérente avec les conclusions suivantes :

12. L'hypothèse d'affinité entre les déformations de fluage linéaire et non linéaire permet de formuler une relation simple et efficace pour estimer l'évolution des déformations inélastiques dans le béton pour une histoire de chargement donné. Il explique de manière explicite le développement des déformations de fluage tertiaire
13. Le calcul analytique de la rupture sous des scénarios de chargement soutenu à long terme peut être effectué par intersection entre la relation définissant le développement de déformations inélastiques pour une histoire de chargement donné (basé sur l'hypothèse d'affinité) et le critère de rupture défini par la capacité de déformation inélastique de béton. Cette approche permet d'estimer de manière cohérente la résistance et la déformation associée pour différentes histoires de chargement, comme le confirment les résultats des tests sous charge soutenue ainsi que sous des vitesses de contrainte et de déformation variables
14. Sur la base du modèle théorique, certains effets peuvent être clairement reproduits et étudiés, comme par exemple :
    a. Des scénarios de chargement constant soutenu dans le temps conduisent plus rapidement à des ruptures avec des niveaux de contrainte plus faibles comparés à des vitesses de contrainte ou de déformation variables (le béton est soumis à des niveaux de contrainte plus élevés depuis le début du processus de chargement)
    b. Le vieillissement du béton (augmentation de la résistance du béton dans le temps) est un phénomène déterminant, car il compense

l’endommagement du matériau. Pour les bétons soumis à une charge soutenue à jeune âge, la rupture ne peut se produire qu'après quelques heures ou quelques jours, car l’augmentation de la résistance dans le temps le compensera, alors que pour les bétons chargés à un âge plus avancé, une rupture à long terme peut se produire plusieurs années après (car il n'y a presque pas de réserve d'augmentation de résistance)

10.2 Résistance des membres critiques à l’effort tranchant

Sur la base d’une campagne expérimentale sur des éléments élancés et trapus critiques à l’effort tranchant et sans armature transversale soumises à des vitesses d’augmentation de la charge variables, il est possible de tirer les conclusions suivantes sur la résistance au cisaillement des éléments en béton armé en fonction du temps :

5. Les essais effectués ne montrent pas de diminution marquée de la résistance à l’effort tranchant pour des durées d'application plus longues de la charge ou pour de faibles vitesses d’augmentation de la charge par rapport aux tests d’effort tranchant typiques
6. Pour des vitesses d’augmentation de la charge supérieures aux tests d’effort tranchant typiques (associés à des ruptures au bout de quelques secondes), une augmentation relativement constante de la résistance peut être observée pour les échantillons élancés. Une analyse des modes de transmission de l’effort tranchant montre que cela peut être justifié par une géométrie plus favorable de la fissure critique en cas de vitesses d’augmentation de la charge élevées. Les résultats ne sont pas aussi clairs pour les éléments trapus, mais indiquent une réponse similaire
7. Pour les éléments élancés, la résistance à l’effort tranchant relativement constante pour des niveaux de charge soutenue élevés peut être justifiée par la capacité potentielle de redistribution et de confinement du béton entourant la bielle de compression portant l’effort tranchant
8. Pour les éléments élancés, la sensibilité limitée de la résistance à l’effort tranchant aux faibles vitesses d’augmentation de la charge peut être justifiée par la forme et les ouvertures similaires de la fissure critique ainsi que par l'ouverture et le glissement relativement rapides (mais stables) de la fissure critique proche à la rupture. Cela permet d'engager de manière significative l’engrènement d’agrégats, le mode dominant de transmission d’effort tranchant dans ces éléments, d'une manière relativement rapide (cette contribution est donc peu influencée par la durée totale d’application de la charge).

10.3 Considérations de conception

Sur la base des travaux expérimentaux et analytiques de ce rapport, une approche simplifiée a été développée pour les ingénieurs de la pratique. Certains aspects importants sont :

1. Le phénomène de fluage du béton doit être pris en compte à la fois pour les états limites de service (ELS) et les états limites ultimes (ELU)
2. Des expressions simples peuvent être dérivées pour caractériser la charge de rupture du béton sous charge soutenue. La combinaison de ces expressions avec l’approche de Palmgren-Miner fournit un moyen pratique de quantifier l’accumulation de dommages et d’estimer la charge et le temps de rupture
3. Il a pu être confirmé que l'effet bénéfique d'une hydratation continue du ciment compense généralement l'effet défavorable d'une charge soutenue. Cela est vrai à condition que la résistance du béton soit déterminée à 28 jours et que l’ELU ait lieu après une période suffisamment longue. Si la résistance du béton est déterminée après 28 jours (particulièrement utile pour l’évaluation des structures existantes), une réduction de la résistance du béton tenant compte d’une charge élevée soutenue est nécessaire
4. Pour un niveau donné de contrainte totale, une combinaison d'actions permanentes et une action variable rapide est moins défavorable pour la

résistance à la compression du béton qu'une action permanente complète. Ce phénomène peut être décrit par de simples expressions aboutissant à une interpolation linéaire entre la réponse d'un membre amené à la ruine sous une charge constante et le cas où des effets de charge permanents peuvent être négligés. En outre, dans les cas où l'action variable est maintenue sur une période donnée, une approche similaire peut être suivie

10. Bien que, pour le comportement du matériau béton, une diminution de la résistance ait été largement documentée et vérifiée, pour les membres critiques à l'effort tranchant, il semble qu'une réduction de la résistance n'est pas nécessaire pour les charges élevées maintenues pendant de longues périodes.

Jusqu'à présent très peu de recherches ont été menées sur les effets d'une charge soutenue sur la résistance au poinçonnement, qui ne faisait pas partie de ce projet de recherche. Par conséquent, des considérations supplémentaires sont nécessaires avant que le facteur de réduction de la résistance à l'effort tranchant dans SIA 262:2013 puisse être supprimé.

10.4 Propositions de recherches dans le futur

Sur la base de l'avancement des connaissances présentées dans le cadre de cette recherche, certains sujets ont été identifiés comme nécessitant des efforts de recherche supplémentaires :

1. En ce qui concerne le thème de la réponse du béton en compression uni-axiale ainsi qu'à long terme dans les zones comprimées des éléments en flexion :
    a. L'effet du confinement, qui peut influencer la capacité de déformation inélastique et donc le critère de rupture du béton
    b. L'activation de l'armature de compression dans les colonnes et les zones comprimées sous l'effet du fluage non-linéaire
2. En ce qui concerne la réponse à l'effort tranchant sous actions soutenues :
    c. Réaliser une étude expérimentale plus complète, à la fois sur des échantillons en grandeur réelle et sur de petits échantillons permettant de caractériser la réponse du matériau
    d. Etudier les ruptures au poinçonnement

11 Conclusions (DE)

Die in diesem Bericht beschriebenen Untersuchungen tragen zum besseren Verständnis des Phänomens der zeitabhängigen Festigkeit von Beton bei verschiedenen Belastungsgeschichten bei (von schnellen Einwirkungen bis zu Dauerlasteinwirkungen). Dieses Phänomen wurde sowohl an einachsigen Druckproben als auch an querkraftkritischen Stahlbetonbauteilen untersucht.

11.1 Einachsige Druckfestigkeit

Basierend auf einer experimentellen Kampagne von einachsigen Druckproben mit unterschiedlichen Dehnungs- und Spannungsraten können die folgenden Schlussfolgerungen zum zeitabhängigen Verhalten von Beton unter hohen Dauerbelastungen gezogen werden:

1. Die Druckfestigkeit von Beton fällt aufgrund von Dauerbelastung oder niedrigen Dehnungs- oder Spannungsraten ab. Dies ist ein nachteiliger Effekt bei Bauteilen, die hohen Belastungen ausgesetzt sind.
2. Die entsprechende Bruchverformung steigt bei hohen Dauerbelastungen. Dies kann sich positiv auf statisch redundante Systeme auswirken, in denen Spannungsumlagerungen und eine erhöhte Aktivierung der Druckbewehrung möglich sind.
3. Bruch unter Dauerbelastung hängt von der inelastischen Verformungskapazität von Beton ab. Wenn die inelastische Verformung des Betons der inelastischen Verformungskapazität entspricht, tritt ein Versagen durch fortschreitendes Zusammenwachsen der Risse auf.
4. Für ein gegebenes Belastungsniveau, kann die inelastische Verformungskapazität als die Differenz zwischen den Verformungen vor und nach dem Bruch (ermittelt mit einem im Kurzzeittest gemessenen Spannungs-Dehnungs-Diagramm) geschätzt werden. Dies ermöglicht die Definition eines Versagenskriteriums für die verfügbare inelastische Verformungskapazität.

Darüber hinaus wurde die Entwicklung von linearen und nichtlinearen Kriechverformungen, die möglicherweise zum Bruch unter Dauerbelastung führen, auf analytische Weise untersucht. Hierfür wurden vorhandene Kriechmodelle und eine Reihe von Annahmen verwendet, die auf dem mechanischen Verhalten von Beton basieren. Diese analytische Studie hat zu einem konsequenten Ansatz geführt, aus dessen Ergebnissen die folgenden Schlussfolgerungen gezogen werden können:

5. Die Affinitätshypothese zwischen linearen und nichtlinearen Kriechverformungen ermöglicht die Formulierung einer einfachen und konsequenten Beziehung, um die Entwicklung inelastischer Verformungen in Beton für eine gegebene Belastungsgeschichte abzuschätzen. Es beschreibt die Entwicklung von Tertiär-Kriechverformung auf explizite Weise.
6. Die analytische Berechnung vom Bruch unter Dauerlastszenarien kann als Schnittpunkt bestimmt werden zwischen der Beziehung, welche die Entwicklung inelastischer Verformungen für eine gegebene Belastungsgeschichte (laut Affinitätshypothese) definiert und dem durch die inelastische Verformungskapazität definierten Versagenskriterium. Dieser Ansatz ermöglicht die konsequente Abschätzung der Festigkeit und der damit verbundenen Verformung für verschiedene Belastungsgeschichten, wie die Testergebnisse sowohl unter konstante Dauerbelastung als auch mit verschiedenen Spannung- und Dehnungsraten bestätigen.
7. Auf der Grundlage des theoretischen Modells können einige Effekte klar reproduziert und untersucht werden, wie zum Beispiel:
    a. Konstante Dauerbeanspruchungen führen zu Versagen bei niedrigeren Beanspruchungsstufen und schneller als bei Spannungs- oder

Dehnungsraten (der Beton ist seit Beginn des Belastungsprozesses höheren Belastungsniveaux ausgesetzt).

b. Die Alterung des Betons (Erhöhung der Betonfestigkeit mit der Zeit) wird als ein instrumentelles Phänomen angesehen, da sie den Materialschaden kompensiert. Bei einer Lastaufbringung im frühen Alter kann ein Versagen erst nach einigen Stunden oder Tagen auftreten, während bei einer Lastaufbringung im späten Alter das Versagen unter Dauerbelastung auch mehrere Jahre danach auftreten kann (da die Festigkeit durch die Alterung mit der Zeit kaum zunimmt).

11.2 Querkraftwiderstand von Stahlbetonbauteilen

Basierend auf einer experimentellen Kampagne von schlanken bzw. gedrungenen querkraftkritischen Bauteilen ohne Schubbewehrung mit unterschiedlichen Belastungsgeschwindigkeiten können die folgenden Schlussfolgerungen zum zeitabhängigen Querkraftwiderstand von Stahlbetonbauteilen gezogen werden:

1. Die durchgeführten Tests zeigen keine merkliche Abnahme des Querkraftwiderstands für höhere Belastungsdauern oder für niedrige Belastungsgeschwindigkeiten im Vergleich zu typischen Querkraftwiderstandstests.
2. Bei höheren Belastungsraten im Vergleich zu typischen Querkraftwiderstandstests (Bruch nach einigen Sekunden) kann bei schlanken Bauteilen eine relativ konsequente Zunahme des Querkraftwiderstands beobachtet werden. Eine Analyse der Querkrafttragmechanismen zeigt, dass dies durch eine günstigere Geometrie des kritischen Schubrisses bei hohen Belastungsgeschwindigkeiten gerechtfertigt werden kann. Die Ergebnisse sind für gedrungene Bauteile nicht so eindeutig, weisen jedoch auf ein ähnliches Verhalten hin.
3. Bei gedrungenen Bauteilen kann der relativ konstante Querkraftwiderstand für hohe Dauerbelastungen durch die potentielle Umlagerung der inneren Kräfte sowie die Umschnürung der querkrafttragenden Druckstrebe gerechtfertigt werden.
4. Für schlanke Bauteile kann die begrenzte Empfindlichkeit des Querkraftwiderstands gegenüber niedriger Belastungsgeschwindigkeiten durch die ähnliche Form und Öffnung des kritischen Schubes und durch das relativ schnelle (jedoch stabile) Öffnen und Gleiten des kritischen Schubes kurz vor Versagen begründet werden. Dies ermöglicht es, die Schubrissverzahnung (der dominante Querkrafttragmechanismus in diesen Bauteilen) auf relativ schnelle Art und Weise zu aktivieren (dieser Beitrag wird daher wenig durch die Gesamtdauer des Belastungsvorgangs beeinflusst).

11.3 Bemessungsfolgerungen

Basierend auf den experimentellen und analytischen Arbeiten dieses Berichts könnte ein vereinfachter normenähnlicher Ansatz für die Ingenieurpraxis entwickelt werden. Einige wichtige Aspekte sind:

1. Das Phänomen des Betonkriechens soll sowohl im Grenzzustand der Gebrauchstauglichkeit als auch im Grenzzustand der Tragfähigkeit berücksichtigt werden.
2. Einfache Gleichungen können hergeleitet werden, um die Bruchlast von Beton unter Dauerbelastung zu charakterisieren. Die Kombination dieser Ausdrücke mit dem Verfahren von Palmgren-Miner bietet eine praktische Möglichkeit, um die Schadensakkumulation im Beton zu berücksichtigen und die Bruchlast und -zeit abzuschätzen.
3. Es konnte bestätigt werden, dass die vorteilhafte Wirkung der fortgesetzten Zementhydratation normalerweise die nachteiligen Auswirkungen der Dauerbelastung kompensiert. Dies gilt, sofern die Betonfestigkeit nach 28 Tagen bestimmt wird und der Grenzzustand der Tragfähigkeit nach einer ausreichend langen Zeit auftritt. Wenn die Betonfestigkeit später als 28 Tage ermittelt wird

(besonders relevant für die Instandsetzung vorhandener Strukturen), ist die Abminderung der Betonfestigkeit unter Berücksichtigung langfristiger und hoher Dauerbelastung gerechtfertigt.

4. Bei einem gegebenen Gesamtspannungsniveau ist eine Kombination aus dauerhafte Einwirkungen und einer schnellen variablen Einwirkung für die Betondruckfestigkeit weniger nachteilig als eine vollständige dauerhafte Einwirkung. Dieses Phänomen kann durch einfache, normenähnliche Gleichungen beschrieben werden, die auf einer linearen Interpolation zwischen dem Fall eines unter Dauerlast brechenden Bauteils und dem Fall basieren, wo Dauerlasteffekte vernachlässigt werden können. In Fällen, in denen die veränderliche Aktion über einen bestimmten Zeitraum einwirkt, kann ein ähnlicher Ansatz verfolgt werden.
5. Trotz der Tatsache, dass für das reine Materialverhalten eine Abnahme der Festigkeit weitgehend dokumentiert und verifiziert wurde, scheint für querkraftkritische Bauteile keine Verringerung des Querkraftwiderstands bei hohen Dauerbelastungen über lange Zeit erforderlich zu sein.

Zu den Auswirkungen der Dauerbelastung auf den Durchstanzwiderstand, die nicht Teil dieses Forschungsprojekts waren, wurde bisher wenig erforscht. Folglich sind zusätzliche Überlegungen erforderlich, bevor der Festigkeitsreduzierungsfaktor für die Berechnung des Bemessungswerts des Querkraftwiderstands in SIA 262:2013 entfernt werden kann.

11.4 Vorschläge für die zukünftige Forschung

Die vorliegende Forschungsarbeit erlaubt folgende Themen zu identifizieren, die, zukünftigen Forschungsarbeiten erfordern:

1. In Bezug auf die Betondruckfestigkeit unter einachsiger Beanspruchung und das Langzeitverhalten von Biegedruckzonen:
    a. Der Einfluss einer Umschnürbewehrung, die die unelastische Verformungsfähigkeit und damit das Versagenskriterium von Beton beeinflussen können.
    b. Die Aktivierung der Druckbewehrung in Stützen und Biegedruckzonen durch nichtlineares Kriechen
2. In Bezug auf den Querkraftwiderstand bei Dauereinwirkungen:
    c. Durchführung einer umfassenderen experimentellen Untersuchung mit Grossversuchen an Betonträgern und Versuchen an kleinen Proben, um das Materialverhalten zu charakterisieren.
    d. Untersuchung des Durchstanzwiderstands von Betonplatten unter Dauerlast.

Appendix A

This Appendix presents the crack kinematics patterns and principal compressive strain (ε_2) vectors of specimens RT13.16 - RT18.25 of the squat beam series (*Fig. 1* - *Fig. 3*) as well as the longitudinal strain profiles in the compression strut for all specimens of the squat beam series (*Fig. 4*).

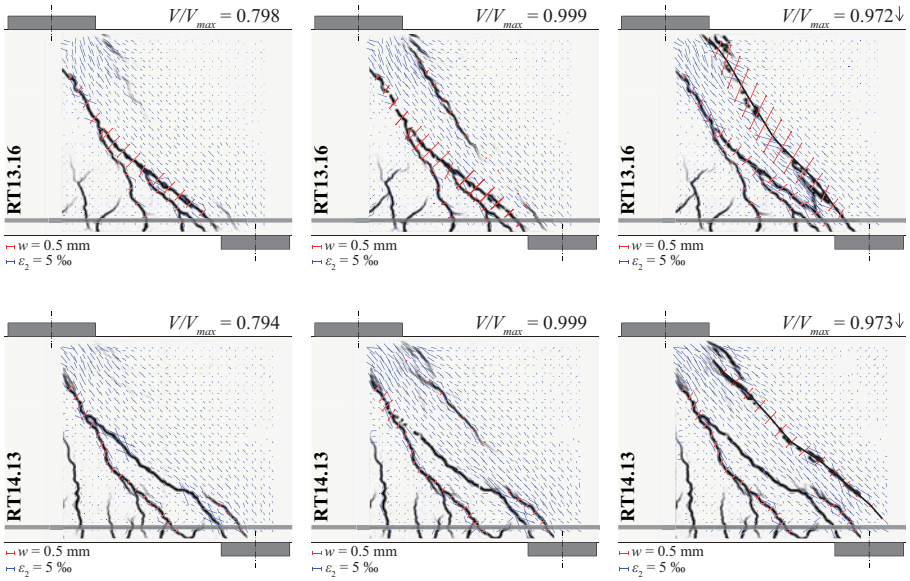

Fig. 1 Crack kinematics patterns and principal compressive strain (ε_2) vectors for specimens RT13.16 and RT14.13 at three load stages: approx. $0.8 \cdot V_{max}$, approx. V_{max} and instants before failure

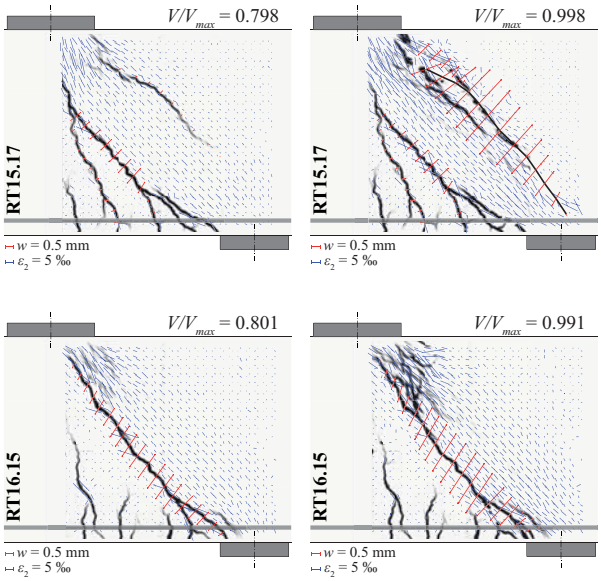

Fig. 2 Crack kinematics patterns and principal compressive strain (ε_2) vectors for specimens RT15.17 and RT16.15 at two load stages: approx. $0.8 \cdot V_{max}$ and approx. V_{max}

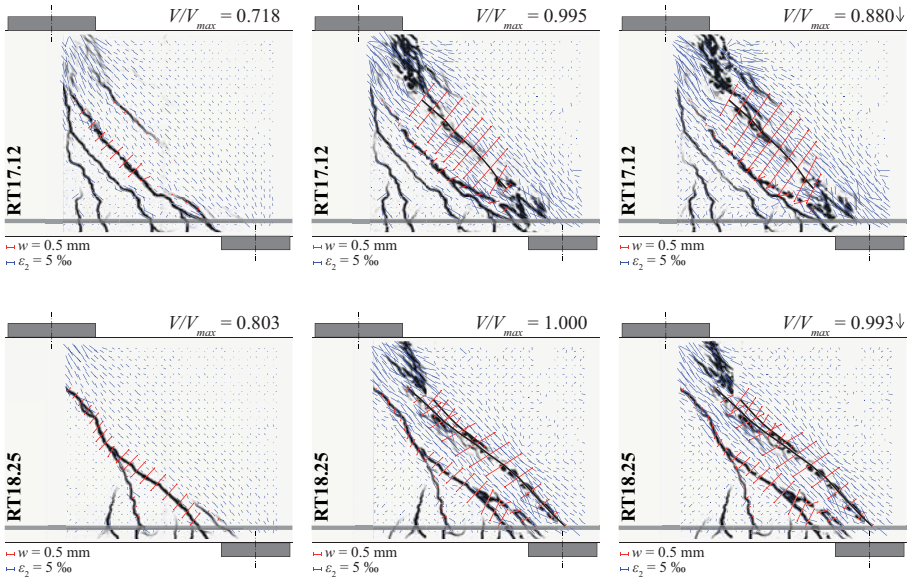

Fig. 3 Crack kinematics patterns and principal compressive strain (ε_2) vectors for specimens RT17.12 and RT18.25 at three load stages: approx. 0.72-0.8·V_{max}, approx. V_{max} and instants before failure

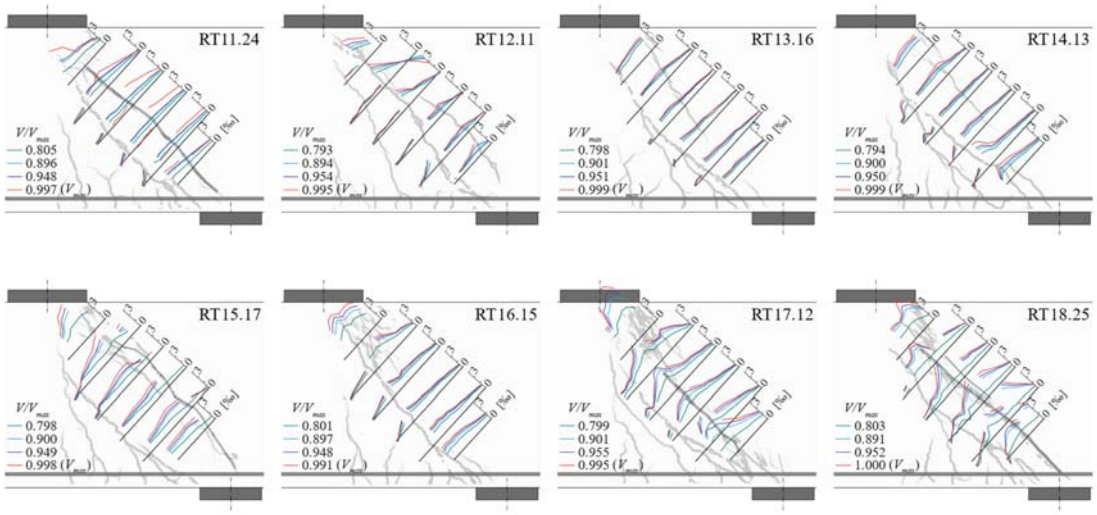

Fig. 4 Longitudinal strain profiles in the compression strut of the squat beam series (a/d = 1.0)

Notation

Term	Signification
Variables	
a	shear span (distance between load axis and support axis)
A_s	area of flexural reinforcement
b	width of the member
d	effective depth
d_g	aggregate size
E_c	modulus of elasticity of concrete
E_s	modulus of elasticity of reinforcing steel
f_c	uniaxial compressive strength of concrete [MPa]
$f_{c,ref}\,(t_0)$	reference compressive strength obtained at a strain rate of 0.02 ‰·s^{-1} and at an age t_0 [MPa]
$f_{c,28}$	reference compressive strength obtained at an age of 28 days [MPa]
$f_{c,\Delta t}$, $f_{c,\Delta tF}$	compressive stress at failure for a given long-term loading pattern [MPa]
$f_{c,var}$	compressive stress at failure under variable action after a permanent load σ_{perm} [MPa]
f_y	yield strength of reinforcement (corresponding to the 0.2% proof stress)
h	height of the member (or cylinder)
k_1, k_2	constants
k_t	strength reduction factor of concrete accounting for sustained load action
l_b	length of the region of the beam contributing to the critical shear crack opening
M_F	bending moment at the section of the tip of the shear crack
RH	relative humidity
s	coefficient characterizing the increase of concrete strength with time, depending on the strength class of cement
T	temperature
t	time
t_0	concrete age at loading [days]
t_F	time to failure since beginning of tests
$t_{F,100kN}$	time to failure after reaching a load of 100 kN
t_{ref}	concrete age at reference strength testing [days]
t_s	concrete age at the beginning of drying [days]
Δt	time under sustained stress for a constant stress level test or time after beginning of a strain or stress rate test (in the case of rapid initial loading, time after the initial loading ramp)
Δt_F	time under sustained stress required to attain failure
u_A	measured horizontal opening of the critical shear crack at the flexural reinforcement level
$u_{0.4d}$	measured horizontal opening of the critical shear crack at distance of 0.4d from the compression face
V	shear force
V_{calc}	calulated shear strength
V_{exp}	experimentally measured shear strength

V_{max}	maximum measured shear force
w	crack opening perpendicular to the crack surface
α	parameter governing the shape of tertiary creep strain development curve
β_{cc}	parameter to describe the development of concrete strength with time acc. to MC 2010
$\beta_{c,sus}$	parameter which depends on the time under high sustained loads acc. to MC 2010
γ	parameter characterizing tertiary creep
δ	deflection at the load introduction (at the edge support)
δ_{corr}	corrected deflection after considering rigid body movements
$\dot{\varepsilon}$	strain rate
$\dot{\varepsilon}_{ref}$	reference strain rate for uniaxial compressive strength testing
ε_c	concrete strain
ε_{c0}	instantaneous pre-peak strain
ε_{cc}	creep strain
ε_{cs}	shrinkage strain
$\varepsilon_{c,trans}$	transverse strain
$\varepsilon_{c,long}$	longitudinal strain
ε_2	second principal strain
$\varnothing$	concrete cylinder diameter
φ	creep coefficient
φ_{lin}	linear creep coefficient
φ_{nl}	nonlinear creep coefficient
λ	constant in [days]
η, η_T	affinity coefficient
ν	efficiency factor for the concrete strut
ν_{eff}	effective Poisson's ratio
ρ	flexural reinforcement ratio
$\dot{\sigma}$	stress rate
σ_c	concrete stress
σ_{perm}	stress due to permanent actions
σ_{tot}	total applied stress
Indexes	
av	available
c	concrete
calc	calculated
cc,1	primary creep
cc,2	secondary creep
cc,3	tertiary creep
cs	shrinkage
eff	effective
F	at failure

in	inelastic
init	initial
lin	linear
nl	nonlinear
perm	Permanent load
ref	reference
test	value form experimental result
tot	total
τ	time-related
var	variable action

Glossary

Term	Signification
ACI	American concrete institute
CEB	European concrete committee
CEN	European committee for standardization
fib	International federation of structural concrete
ISO	International organisation for standardisation
SIA	Swiss society of engineers and architects
SN	Swiss norms
USSR	Union of Soviet Socialist Republics

Bibliography

[1] Smeaton J (1791), « **A Narrative of the Building and a Description of Construction of the Eddystone Lighthouse with Stone** », *Publisher: H. Hughs, London, 198 p.*

[2] Swiss society of engineers and architects SIA (1903), « **Provisorische Normen für Projektierung, Ausführung und Kontrolle von Bauten in armiertem Beton** », *Publisher: V. F. Lohbauer, Zürich, 8 p*.

[3] Mörsch E (1912), « **Der Eisenbetonbau, seine Theorie und Anwendung** », *4th Ed., Publisher: Konrad Wittwer, Stuttgart, 710 p*.

[4] Kaltakci MY, Arslan MH, Korkmaz HH, and Ozturk M (2007), « **An investigation on failed or damaged reinforced concrete structures under their own-weight in Turkey** », *Engineering Failure Analysis*, *vol. 14, no. 6 SPEC. ISS.*, *pp. 962–969*.

[5] Hamed E (2014), « **Modelling of creep in continuous RC beams under high levels of sustained loading** », *Mechanics of Time-Dependent Materials*, *vol. 18, no. 3*, *pp. 589–609*.

[6] Shank JR (1949), « **Plastic Flow of Concrete at High Overload** », *ACI Journal*, *vol. 20, no. 6*, *pp. 493–498*.

[7] Rüsch H (1956), « **Versuche zur Bestimmung des Einflusses der Zeit auf Festigkeit und Verformung** », in *IABSE Kongressbericht, no. 5, pp. 237-244*.

[8] Rüsch H, (1960), « **Researches Toward a General Flexural Theory for Structural Concrete** », *ACI Journal*, *vol. 57, no. 1*, *pp. 1–28*.

[9] Rüsch H, Sell. R, Rasch C, Grasser E, Hummel A, Wesche K, and Flatten H (1968), « **Festigkeit und Verformung von unbewehrtem Beton unter konstanter Dauerlast** », *Deutscher Ausschuss für Stahlbeton*, *no. Heft 198*.

[10] International Organization for Standardization ISO (2005), « **ISO 1920-4:2005 Testing of Concrete - Part 4: Strength of hardened concrete** », *ISO Standard, Geneva, Switzerland, 27 p.*

[11] Stöckl S (1972), « **Strength of Concrete under Uniaxial Sustained Loading** », *SP-34 Concrete for Nuclear Reactors*, *vol. 1*, *pp. 313–326*.

[12] International Federation of Structural Concrete *fib* (2013), « **Bulletin 70: Code-type models for structural behaviour of concrete: Background of the constitutive relations and material models in the fib Model Code for Concrete Structures 2010** », *Ernst and Sohn, Germany, p. 196.*

[13] Tasevski D, Fernández Ruiz M, and Muttoni A (2018), « **Compressive Strength and Deformation Capacity of Concrete under Sustained Loading and Low Stress Rates** », *Journal of Advanced Concrete Technology*, *vol. 16, no. 8*, *pp. 396–415*.

[14] Fernández Ruiz M, Muttoni A, and Gambarova PG (2007), « **Relationship between nonlinear creep and cracking of concrete under uniaxial compression** », *Journal Of Advanced Concrete Technology*, *vol. 5, no. 3*, *pp. 383–393*.

[15] Schlappal T, Schweigler M, Gmainer S, Peyerl M, and Pichler B (2017), « **Creep and cracking of concrete hinges: insight from centric and eccentric compression experiments** », *Materials and Structures*, *vol. 50, no. 244, pp. 1-16*.

[16] Shah SP and Chandra S (1970), « **Fracture of Concrete Subjected to Cyclic and Sustained Loading** », *ACI Journal Proceedings*, *vol. 67, no. 10*, *pp. 816–827*.

[17] Awad ME and Hilsdorf HK (1971), « **Strength and Deformation Characteristics of Plain Concrete Subjected to High Repeated and Sustained Loads** », *Structural Research Series*, *vol. 372, no. February 1971*, *p. 266*.

[18] Diaz SI and Hilsdorf HK (1971), « **Fracture mechanisms of concrete under static, sustained, and repeadted compressive loads** », *Structural Research Series*, *vol. 382, no. August 1971*, *p. 198*.

[19] Wittmann FH and Zaitsev J (1972), « **Behaviour of Hardened Cement Paste and Concrete under Sustained Load** », *in Society of Materials Science Conference on the Mechanical Behavior of Materials*, *vol. 4, pp. 84–95*.

[20] Coutinho SA (1977), « **A contribution to the mechanism of concrete creep** », *Matériaux et Constructions*, *vol. 10, no. 55*, *pp. 3–16*.

[21] Fouré B (1985), « **Long–term strength of concrete under sustained loading (in French, Résistance potentielle à long terme du béton soumis à une contrainte soutenue)** », *Annales de l'Institut Technique du Batiment et des Travaux Publics, Paris, France, pp. 45-64.*

[22] Smadi MM, Slate FO, and Nilson AH (1985), « **High-, Medium-, and Low-Strength Concretes Subject to Sustained Overloads - Strains, Strengths, and Failure Mechanisms** », *ACI Materials Journal*, *vol. 82, no. 5*, *pp. 657–664*.

[23] Ngab AS, Nilson AH, and Slate FO (1981), « **Shrinkage and Creep of High-Strength Concrete** », *ACI Journal Proceedings*, *vol. 78, no. 4*, *pp. 255–261*.

[24] Smadi MM (1983), « **Time-Dependent Behavior of High-Strength Concrete under High Sustained Compressive Stresses** », *PhD Thesis, Cornell University, 297 p*.

[25] Han N and Walraven JC (1994), « **Properties of High-Strength Concrete Subjected to Uniaxial Loading** », *ACI Special Publication*, *vol. 149*, *pp. 269–288*.

[26] Iravani S and MacGregor JG (1998), « **Sustained load strength and short-term strain behavior of high-strength concrete** », *ACI Materials Journal*, *vol. 95, no. 5*, *pp. 636–647*.

[27] Müller HS, Burkart I, Bundelmann H, Ewert J, Mechtcherine V, Dudziak L, Müller C, and Eppers S (2010), « **Time-dependent behaviour of ultra high performance concrete (UHPC)** », *in 3rd International fib Congress, Washington D.C., 29 May – 2 June 2010*, *pp. 1–15*.

[28] Domone PL (1974), « **Uniaxial tensile creep and failure of concrete** », *Magazine of concrete research*, *vol. 26, no. 88*, *pp. 144–152*.

[29] Reinhardt H-W and Cornelissen HAW (1985), « **Zeitstandzugversuche an Beton** », *Baustoffe 85, Karlhans Wesche gewidmet.*, *Wiesbaden*, *pp. 162–167*.

[30] Reinhardt H-W and Rinder T (2006), « **Tensile Creep of High-Strength Concrete** », *Journal of Advanced Concrete Technology*, *vol. 4, no. 2*, *pp. 277–283*.

[31] El-Kashif KF and Maekawa K (2004), « **Time-Dependent Nonlinearity of Compression Softening in Concrete** », *Journal of Advanced Concrete Technology*, *vol. 2, no. 2*, *pp. 233–247*.

[32] Fischer I, Pichler B, Lach E, Terner C, Barraud E, and Britz F (2014), « **Compressive strength of cement paste as a function of loading rate: Experiments and engineering mechanics analysis** », *Cement and Concrete Research*, *vol. 58*, *pp. 186–200*.

[33] Berthollet A, Georgin J-F, and Reynouard J-M (2004), « **Fluage tertiaire du béton en traction** », *Revue Française de Génie Civil*, *vol. 8, no. 2–3*, *pp. 235–260*.

[34] Rossi P, Tailhan J-L, and Le Maou F (2013), « **Creep strain versus residual strain of a concrete loaded under various levels of compressive stress** », *Cement and Concrete Research*, *vol. 51*, *pp. 32–37*.

[35] Wittmann FH and Zaitsev J (1974), « **Verformung und Bruchvorgang poröser Baustoffe bei kurzzeitiger Belastung und Dauerlast** », *Deutscher Ausschuss für Stahlbeton*, *no. Heft 232, pp. 67-145*.

[36] Claisse P and Dean C (2013), « **Compressive strength of concrete after early loading** », *Proceedings of the Institution of Civil Engineers - Construction Materials*, *vol. 166, no. 3*, *pp. 152–157*.

[37] Swiss society of engineers and architects SIA (2013), « **Code 262 for concrete structures** », *Code SIA 262, Zürich, Switzerland, p. 102.*

[38] International Federation of Structural Concrete *fib* (2013), « **Model Code for concrete structures 2010** », *Ernst and Sohn, Germany, p. 434*.

[39] European committee for standardization CEN (2004), « **Eurocode 2. Design of concrete structures - General rules and Rules for Buildings** », *EN 1992-1-1. Brussels, Belgium, p. 225.*

[40] Gilbert RI and Ranzi G (2011), « **Time-Dependent Behaviour of Concrete Structures** », *Spon Press, New York, p. 428.*

[41] Ghali A, Favre R, and Eldbadry M (2002), « **Concrete Structures. Stresses and Deformation: Analysis and Design for Serviceability** », 3rd ed. Taylor&Francis, 2002, p. 608.

[42] Sarkhosh R (2014), « **Shear Resistance of Reinforced Concrete Beams without Shear Reinforcement under Sustained Loading** », *PhD Thesis, TU Delft, p. 259.*

[43] Sarkhosh R (2013), « **Shear Capacity of Concrete Beams under Sustained Loading** », *in International IABSE Conference, Rotterdam, pp. 1–8.*

[44] Muttoni A and Fernández Ruiz M (2008), « **Shear strength of members without transverse reinforcement as function of critical shear crack width** », *ACI Structural Journal*, *vol. 105, no. 2*, *pp. 163–172*.

[45] Cavagnis F, Fernández Ruiz M, and Muttoni A (2018), « **A mechanical model for failures in shear of members without transverse reinforcement based on development of a critical shear crack** », *Engineering Structures*, *vol. 157*, *pp. 300–315*.

[46] Fernández Ruiz M, Muttoni A, and Sagaseta J (2015), « **Shear strength of concrete members without transverse reinforcement: A mechanical approach to consistently account for size and strain effects** », *Engineering Structures*, *vol. 99*, *pp. 360–372*.

[47] Saifullah HA, Nakarai K, Piseth V, Chijiwa N, and Maekawa K (2017), « **Shear creep failures of reinforced concrete slender beams without shear reinforcement** », *ACI Structural Journal*, *vol. 114, no. 6*, *pp. 1581–1590.*

[48] Cavagnis F, Fernández Ruiz M, and Muttoni A (2018), « **An analysis of the shear-transfer actions in reinforced concrete members without transverse reinforcement based on refined experimental measurements** », *Structural Concrete*, *vol. 19, no. 1*, *pp. 49–64*.

[49] Sagaseta J and Vollum R (2010), « **Shear design of short-span beams** », *Magazine of Concrete Research*, *vol. 62, no. 4*, *pp. 267–282*.

[50] Maekawa K, Zhu X, Chijiwa N, and Tanabe S (2016), « **Mechanism of Long-Term Excessive Deformation and Delayed Shear Failure of Underground RC Box Culverts** », *Journal of Advanced Concrete Technology*, *vol. 14, no. 5*, *pp. 183–204*.

[51] Bugalia N and Maekawa K (2017), « **Time-Dependent Capacity of Large Scale Deep Beams under Sustained Loads** », *Journal of Advanced Concrete Technology*, *vol. 15, no. 7*, *pp. 314–327*.

[52] ACI Committee 318 (2014), « **Building Code Requirements for Structural Concrete** », *Code ACI 318-14, p. 520*.

[53] Hellesland J and Green R (1972), « **A Stress and Time Dependent Strength Law for Concrete** », *Cement and Concrete Research*, *vol. 2, no. 3*, *pp. 261–275*.

[54] Carol I and Murcia J (1989), « **A model for the non-linear time-dependent behaviour of concrete in compression based on a Maxwell chain with exponential algorithm** », *Materials and Structures*, *vol. 22, no. 3*, *pp. 176–184*.

[55] Mazzotti C and Savoia M (2003), « **Nonlinear Creep Damage Model for Concrete under Uniaxial Compression** », *ASCE, Journal of Engineering Mechanics*, *vol. 129, no. 9*, *pp. 1065–1075*.

[56] Bockhold J and Stangenberg F (2004), « **Modellierung des nichtlinearen Kriechens von Beton** », *Beton- und Stahlbetonbau*, *vol. 99, no. 3*, *pp. 209–216*.

[57] Challamel N, Lanos C, and Casandjian C (2005), « **Creep damage modelling for quasi-brittle materials** », *European Journal of Mechanics - A/Solids*, *vol. 24, no. 4*, *pp. 593–613*.

[58] Zhou FP (1992), « **Time-dependent crack growth and fracture in concrete** », *PhD Thesis, Lund Institute of Technology, 132 p*.

[59] van Zijl GPAG, de Borst R, and Rots JG (2001), « **The role of crack rate dependence in the long-term behaviour of cementitious materials** », *International Journal of Solids and Structures*, *vol. 38, no. 30*, *pp. 5063–5079*.

[60] Barpi F and Valente S (2002), « **Creep and fracture in concrete: a fractional order rate approach** », *Engineering Fracture Mechanics*, *vol. 70, no. 5*, *pp. 611–623*.

[61] Di Luzio G, (2009) « **Numerical Model for Time-Dependent Fracturing of Concrete** », *Journal of Engineering Mechanics*, *vol. 135, no. 7*, *pp. 632–640*.

[62] Karsan AI and Jirsa JO (1969), « **Behavior of Concrete under Compressive Loadings** », *Journal of the Structural Division, ASCE*, *vol. 95*, *pp. 2535–2563*.

[63] Zanuy C, Albajar L, and De La Fuente P (2010), « **Sectional analysis of concrete structures under fatigue loading** », *ACI Structural Journal*, *vol. 106, no. 5*, *pp. 667–677*.

[64] Tasevski D, Fernández Ruiz M, and Muttoni A (2016), « **Behaviour of concrete in compression and shear under varying strain rates: from rapid to long-term actions** », *in 11th fib International PhD Symposium in Civil Engineering, Tokyo*, *29-31 August 2016, pp. 881–886*.

[65] Tasevski D, Fernández Ruiz M, and Muttoni A (2015), « **Analogy between Sustained Loading and Strain Rate Effects on the Nonlinear Creep Response of Concrete** », in *CONCREEP-10, Vienna, 21-23 September 2015, pp. 1187-1193*.

[66] European Concrete Committee CEB (1962), « **Principes de Calcul du Béton Armé Sous des états de Contraints Monoaxiaux** », *CEB Bulletin d'information No. 36, Luxembourg, p. 112.*

[67] Palmgren AG (1924), « **Life Length of Roller Bearings** », *Zeitschrift des Vereins Deutscher Ingenieure*, *vol. 68, no. 14*, *pp. 339–341*.

[68] Miner M (1945), « **Cumulative damage in fatigue** », *Journal of Applied Mechanics*, *vol. 67, no. September*, *pp. 159–164*.

[69] Oh BH (1991), « **Cumulative Damage Theory of Concrete under Variable-Amplitude Fatigue Loadings** », *ACI Materials Journal*, *vol. 88, no. January-February*, *pp. 41–48*.

[70] Miller KJ, Mohamed HJ, and de Los Rios ER (1986), « **Fatigue damage accumulation above and below fatigue limit** », *in Report: The Behaviour of short fatigue cracks, Ed. Miller KJ and de los Rios ER, EGF Pub. 1, London, pp. 491–511.*

[71] Zhang B, Phillips D V., and Wu K (1996), « **Effects of loading frequency and stress reversal on fatigue life of plain concrete** », *Magazine of Concrete Research*, *vol. 48, no. 177*, *pp. 361–375.*

[72] Holmen JO (1982), « **Fatigue of Concrete by Constant and Variable Amplitude loading** », *ACI Special Publication*, *vol. 75*, *pp. 71–110*.

[73] Hilsdorf HK and Kesler C (1966), « **Fatigue Strength of Concrete under Varying Flexural Stresses** », *ACI Materials Journal*, *vol. 63, no. 10*, *pp. 1059–1076*.

[74] Mattock AH, Kriz LB, and Hognestad E (1961), « **Rectangular Concrete Stress Distribution in Ultimate Strength Design** », *ACI Journal Proceedings*, *vol. 57, no. 2*, *pp. 875–928*.

[75] Fernández Ruiz M (2003), « **Nonlinear Analysis of the Structural Effects of the Delayed Strains of Steel and Concrete** », *PhD Thesis, Polytechnic University of Madrid, Ed. ACHE, 175 p.*

[76] CorrelatedSolutions (2007), « *VIC3D-8 Manual* », www.correlatedsolutions.com, *User manual, p. 114*.

[77] Campana S, Fernández Ruiz M, Anastasi A, and Muttoni A (2013), « **Analysis of shear-transfer actions on one-way RC members based on measured cracking pattern and failure kinematics** », *Magazine of Concrete Research*, *vol. 65, no. 6*, *pp. 386–404*.

[78] Cavagnis F, Fernández Ruiz M, and Muttoni A (2015), « **Shear failures in reinforced concrete members without transverse reinforcement: An analysis of the critical shear crack development on the basis of test results** », *Engineering Structures*, *vol. 103*, *pp. 157–173*.

[79] Cavagnis F (2017), « **Shear in reinforced concrete without transverse reinforcement: from refined experimental measurements to mechanical models** », *PhD Thesis, EPFL, p. 201.*

[80] Das Adhikary S, Li B, and Fujikake K (2014), « **Effects of High Loading Rate on Reinforced Concrete Beams** », *ACI Structural Journal*, *vol. 111, no. 3*, *pp. 651–660*.

[81] Muttoni A, Fernández Ruiz M, and Niketić F (2015), « **Design versus Assessment of Concrete Structures Using Stress Fields and Strut-and-Tie Models** », *ACI Structural Journal*, *vol. 112, no. 5*, *pp. 605–616*.

[82] Fernández Ruiz M and Muttoni A (2008), « **On Development of Suitable Stress Fields for Stuctural Concrete** », *ACI Structural Journal*, *no. 104*, *pp. 495–502*.

[83] Simões JT, Faria DMV, Fernández Ruiz M, and Muttoni A (2016), « **Strength of reinforced concrete footings without transverse reinforcement according to limit analysis** », *Engineering Structures*, *vol. 112*, *pp. 146–161*.

[84] Swiss society of engineers and architects SIA (2014), « **National annex NA to SN EN 1992-1-1:2004 (Eurocode 2)** », *Zürich, Switzerland, p. 123.*

[85] Gvozdev AA (1966), « **Creep of concrete** », *Mekhanika Tverdogo Tela, Moscow, p. 137-152.*

[86] Neville AM (1970), « **Creep of concrete: Plain Reinforced and Prestressed** », *Elsevier, Amsterdam, p. 622.*

[87] Jensen RS, Richart FE (1938), « **Short-time creep test of concrete in compression** », *ASTM Proceedings 38, Part 2, p. 410-417.*

[88] Becker J, Bresler B (1974), « **FIRES-RC, A computer program for the fire resistance of structures and reinforced concrete frames** », *UC-FRG Report No, 74-3, University of California, Berkeley*.

[89] Pérez Caldentey A, Arroyo Portero JC (1998) « **Caracterización de las propriedades diferidas del horigón y su incidencia estructural** », *GT II/3 GEHO, Boletín 22, Madrid.*

[90] Karapetan KS (1959), « **Vlianie starenia betona na zavisimosti medju napreajeniami I deformatiami polzucesti** », *Izvestia AN. Armeanskoi SSR. Fizico-matematiceskie nauki, XII(4).*

[91] Avram C, Facaoaru I, Filimon I, Mirsu O, Tertea I (1981) « **Concrete strength and strain** », *Vol. 3, Elsevier, Amsterdam, p. 557*.

[92] Ulitkii II (1967), « **Teoria I rasciot jelezobetonnih sterjnevihkonstruktii s uciotom dlitelinih protesov** », *Izd. Budivelnik, Kiev*.

Project closure

Schweizerische Eidgenossenschaft
Confédération suisse
Confederazione Svizzera
Confederaziun svizra

Département fédéral de l'environnement, des transports, de l'énergie et de la communication DETEC
Office fédéral des routes OFROU

RECHERCHE DANS LE DOMAINE ROUTIER DU DETEC

Version du 09.10.2013

Formulaire N° 3 : Clôture du projet

établi / modifié le : 22.05.2019

Données de base

Projet N° : AGB 2013-001

Titre du projet : Influence de la durée et de la vitesse de chargement sur la résistance des structures en béton

Echéance effective :

Textes :

Résumé des résultats du projet :

L'objectif de ce travail de recherche était d'étudier l'effet des charges soutenues et de la vitesse de chargement sur la résistance à la compression du béton ainsi que ses implications aux éléments de structure.
La première partie du travail était concentrée sur l'amélioration d'un modèle mécanique, qui a été validé par deux séries d'essais supplémentaires sur des cylindres en béton non armés chargés en compression. Sur la base de ce modèle, il a été montré que la diminution de résistance sous charges soutenues peut atteindre environ 20%. Cette diminution est plus importante dans le cas d'une charge soutenue constante que dans le cas de charges augmentant progressivement. De plus, il a été montré que l'âge de chargement joue un rôle important, car la diminution de résistance peut être compensée par une augmentation due à la poursuite du processus d'hydratation du ciment. Les résultats du modèle montrent aussi que l'effet défavorable d'une charge soutenue est accompagné d'une plus grande capacité de déformation à la rupture, ce qui peut être très favorable pour la redistribution des efforts et la diminution des concentrations d'efforts.
Pour la deuxième partie du travail, deux séries d'essais avec des vitesses d'augmentation de la charge ont été effectués sur des éléments élancés et trapus dans le but de déterminer si une réduction de la résistance à l'effort tranchant sous charges soutenues devrait également être considérée dans les normes. Les résultats montrent qu'il n'y a pas de diminution marquée de la résistance à l'effort tranchant pour des durées d'application de la charge longues ni pour des vitesses de chargement plus faibles. De plus, des vitesses de chargement plus rapides qu'utilisées habituellement montrent une augmentation systématique de la résistance.
Cette recherche a aussi permis de vérifier les règles de la norme SIA 262:2013 ainsi que l'annexe nationale EN 1992-1-1/CH-NA:2014 de l'Eurocode 2. La présente étude montre que les provisions pour le facteur de réduction de la résistance en compression devraient être légèrement adaptées. Pour l'évaluation de structures existantes qui sont critiques à l'effort tranchant, le facteur de réduction de la résistance peut être omis. Pour l'effet des charges soutenues sur la résistance au poinçonnement, qui ne faisait pas partie de ce projet de recherche, des considérations supplémentaires sont requises.

Schweizerische Eidgenossenschaft
Confédération suisse
Confederazione Svizzera
Confederaziun svizra

Département fédéral de l'environnement, des transports, de l'énergie et de la communication DETEC
Office fédéral des routes OFROU

Atteinte des objectifs :

Les objectifs initiaux du projet sont considérés comme atteints :
- Le modèle de calcul de la réponse du béton en compression sous charge soutenue a été amélioré et validé par deux séries d'essais sur cylindres. Un critère de rupture a été établi, permettant de calculer la résistance sous charge soutenue élevée
- La différence entre le cas d'une charge soutenue constante et le cas d'une charge augmentant progressivement a été clarifiée et une approche a été proposée pour prendre en compte cette différence ainsi que pour considérer des histoires de chargement complexes
- Il a été clarifié que les durées de chargement de plus qu'une heure peuvent influencer la résistance du béton
- Une amélioration des normes de dimensionnement pour la résistance à la compression a été proposée
- Il a été vérifié sur la base de deux séries d'essais qu'une réduction de la résistance à l'effort tranchant due aux charges soutenues n'est pas nécessaire pour les éléments sans armature transversale.

Déductions et recommandations :

Pour le calcul de la résistance de calcul à la compression du béton, en principe, l'approche de la norme SIA 262 :2013 et de l'annexe nationale EN 1992-1-1/CH-NA:2014 de l'Eurocode 2 est confirmée. Néanmoins, des modifications mineures sont proposées pouvant être implémentées dans une prochaine révision des normes.
Pour la résistance à l'effort tranchant des éléments sans armature d'effort tranchant, ce projet a montré qu'il n'est pas nécessaire de réduire la résistance en cas de charge soutenue et une proposition de modification de la norme SIA 262 :2013 est faite dans ce sens. Néanmoins, très peu de recherche sur l'effet des charges soutenues sur la résistance au poinçonnement (qui ne faisait pas partie de ce projet de recherche) a été effectuée jusqu'à présent. En conséquence, des considérations supplémentaires sont requises avant de pouvoir supprimer le facteur de réduction de la résistance pour le calcul de la valeur de dimensionnement de la contrainte limite de cisaillement de la SIA 262:2013.

Publications :

- Tasevski D, Fernández Ruiz M, and Muttoni A (2019). « Influence of load duration on shear strength of reinforced concrete members », ACI Structural Journal, submitted for publication.
- Tasevski D, Fernández Ruiz M, and Muttoni A (2019), « Assessing the compressive strength of concrete under sustained actions: from refined models to simple design expressions », Structural Concrete, accepted for publication.
- Tasevski D, Fernández Ruiz M, and Muttoni A (2018), « Compressive Strength and Deformation Capacity of Concrete under Sustained Loading and Low Stress Rates », Journal of Advanced Concrete Technology, vol. 16, no. 8, pp. 396–415.
- Tasevski D, Fernández Ruiz M, and Muttoni A (2016), « Behaviour of concrete in compression and shear under varying strain rates: from rapid to long-term actions », in 11th fib International PhD Symposium in Civil Engineering, Tokyo, 29-31 August 2016, pp. 881–886.
- Tasevski D, Fernández Ruiz M, and Muttoni A (2015), « Analogy between Sustained Loading and Strain Rate Effects on the Nonlinear Creep Response of Concrete », in CONCREEP-10, Vienna, 21-23 September 2015, pp. 1187-1193.

Chef/cheffe de projet :

Nom : Muttoni Prénom : Aurelio

Service, entreprise, institut : École Polytechnique Fédérale de Lausanne, Laboratoire de Construction en Béton IBETON

Signature du chef/de la cheffe de projet :

Prof. Dr. Aurelio Muttoni, Lausanne, le 22.05.2019

Schweizerische Eidgenossenschaft
Confédération suisse
Confederazione Svizzera
Confederaziun svizra

Département fédéral de l'environnement, des transports, de l'énergie et de la communication DETEC
Office fédéral des routes OFROU

RECHERCHE DANS LE DOMAINE ROUTIER DU DETEC

Formulaire N° 3 : Clôture du projet

Appréciation de la commission de suivi :

Evaluation :

Ce rapport de recherche montre que l'approche de la norme SIA 262:2013 concernant l'effet des actions permanentes sur la résistance à la compression du béton est, avec quelque adaptation proposée, pertinente. L'étude permet aussi de définir la limite entre charges de longue durée (pour lesquelles il faut considérer la diminution de résistance) et les charges de courte durée (pour lesquelles la diminution de résistance peut être négligée). Pour ce qui concerne la résistance à l'effort tranchant des éléments sans armature transversale (typiquement les dalles, les radiers de fondation, les murs de soutènement, les dalles de pont et les pont-dalles), cette recherche montre que l'effet des charges de longue durée sur la résistance peut être négligé.

Mise en oeuvre :

Ces nouvelles connaissances peuvent être considérées dans le cadre d'une future révision de la norme SIA 262. Surtout la partie sur l'effort tranchant donne des indications pouvant être très importantes dans le cadre de l'évaluation de structures existantes. Dans une phase intermédiaire, avant la révision de la norme SIA 262, ces nouvelles connaissances pourraient éventuellement être appliquées dans la vérification de structures existantes, mais, pour ce qui concerne l'effort tranchant, à condition de considérer aussi les nouvelles connaissances acquises dans le projet AGB 2011-015.

Besoin supplémentaire en matière de recherche :

Cette recherche fournit les bases pour traiter d'autres cas intéressants dans la pratique (par exemple l'effet favorable du fluage non-linéaire en cas de redistribution des efforts) qui pourrait faire l'objet d'autres recherches futures. L'effet potentiellement défavorable des charges de longue durée sur la résistance au poinçonnement des dalles, dont l'étude ne faisait pas partie de ce projet de recherche, mériterait aussi d'être étudié plus en détail.

Influence sur les normes :

Ce projet de recherche fournit les bases pour la révision des clauses 2.3.2.4 (contrainte limite de cisaillement) et 4.2.1.3 (effet des charges de longue durée sur la résistance du béton) de la norme SIA 262 :2013 « Construction en béton ».

Président/Présidente de la commission de suivi :

Nom : Dr. Käser Prénom : Martin

Service, entreprise, institut : Baudirektion des Kt. Zürich, Tiefbauamt

Signature du président/ de la présidente de la commission de suivi :

M. Käser

List of previous road research reports from the Federal Roads Office FEDRO

L'index actuel des rapports publiés dernièrement est à télécharger sur notre site www.astra.admin.ch (Service --> Recherche en matière de routes --> Downloads --> Formulaires)